SYNTHESIS AND DYNAMICS OF γ-ALUMINA SUPPORTED MOLYBDENUM SUBCARBONYLS AND MODEL COMPOUNDS

by

George Wayne Wagner

Dissertation submitted to the Faculty of the
Virginia Polytechnic Institute and State University
in partial fulfillment of the requirements for the degree of

DOCTOR OF PHILOSOPHY

in

Chemistry

APPROVED:

B. E. Hanson, Chairman

J. G. Dillard

J. G. Mason

J. W. Viers

J. M. Tanko

July, 1987

Blacksburg, Virginia

SYNTHESIS AND DYNAMICS OF γ-ALUMINA SUPPORTED MOLYBDENUM SUBCARBONYLS AND MODEL COMPOUNDS

by

George Wayne Wagner

Committee Chairman: Brian E. Hanson
Chemistry

(ABSTRACT)

Molybdenum hexacarbonyl supported on γ-alumina is a precursor to an active olefin metathesis catalyst. Surface sites on the alumina act as coordinating ligands to stabilize various molybdenum subcarbonyl species. The formation of these species can be controlled by appropriate activation conditions. In particular, $Mo(CO)_3$(ads) can be quantitatively formed upon activation of $Mo(CO)_6$ on γ-alumina at 100°C in flowing helium. In the reaction, three carbon monoxide ligands are replaced by either surface OH^- or O^{2-} depending on the degree of surface hydroxylation. This species has been shown to be active for olefin metathesis.

The intent of this dissertation is twofold. The first part is an investigation of alternate, low temperature synthetic routes to $Mo(CO)_3$(ads) via ligand displacement reactions using the molybdenum tricarbonyl complexes, $Mo(CO)_3(CH_3CN)_3$ and $Mo(CO)_3(\eta^6\text{-}C_6H_6)$. Molybdenum hexacarbonyl can be impregnated onto γ-alumina using an inert hydrocarbon solvent such as pentane or benzene and these solvents are also used to adsorb $Mo(CO)_3(\eta^6\text{-}C_6H_6)$. However, a polar solvent such as acetone is necessary in the case of $Mo(CO)_3(CH_3CN)_3$. The resulting surface species using these complexes are characterized by FTIR, reaction stoichiometry and propylene metathesis activity and are compared with results obtained for γ-alumina supported $Mo(CO)_6$. In order to interpret the results for $Mo(CO)_3(CH_3CN)_3$, the interaction of acetone with γ-alumina was investigated since acetone is highly reactive with the surface. The results of this in situ FTIR-MS study of acetone on γ-alumina are also reported.

The second part of this dissertation involves using cross polarization-magic angle spinning ^{13}C NMR to probe the dynamic natures of $Mo(CO)_3$(ads) and $Mo(CO)_5$(ads). Crystalline samples of

metal tricarbonyl complexes, which serve as model compounds for $Mo(CO)_3$(ads), are characterized by variable temperature CP-MAS ^{13}C NMR in order to determine the presence of motional processes involving the carbonyl ligands. These findings yield additional information about the nature of molybdenum subcarbonyls on γ-alumina.

DEDICATION

to my father

George William Wagner

and in memory of my mother

Mildred Elizabeth Sheesley-Wagner

ACKNOWLEDGEMENTS

I would like to thank my advisor, Dr. Brian E. Hanson, for his help, guidance and patience during the course of this work as well as the rest of my advisory committee for their role in my professional development. I would like to thank Dr. Larry Weiserman and Ms. Ruth Kaufman for their assistance in using the FTIR-MS at Alcoa Laboratories and also Dr. George Marcelin for the use of the MSL-300 NMR at the University of Pittsburgh. Grants from the National Science Foundation supporting this research are gratefully acknowledged.

TABLE OF CONTENTS

FIGURES

TABLES

CHAPTER 1
INTRODUCTION

1A HISTORICAL

Molybdenum hexacarbonyl supported on alumina was discovered by Banks and Bailey[1] in 1964 to catalyze a new olefin disproportionation reaction now termed olefin metathesis.[2] They reported the reaction in which olefins of three to eight carbon atoms were converted to olefins of shorter and longer chains in approximately equimolar quantities. For propylene, the metathesis reaction would be represented by:

$$2\ CH_3\text{-}CH=CH_2 \rightleftharpoons H_3C\text{-}CH=CH\text{-}CH_3 + CH_2=CH_2$$

Besides molybdenum hexacarbonyl, the coworkers reported that tungsten hexacarbonyl and molybdenum oxide supported on alumina would also catalyze the reaction.

Since then, much research has been devoted to characterize the nature of the molybdenum catalysts. Studies have been done to determine the molybdenum species present on the γ-alumina surface[3-11] as well as the activities of differently prepared catalysts for a variety of reactions. These include olefin metathesis,[4,5,7,12,13] hydrogenation of propylene and hydrogenolysis of cyclopropane,[14] and methanation.[15,16] Also, a mechanism has been proposed for olefin metathesis in a homogeneous catalytic system by Chauvin and Herisson[17] and has been discussed by others.[2,18-21] A discussion of the results of these previous studies follows.

In an early study, Kemball, et al.[3] studied catalyst samples by IR using nujol mulls of the materials. An unactivated sample of $Mo(CO)_6$ adsorbed on γ-alumina yielded a single carbonyl stretch at 1985 cm^{-1} which was assigned to physisorbed $Mo(CO)_6$. This material was found to be inactive for olefin metathesis. Another sample activated at 100°C for 1 h under vacuum proved to be active for metathesis and two bands were present in the IR spectrum at 1880 and 2020 cm^{-1}. The researchers noted that this indicated a loss of symmetry from that of the original octahedral symmetry of $Mo(CO)_6$. It was found that exposing the sample to air caused all carbonyl bands to disappear and also the loss of catalytic activity. When the sample activated at 100°C was treated with

cycloheptatriene, the pale yellow color of the catalyst became orange and three IR bands were present at 1890, 1940 and 2020 cm^{-1} which were similar to those expected for the orange-red complex, $Mo(CO)_3(\eta^6\text{-}C_7H_8)$ (1890, 1929 and 2000 cm^{-1}). Exposing an identically prepared sample to bicycloheptadiene caused the pale yellow color to deepen but a satisfactory IR spectrum of this material was not obtained in order to compare it to the yellow bicycloheptadiene-$Mo(CO)_4$ complex. On the basis of the ease of complex formation, the workers suggested that in the case of the active catalyst the hexacarbonyl had lost at least two and probably three carbonyl groups.

In a later paper, Kemball, et al.,[12] in a study of propylene metathesis over γ-alumina supported molybdenum hexacarbonyl catalysts, confirmed by mass spectroscopy that carbon monoxide was evolved when the catalysts were activated between 50 and 150°C. The yellow color of the catalysts was attributed to an $Mo(CO)_5$ species being formed on the surface on the basis of the yellow color of molybdenum pentacarbonyl ether complexes in solution. It was noted that activation for 1 h at 100°C produced a catalyst of maximum activity. The workers postulated that the fully active catalyst involved the loss of two or probably more carbonyl ligands which would allow for the co-ordination of propylene to form species of the type, $Mo(CO)_x(CH_2=CH\text{-}CH_3)_{6-x}$ where x is less than six and probably three or four. On the basis of quantitative analyses for the Mo content of the catalysts, it was reported that loadings of only about 1% Mo could be achieved.

In an IR study, Howe, et al.[4] investigated the adsorption of molybdenum hexacarbonyl on alumina, magnesia and silica and the metathesis activities of the materials. They observed that $Mo(CO)_6$ lost carbon monoxide upon activation at 45°C under vacuum to form subcarbonyls and that the process could be reversed by admitting carbon monoxide into the IR cell. The researchers suggested that at least three and possibly four different subcarbonyls were present on the surface due to the various intensities of four IR bands observed in separate samples. It was pointed out that three IR bands would be expected for $Mo(CO)_5$(ads) (C_{4v}) and assigned bands at 2080, 1945 and 1895 cm^{-1} to this species. Two bands at 1790 and 1725 cm^{-1} were assigned to

$Mo(CO)_4$(ads) since these bands indicated a reversible reaction with carbon monoxide to generate the bands assigned to $Mo(CO)_5$(ads). Two other bands at 1935 and 2020 cm^{-1} were assigned to lower subcarbonyl species of the type $Mo(CO)_x$ where x = 1, 2 or 3. These species were not observed to react with carbon monoxide. It was mentioned that the stabilities of the subcarbonyls might be due to interactions with surface OH^- and would explain the low CO stretching frequencies. A sample activated at 200°C indicated nearly complete loss of the above bands and the appearance of two new bands at 1965 and 1835 cm^{-1}. It was noted that this species was more active for olefin metathesis than the previous species, but its structure was not postulated. Exposure of the sample to oxygen caused the bands to disappear yet the catalytic activity of the material greatly increased. This information, plus the fact that propylene adsorption does not alter the IR spectra of the samples, suggested that the active species was devoid of carbonyl ligands. Also, no correlation was found between the concentration of subcarbonyls and activity. However, the researchers pointed out that a weak propylene interaction with only a small fraction of the subcarbonyls would not have been detected by IR.

In a later IR study, Howe[8] assigned two bands at 2120 and 1985 cm^{-1} to physisorbed $Mo(CO)_6$. The band at 2120 cm^{-1} was due to a lowering of the octahedral symmetry in $Mo(CO)_6$ after adsorption which allowed the normally inactive stretching mode to become IR active. As in the previous paper,[4] bands at 2075, 1950 and 1910 cm^{-1} were assigned to $Mo(CO)_5(OH^-)$ (C_{4v}) where OH^- is a surface hydroxyl group. Howe also observed reversible CO adsorption and the expected isotopic shifts in the IR spectra upon ^{13}CO adsorption. He noted that bands at 2020 and 1935 cm^{-1} exchanged CO very slowly. The bands present at 2020, 1935, 1790 and 1725 cm^{-1} were assigned to subcarbonyls of the form $Mo(CO)_x$. The results suggested that there were at least two and possibly three stable subcarbonyl species present on the surface, however they could not be identified by the available data. Howe also noted that the species responsible for the lower frequency bands at 1790 and 1725 cm^{-1} would undergo rapid CO exchange and that carbonyl frequencies below 1900 cm^{-1} are generally indicative of bridging carbonyl ligands or

anionic species, but he did not speculate as to how these observations might apply to the structure of the subcarbonyl species.

A more recent IR study by Kazusaka and Howe[10] gives further insight into the individual subcarbonyls. They observed that the interaction of physisorbed $Mo(CO)_6$ with surface OH^- causes a broadening of the IR OH bands. Two low frequency CO bands at 1680 and 1590 cm^{-1} were assigned to a terminal and bridging CO coordinated to surface Al^{3+}. The coworkers suggested that "$Mo(CO)_3$" is a mixture of the bimolecular and monomer species: $(X)(CO)_2Mo(CO:Al)_2Mo(CO)_2(X)$ and $(X)(CO)_2Mo(CO:Al)$ where X represents surface OH^- or O^{2-}. The IR bands assigned to these species are 2000, 1900 and 1590 cm^{-1} for the bimolecular species and 2000, 1900 and 1680 cm^{-1} for the monomer. They noted that the addition of CO would reverse the decarbonylation to yield "$Mo(CO)_4$" which was postulated to also be a mixture of bimolecular and monomer species: $(X)(CO)_3Mo(CO:Al)_2Mo(CO)_3(X)$ and $(X)(CO)_3Mo(CO:Al)$. The bands assigned to the bimolecular species were 2040, 1960 and 1640 cm^{-1} and for the monomer the bands were at 2040, 1960 and 1750 cm^{-1}. Again, the low frequency bands at 1640 and 1750 cm^{-1} were assigned to bridging and terminal CO coordinated to surface Al^{3+}. In the spectra, a weak shoulder was observed at 2085 cm^{-1} and was assigned to square pyramidal $Mo(CO)^5$(ads). However, the other bands expected for this species were not resolvable. The coworkers postulated that the reversiblity of the decomposition of $Mo(CO)_6$ suggested the existence of bridge-terminal CO exchange:

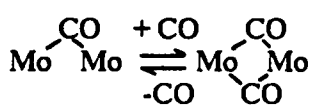

They also noted that "$Mo(CO)_3$" is less stable on hydroxylated γ-alumina (HA) than on partially dehydroxylated γ-alumina (PDA) and could be explained by the absence of surface Al^{3+} available for coordination with carbonyl ligands. "$Mo(CO)_3$" appeared to be coordinatively unsaturated as a result of an ammonia-d_3 adsorption experiment in which the terminal IR bands at 2000 and 1900 cm^{-1} shifted to 1910 and 1780 cm^{-1}, respectively, due to ND_3 adsorption. Also, the bridging CO

bands shifted from 1590 cm^{-1} to 1750 cm^{-1} as the result of being displaced from coordination with Al^{3+} by ND_3. It was noted that catalysts containing "$Mo(CO)_3$" had some activity but that outgassing at 400°C yielded a maximum activity and loss of all surface carbonyls. The workers were unable to conclude whether "$Mo(CO)_3$" is an active metathesis species or if the apparent activity was due to non-carbonyl containing species characteristic of higher temperature activation.

On the basis of stoichiometric carbon monoxide evolution measurements, Burwell and Brenner[5-7,9] have shown that the subcarbonyl species, $Mo(CO)_5$(ads), $Mo(CO)_4$(ads) and $Mo(CO)_3$(ads), can be selectively generated on the PDA surface and can be interconverted by the addition or removal of carbon monoxide at various temperatures. $Mo(CO)_3$(ads) is the most stable towards further CO loss and is nearly quantitatively formed at 100°C in flowing helium. The workers noted that the steric hinderance of the CO ligands around $Mo(CO)_5$(ads), along with the ready interconversion between the subcarbonyls, suggests that the species are molecularly dispersed on the surface and that they are readily accessible. However, a bridged species could not be ruled out. These subcarbonyls were considered to be bonded to the surface via OH^- or O^{2-} groups on the PDA surface. It was pointed out that $Mo(CO)_3$(ads) would be analogous to the complex, (diglyme)$Mo(CO)_3$ (diglyme = $CH_3OCH_2CH_2OCH_2CH_2OCH_3$);[22] both being eighteen electron complexes. They further noted that the diglyme complex is very labile and suggested the same behavior for $Mo(CO)_3$(ads) which would explain its ability to coordinate olefins in a metathesis reaction.

Burwell and Brenner[9] also noted that the separation of OH^- groups on the PDA surface is 0.27 nm[23] which is close to the value of 0.29 nm between carbon atoms in $Mo(CO)_6$.[24] The PDA surface is about 36% hydroxylated[23] which at the maximum loading of 2.2% Mo observed would yield a ratio of 6.5 OH^-/Mo. However, when taking into account the number of suitable OH^- triads, the ratio is 2.8 OH^-/Mo and is close to the theoretical value of 3 required for $Mo(CO)_3$(ads). Thus, the species, $Mo(CO)_3$(ads), was postulated to be either $Mo(CO)_3(OH^-)_3$ or $Mo(CO)_3(OH^-)_2(O_2^-)$ on the PDA surface.[9]

In a propylene metathesis study, Burwell and Brenner[13] noted that the activity of $Mo(CO)_3$(ads) indicated the presence of non-uniformity among the active sites. This behavior was rationalized by the fact that the geometries of the three surface ligands would vary as well as the ratio of O^{2-}/OH^-. Their results suggested that a very small number, < 1%, of the $Mo(CO)_3$(ads) surface complexes were generated to catalytically active sites. These active sites were postulated to be carbene complexes which have been shown to be intermediates in olefin metathesis reactions.[25] Irreversible propylene adsorption was not detected which was in agreement with the proposed small number of active sites generated. Brenner[5] has also noted the possibility of a hydride formation on the surface: $(OH^-)_2(O^{2-})HMo(CO)_3$. This structure was suggested as a result of H_2 chemisorption experiments and the fact that there are many examples of hydrido carbonyl complexes. Hydrides have also been proposed as catalysts for olefin metathesis.[26]

Laniecki and Burwell[11] indicated on the basis of the above information and their IR results that $Mo(CO)_3$(ads) on PDA is a mixture of $Mo(CO)_3(O_2^-)_2(OH^-)$ and $Mo(CO)_3(O^{2-})(OH^-)_2$. They also proposed a structure in which one of the carbonyl ligands is interacting with an adjacent O^{2-} in a bridging fashion. This structure was invoked to explain the species responsible for an IR band at about 1584 cm^{-1} which is in close agreement with the values of about 1580 cm^{-1} reported for M-COOH and $M\text{-}CO_2^-$ complexes.[27,28] The workers also noted that a dinuclear species in which a bridging carbonyl oxygen is coordinated to exposed Al^{3+} as proposed by Kazusaka and Howe[10] would also fit the available data and that it would be difficult to devise experiments to distinguish between the two structures.

In reviewing the previous evidence, Brown[29] discussed the structures proposed for $Mo(CO)_3$(ads) shown in Figures 1(a), (b) and (c). He noted that if $Mo(CO)_3$(ads) had approximately three-fold symmetry, then two IR stretching bands would be expected as seen in complexes of the type $Mo(CO)_3L_3$ (see Table 1). However, researchers had reported more than two and must represent structures with modified terminal or bridging CO ligands. The first structure considered was proposed by Laniecki and Burwell[11] and involved the interaction of a carbonyl group with a

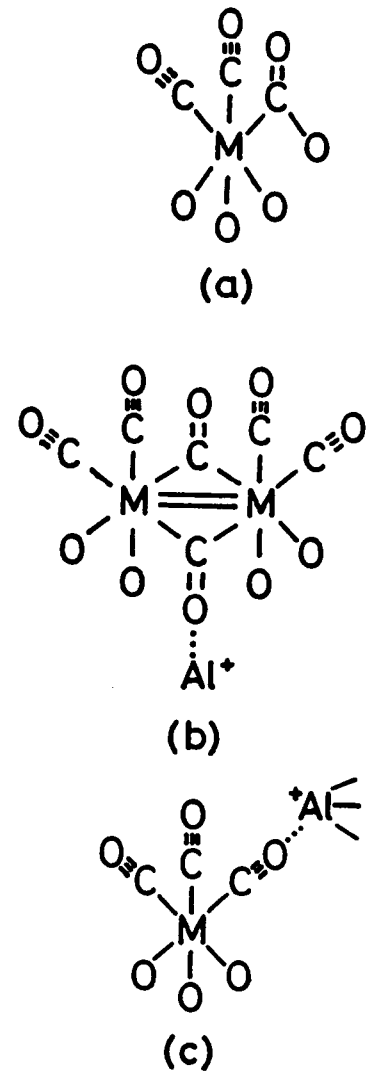

Figure 1. Proposed Structures for $Mo(CO)_3$(ads)

Table 1[a]

Infrared Stretching Frequencies of CO Groups in fac-$M(CO)_3L_3$ Compounds

Compound	A_1 (cm^{-1})	E (cm^{-1})
[b] $Mo(CO)_3(py)_3$	1908	1777
[c] $Mo(CO)_3$(dien)	1898	1758
[d] $Mo(CO)_3$(diglyme)	1905	1835
[e] $Mo(CO)_3(CH_3CN)_3$	1915	1783
[f] $Mn(CO)_3(py)_3^+$	2041	1947

[a] Data compiled by Brown.[29]
[b] Houk, L. W.; Dobson, G. R. J. Chem. Soc. (A), (1966) 317.
[c] Abel, E. W.; Bennett, M. A.; Wilkinson, G. J. Chem. Soc., (1959) 2323.
[e] Werner, R. P. M.; Coffield, T. H. Chem. Ind. (London), (1960) 936.
[f] Ross; B. L.; Grasselli, J. G.; Ritchey, W. M.; Kaesz, H. D. Inorg. Chem., 2 (1963) 1023.

surface O^{2-} group. A CO stretch at 1595 cm^{-1} was assigned to the interacting CO ligand. The other two bands at 2008 and 1919 cm^{-1} were assigned to the stretching frequencies of the other two CO groups. Brown pointed out that the interacting CO would increase electron density at the metal atom, thus causing an increased π-bonding interaction between the metal atom and the two remaining CO groups. However, the stretches assigned to these two groups are actually about 100 cm^{-1} higher than would be expected for compounds of the type $Mo(CO)_3L_3$. In fact, the frequencies assigned to $Mo(CO)_3$(ads) more closely resembled the stretching frequencies observed in a metal tricarbonyl complex in which the metal is in the + 1 oxidation state.

The bridged structure proposed for $Mo(CO)_3$(ads) by Kazusaka and Howe[10] was judged to be unfavorable by Brown[29] for several reasons. The first consideration was that Group VIb metal compounds show little tendency to form bridged species and σ-donating ligands such as surface OH^- and O^{2-} would further reduce any ability to form bridged species. Also, the Lewis acid adduct-CO bands assigned to the bimolecular and monomer species at 1590 and 1680 cm^{-1} grow nearly concurrently when $Mo(CO)_6$ is adsorbed in small quantities at very mild conditions such as 1 h at 25°C under vacuum. Moreover, a band is not observed for a bridging carbonyl group which is not coordinated to a Lewis acid site.

Brown[29] supported the other model proposed by Kazusaka and Howe[10] in which a carbonyl group of a monomer species is coordinated to a Lewis acid site. The coordination of a CO to Al^{3+} would lower its stretching frequency and would increase the frequencies of the other two carbonyl groups. Also, the presence of two types of Lewis acid sites has been demonstrated for the γ-alumina surface which would account for the two low frequencies observed at 1680 and 1590 cm^{-1}. Brown pointed out that this model would further be supported by the ND_3 adsorption experiments of Kazusaka and Howe[10] in which the bands at 2000 and 1900 cm^{-1} shifted to 1900 cm^{-1} and a pair of bands at 1780 and 1760 cm^{-1} and the bands at 1680 and 1590 cm^{-1} disappeared. In this case the ND_3 displaced the CO coordinated to the Lewis acid sites and resulted in values of IR stretches more closely resembling those expected for $Mo(CO)_3L_3$. The splitting of the

lower frequency E mode band in the isolated $Mo(CO)_3$ fragment was suggested by Brown to be a manifestation of the lowered symmetry due to ND_3 adsorption at nearby Lewis acid sites or merely surface heterogenity.

However, Brown discussed a few shortcomings associated with this structure. First of all, the CO-Lewis acid adduct seemed to have a relatively higher stretching frequency than would be expected. Secondly, the formation of such a structure on a flat crystal plane would be unfavorable due to geometric constraints but Brown pointed out that this would not be a problem at steps or other surface irregularities. Nevertheless, Brown noted a precedence for the sideways interaction of a CO ligand with a Lewis acid center in the complex, $(\eta^5\text{-}C_5H_5)_3Nb_3(CO)_3$, which has a low frequency stretch.[30,31]

Results of the above studies have shown that molybdenum subcarbonyl species are formed on the γ-alumina surface. On the basis of stoichiometric measurements of carbon monoxide evolution and IR spectroscopy, several discreet species have been identified.[3-11] These include $Mo(CO)_5$(ads), $Mo(CO)_4$(ads) and $Mo(CO)_3$(ads) of which $Mo(CO)_3$(ads) is the most stable and is nearly quantitatively formed at 100°C in flowing helium.[9] The species are coordinated to either surface OH^- or O^{2-} depending on the degree of surface hydroxylation.[5,7-11,29]

1B INTENT OF THESIS

The fact that molybdenum hexacarbonyl forms discreet subcarbonyls which are bonded to surface OH^- and O^{2-} groups on γ-alumina provides an opportunity to: a) synthesize the subcarbonyls via ligand substitution reactions using molybdenum carbonyl complexes and b) characterize the subcarbonyls on the surface by solid state cross polarization-magic angle spinning (CP-MAS) ^{13}C NMR in a manner analogous to studies of solid samples of metal carbonyl complexes.

In this dissertation, the results of the ligand displacement reactions of $Mo(CO)_3(CH_3CN)_3$ and $Mo(CO)_3(\eta^6\text{-}C_6H_6)$ with the γ-alumina surface are compared directly with the results obtained for

the $Mo(CO)_6/\gamma\text{-}Al_2O_3$ system on the basis of reaction stoichiometry, IR spectroscopy, and propylene metathesis activity as determined in this work and the aforementioned studies.[3-13]

Also, the solid state CP-MAS ^{13}C NMR results for the molybdenum subcarbonyls on the γ-alumina surface are presented and interpreted by comparison with studies performed on metal carbonyl complexes in solution[32-36] and the solid state[37-47] as well as the model compounds investigated in this work: $Mo(CO)_3(CH_3CN)_3$, $Mo(CO)_3(\eta^6\text{-}C_6H_6)$, $Mo(CO)_3(\eta^6\text{-}C_6H_5CH_3)$, $Cr(CO)_3(\eta^6\text{-}C_6H_5CH_3)$ and $Mo(CO)_3$(diglyme). Furthermore, the dynamic natures of $Mo(CO)_3$(ads) and $Mo(CO)_5$(ads) are demonstrated by CP-MAS ^{13}C NMR and the results are interpreted by comparision with the intramolecular motions determined in solid organic compounds,[40,41,49-55] metal carbonyl complexes, both in solution[34-36] and in the solid state,[37-42,44-47,50] and the above model compounds. The dynamics of these compounds are characterized by variable temperature CP-MAS ^{13}C NMR.[48,49]

Acetone was used as the solvent for the reaction of $Mo(CO)_3(CH_3CN)_3$ with the surface of γ-alumina and its interaction with the surface was studied independently. This was necessary because acetone is highly reactive with the surface of γ-alumina[56-59] and appears to interfere with the adsorption of metal carbonyl complexes. These results are presented in Chapter 7.

CHAPTER 2
EXPERIMENTAL

The alumina used was CATAPAL SB obtained from Conoco Chemicals (surface area 200 m^2/g, 200-300 mesh) and was calcined at 400°C in flowing oxygen prior to use. This alumina is actually a pseudoboehmite which has a pseudoamorphous structure midway between amorphous and truly crystalline boehmite.[60] It has been demonstrated that poorly crystallized boehmite can be converted to γ-alumina at temperatures approaching 350°C but that a temperature of 450°C is needed to convert crystalline boehmite to γ-alumina.[61] Therefore, all of the pretreatment procedures for the pseudoboehmite involve heating at 450°C before further use and, henceforth, the alumina used in all the experiments in this dissertation will be referred to as γ-alumina.

All experiments were performed using an ultra-pure helium flow reactor system[7] shown in Figure 2. In a typical experiment, 0.25 to 0.80 g alumina was placed in the reactor and supported by a plug of quartz wool. The alumina was heated at 450°C for 1 h in flowing helium to yield partially dehydroxylated γ-alumina (PDA).[7] The reactor was cooled to room temperature under helium flow and a solution containing the desired metal carbonyl complex was injected and slurried with the γ-alumina in flowing helium. The solvent was evaporated at room temperature and trapped at -196°C. The reactor was then heated to activate the material at the desired temperature. Carbon monoxide evolution was measured by the method described by Burwell and Brenner.[7]

Metathesis activities were measured by passing standard pulses of propylene in helium through the fluidized material in the reactor at the desired temperature. The products were detected by G. C. as described by Burwell and Brenner.[7]

All IR and NMR samples were prepared using the helium flow system which allowed for direct measurements of carbon monoxide evolution. The reactor containing the material for subsequent sample preparation was sealed under helium and taken into a Vacuum Atmospheres drybox to avoid exposure to air.

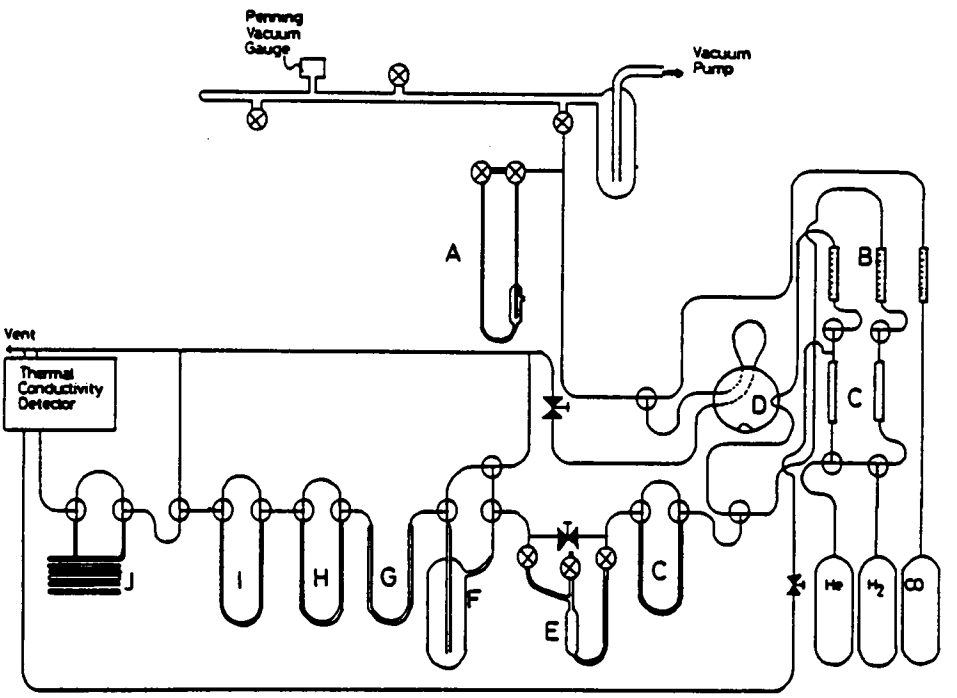

A	manometer	H	5A molecular sieve
B	flowmeter	I	CuO
C	MnO on silica	J	column
D	sample valve	⊗	high vacuum stopcock
E	fused silica reactor	⊕	Whitey 3-way ball valve
F	trap		Nupro bellows valve
G	silica trap		

Figure 2. Helium Flow Reactor System

CHAPTER 3
SYNTHETIC ROUTES TO γ-ALUMINA SUPPORTED MOLYBDENUM SUBCARBONYLS

3A GENERAL

The previous studies discussed in Chapter 1[3-11] have demonstrated that molybdenum hexacarbonyl undergoes a reaction with the γ-alumina surface resulting in the loss of up to three carbonyl ligands per complex at 100°C in flowing helium.[6] The three carbonyl ligands were suggested to be displaced by either surface OH^- or O^{2-} depending on the degree of surface dehydroxylation.[5,7-11,29] Also, the species, $Mo(CO)_3$(ads), has been postulated to be a catalytically active species for the metathesis of olefins.[7,13]

In solution, molybdenum tricarbonyl complexes are typically synthesized from $Mo(CO)_6$ and excess ligand where the substitution process is observed to abruptly halt at the tricarbonyl stage due to its intrinsic stability. Furthermore, ligand displacement reactions between molybdenum tricarbonyl complexes and various other ligands have been well documented.[62] These factors suggest that $Mo(CO)_3$(ads) could be generated on the γ-alumina surface via the substitution of surface OH^- or O^{2-} in place of an appropriate leaving group coordinated to the tricarbonyl complex.

In this chapter, the materials synthesized from the reactions of $Mo(CO)_3(CH_3CN)_3$ and $Mo(CO)_3(\eta^6\text{-}C_6H_6)$ with partially dehydroxylated γ-alumina (PDA) are compared with conventionally prepared $Mo(CO)_3$(ads) (from $Mo(CO)_6$) on the basis of reaction stoichiometry, FTIR spectroscopy and catalytic activity for the metathesis of propylene. These results will also appear in a forthcoming publication.[63]

3B EXPERIMENTAL

$Mo(CO)_3(CH_3CN)_3$ was synthesized by refluxing $Mo(CO)_6$ in acetonitrile. It was characterized by IR bands at 1915 and 1783 cm^{-1} (Nujol mull)[67] and satisfactory elemental analysis.

$Mo(CO)_3(\eta^6\text{-}C_6H_6)$ was prepared from $Mo(CO)_3(\eta^6\text{-}C_6H_5CH_3)$ by refluxing the toluene complex in benzene. The toluene complex was prepared by refluxing $Mo(CO)_6$ in toluene. The compound was characterized by infrared bands at 1984 and 1916 cm^{-1} (pentane solvent) which

corresponded well with literature values.[68] Also, the UV spectrum of the benzene complex in pentane yielded and adsorption at 322 nm which is near the literature value of 323 nm.[69]

The pentane and benzene solvents were freshly distilled over NaK/benzophenone prior to use. Acetone was dried over 4A molsieves and degassed by three freeze-pump-thaw cycles.

The complexes and impregnating solutions were manipulated under an inert atmosphere. The concentration of $Mo(CO)_3(\eta^6\text{-}C_6H_6)$ in pentane was determined by UV spectroscopy.[69]

Carbon monoxide evolution was measured by trapping the evolved CO on a silica gel trap (Figure 2) at -196°C during activation.[7] The CO was then desorbed by removing the liquid nitrogen dewar from the trap and allowing it to warm up to room temperature. A 0.25″ × 6′ glass column packed with 40-60 mesh 5A molecular sieve was used to separate CO from any oxygen or nitrogen which may have been coadsorbed on the silica gel trap. The CO was quantified using a Gow Mac thermal conductivity detector (model 40-200) and a Gow Mac recorder equipped with an integrator (model 70-750). Standard pulses of CO were used to calibrate the T. C. detector for each experiment.

Any $Mo(CO)_6$ or benzene evolved from the reactor during the adsorption experiments was trapped in the solvent trap (Figure 2) along with the impregnation solvent and quantified by UV spectroscopy. A Perkin-Elmer 330 UV-Visible spectrometer was used. The observed detection limit for $Mo(CO)_6$ was 16 μg which corresponds to an absorbance value which is twice the noise level. This value represents an amount which is less than 0.1% of the amount of $Mo(CO)_6$ used to impregnate 0.5 g of γ-alumina in a typical experiment.

For measuring catalytic activities, catalysts were prepared using 0.25 g of the alumina. The activities were measured by passing ~0.2 mL (STP) pulses of propylene in helium through the fluidized catalyst contained in the reactor at a flow rate of 60 mL/min.[5] The reactor was immersed in a silicon oil bath which was heated to the desired temperature. The products were trapped on the silica gel trap (Figure 2) at -196°C for 5 min. The liquid nitrogen dewar was then quickly replaced with a dewar containing hot water in order to quickly desorb the products into the G. C.

column. The products were separated on a 0.25″ × 1′ glass column packed with 25% bis[2-(2-methoxyethoxy)ethyl] ether (Eastman Kodak) supported on 60-80 mesh Gas Chrom RA (Applied Science Div., Milton Roy Lab Group) and detected and integrated with the T. C. detector and recorder.

The percent conversion of a pulse of propylene was calculated from the integrated areas of the ethylene and propylene peaks under the assumption that equimolar amounts of ethylene and 2-butene were formed as described by Brenner[5] and is expressed as:

$$\%\text{conversion} = 200(C_2)/[2(C_2) + C_3]$$

where C_2 and C_3 are the integrated areas of ethylene and propylene, respectively. This is reasonable since ethylene and 2-butene have been reported to represent at least 99.5 % of the products of propylene metathesis.[5,7,13] The contact time of a propylene pulse was calculated using the method described by Brenner.[5] This method assumes that the spreading of a gas pulse is proportional to the volume traversed and inversely proportional to pressure. Thus, by knowing the volume through which a gas pulse travels and the pressure, the width (W) of the pulse can be calculated at any point, i.e. $W = W_0(V_b/V_c)(P_s/P_r)$. The between the gas sample loop and the catalyst bed (V_b) and the volume between the sample loop and the T. C. detector (V_c) were calculated to be 20.46 and 40.68 cm^3, respectively. The pressure in the reactor was measured to be 962 torr at reaction conditions by the use of a manometer connected to its top. Atmospheric pressure was typically 707 torr. The width at half height (W_0) of a propylene pulse at the T. C. detector was measured to be 14.1 s after bypassing the reactor and G. C. column (with a hot water dewar in place on the silica gel trap). Bypassing the G. C. column and sending the pulse through the reactor (with the hot water dewar on the silica gel trap) resulted in a propylene pulse width of 15.6 s. Therefore, the width of a propylene pulse at the front of the catalyst bed under reaction conditions would be: (14.1 s)(V_b /V_c)(707 torr/962 torr) = 5.2 s. Similarly, the width of a pulse at the exit of the catalyst bed would be: (15.6 s)(V_b/V_c)(707 torr/962 torr) = 5.8 s. Thus, the average contact time of a propylene pulse with the catalyst bed is given by: (5.2 s + 5.8 s)/2 = 5.5 s. This value was found to be a rea-

sonable estimate as a result of putting the T. C. detector in place of the reactor and measuring the width of a propylene pulse directly. This resulted in a measured width of 4.5 s which was expected to be slightly less since the T. C. detector had a smaller volume than the reactor. The contact time of 5.5 s was used along with the Mo weight % of the catalysts to calculate the turnover numbers for the conversions of propylene on a per molybdenum per second basis.

Poisoning experiments were performed on active catalysts generated from $Mo(CO)_6$. Initially, a pulse of propylene was passed through the fresh catalyst to demonstrate its activity. Then the catalyst was cooled to room temperature, at which point 1 mL of dry, degassed acetonitrile, acetone or benzene was injected into the reactor. This amount was sufficient to completely wet the catalyst. The solvent was evaporated at room temperature in flowing helium and then the catalyst was activated at 100°C for 0.5 h in flowing helium. The catalytic activity was then again measured by a second propylene pulse.

3C RESULTS FOR $Mo(CO)_3(CH_3CN)_3$

The adsorption of $Mo(CO)_6$ onto γ-alumina can be performed either by the direct sublimation of the volatile carbonyl or via adsorption from an alkane solution of the complex. Alkanes do not react with γ-alumina at temperatures below 100°C and can be completely removed from the support after adsorption[64] which makes them the preferred solvents for metal carbonyl adsorptions.

However, $Mo(CO)_3(CH_3CN)_3$ is insoluble in alkane solvents and does not sublime without substantial decomposition and, thus, the selection of an appropriate solvent for the adsorption experiments is necessary. $Mo(CO)_3(CH_3CN)_3$ is soluble in acetonitrile, diethylether and acetone which allow stable solutions to be formed for use in adsorption experiments. Methylene chloride solutions of $Mo(CO)_3(CH_3CN)_3$ decompose rapidly which renders the solvent unusable for the complex. Methylene chloride has also been observed to react with γ-alumina to produce CO, H_2 and light hydrocarbons.[64]

Attempts at adsorbing $Mo(CO)_3(CH_3CN)_3$ onto PDA using acetonitrile result in very little, if any, adsorption. Evidence for this is given by the persistent yellow color of the solution while in

contact with the PDA. Diethylether solutions are rapidly decolorized by the PDA which attains a yellow appearance indicating an adsorbed molybdenum complex. However, it was found that physisorbed diethylether decomposes to ethylene at 100°C which would have interfered with subsequent metathesis activity measurements. Acetone solutions of $Mo(CO)_3(CH_3CN)_3$ are also quantitatively decolorized by the PDA and blank runs using pure acetone indicate no CO or light olefin formation up to 150°C. However, acetone does chemisorb on the surface of γ-alumina and may compete with the metal carbonyl for adsorption sites. The interaction of acetone with the PDA surface was studied independently[65] and the results are discussed in Chapter 7.

The evolution of carbon monoxide from $Mo(CO)_3(CH_3CN)_3$ supported on PDA via adsorption from acetone solution was quantitatively measured as a function of temperature and the results are shown in Table 2. The evolution of CO is observed to be independent of the level of loading in the range of 0.3 to 2.1 weight percent molybdenum. A reaction period of 2 h was sufficient to quantify the amount of CO evolved and longer times did not show further substantial loss of carbon monoxide. Heating samples to a temperature of 350°C was found to effect the complete evolution of all CO from the surface complexes. The results do not precisely define average stoichiometries for the surface complexes as previously observed for molybdenum subcarbonyl species derived from $Mo(CO)_6$,[5,6] but they do allow the following observations to be made. (i) The adsorption process at 25°C is accompanied by a small but measurable loss of CO. (ii) CO loss increases with temperature until at 150°C, approximately 1 CO/Mo are lost and at 200°C, approximately 2 CO/Mo are lost.

When activated at 25°C, the supported complex from $Mo(CO)_3(CH_3CN)_3$ gives the PDA a yellow-brown color similar to $Mo(CO)_3$(ads) generated from $Mo(CO)_6$ at 100°C.[7,9,15,66] The infrared spectrum of the material after activation at 25°C is shown in Figure 3. The upper spectrum resulted from a Nujol mull of a sample activated for 3 h at 25°C in flowing helium and the lower spectrum shows the Nujol mull spectrum of a sample which was activated for 2 h at 100°C in flowing helium. In the upper spectrum, two peaks are present in the metal carbonyl region at 1907

Table 2

Carbon Monoxide Evolution During Adsorption of $Mo(CO)_3(CH_3CN)_3$ on PDA

Activation Temperature	Solvent	CO/Mo(ads)	Number of Runs
25°C	Acetone	0.2 ± 0.1	5
100°C	"	0.7 ± 0.2	5
150°C	"	1.1 ± 0.1	5
200°C	"	1.9 ± 0.1	5
350°C	"	3.0 ± 0.1	2

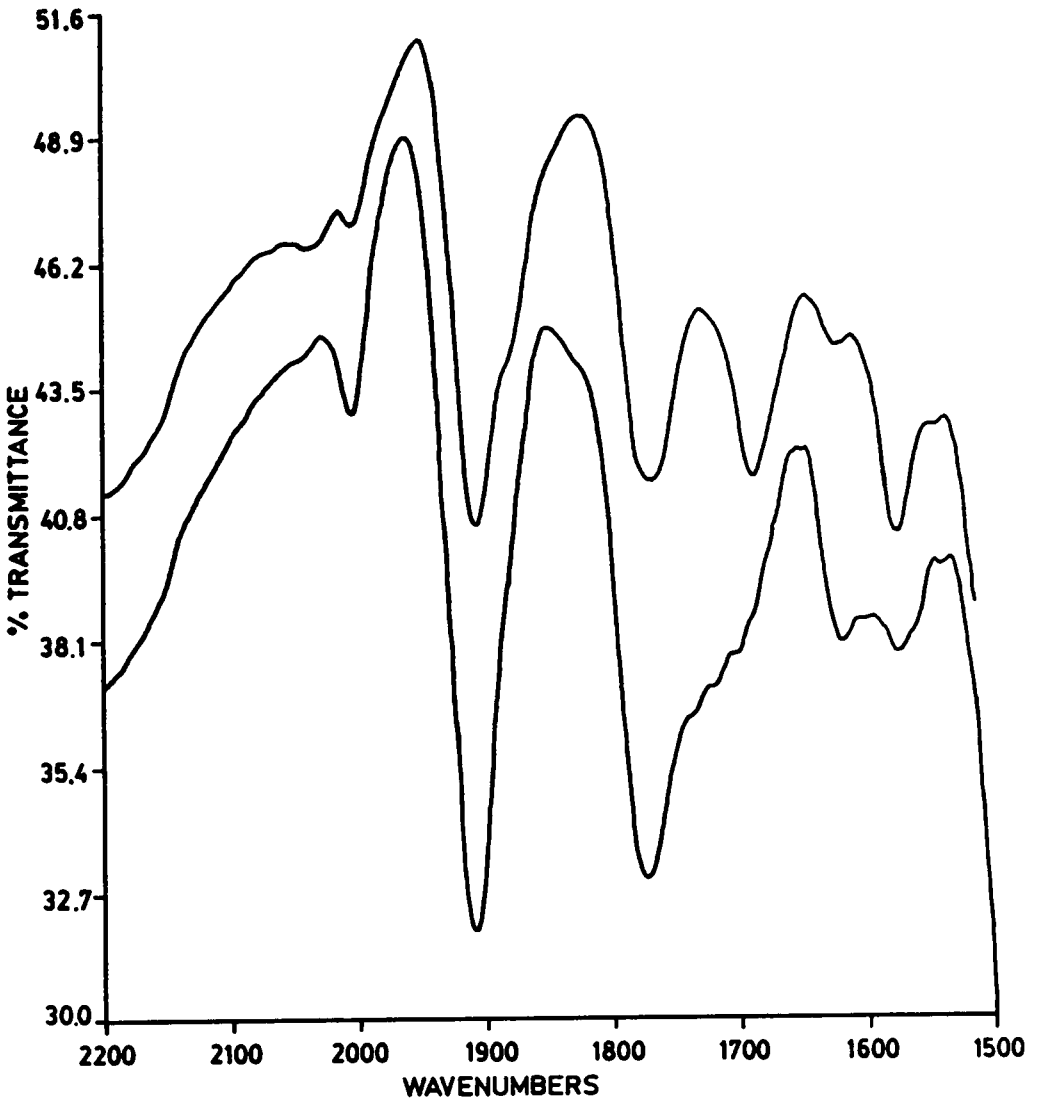

Figure 3. $Mo(CO)_3(CH_3CN)_3$ Adsorbed on PDA

and 1770 cm^{-1} which are shifted by about 10 cm^{-1} to lower wavenumber from the parent complex (Table 1, Chapter 1). The infrared bands below 1700 cm^{-1} are assigned to reaction products of acetone with γ-alumina[65] as discussed in Chapter 7. The infrared results are summarized in Table 3.

Unlike $Mo(CO)_3$(ads) generated from $Mo(CO)_6$, the surface species generated from $Mo(CO)_3(CH_3CN)_3$ was inactive for olefin metathesis.

3D RESULTS FOR $Mo(CO)_3(\eta^6\text{-}C_6H_6)$

The benzene complex, $Mo(CO)_3(\eta^6\text{-}C_6H_6)$, is soluble in benzene and pentane as is typically observed for arene derivatives of molybdenum carbonyl and both solvents were employed for the adsorption of $Mo(CO)_3(\eta^6\text{-}C_6H_6)$ onto PDA. The benzene complex is only slightly soluble in pentane and loadings of up to about 0.4% Mo could be achieved using this solvent. Higher loadings were attained using benzene as the solvent. PDA rapidly decolorized both yellow pentane and benzene solutions of $Mo(CO)_3(\eta^6\text{-}C_6H_6)$. IR spectroscopy, CO evolution and catalytic activity measurements were performed on the supported molybdenum carbonyls generated from both solvents to aid in determining the nature of the supported complex.

The results from the CO evolution measurements are shown in Table 4. All adsorptions from solution were carried out at 25°C followed by activation at either 25 or 100°C. The data in Table 4 shows that $Mo(CO)_3(\eta^6\text{-}C_6H_6)$ is more efficiently adsorbed from benzene than from pentane. This is evidenced by the formation of $Mo(CO)_6$ from the decomposition of the benzene complex when pentane was used as the solvent. The CO evolved when the adsorption was performed from pentane solution was probably due to the adsorption of the in situ-generated $Mo(CO)_6$ onto the PDA which was not completely removed from the reactor by sublimation in flowing helium. When the adsorption was carried out from benzene solution, no evolved $Mo(CO)_6$ could be detected by UV spectroscopy and virtually no CO was evolved at 25°C. At 100°C, where $Mo(CO)_3$(ads) should be stable, the adsorbed carbonyl complex generated from $Mo(CO)_3(\eta^6\text{-}C_6H_6)$ lost CO very slowly which is consistent with the formation of the supported tricarbonyl.

Table 3

Carbonyl Stretching Frequencies for Molybdenum Subcarbonyls Adsorbed on PDA

Source	Activation Temperature	Proposed Structure	$\nu CO^{a,b}$ cm^{-1}	ref.
$Mo(CO)_6$ (sublimed)	100°C, 1h	$Mo(CO)_3$(ads) PDA wafer	2030(w),1994 1885(br),1685,1584	11
$Mo(CO)_6$ (sublimed)	100°C, 1h	$Mo(CO)_3$(ads) PDA wafer	2040(w),2000 1900(br),1680,1590	10
$Mo(CO)_6$ (pentane solution)	100°C, 3h	$Mo(CO)_3$(ads) PDA powder (Nujol mull)	2020(w),1970,1929 1860(br),1750(sh) 1570(sh)	This work
$Mo(CO)_3(CH_3CN)_3$ (acetone solution)	25°C, 3h	$Mo(CO)_3(CH_3CN)$ PDA powder (Nujol mull)	2005(w),1907,1770 (1690),(1625(w)) (1577)	"
	100°C, 2h	"	2004(w),1908,1773 (~1700(sh)),(1618(w)) (1574(w))	"
	150°C, 2h	"	2006(w),1910,1778 (1570)	"
	200°C, 2h	"	2012,1917,1786 1739(w),(1565)	"
$Mo(CO)_6 + ND_3$	25°C	$Mo(CO)_3(ND_3)$ PDA wafer	1900,1780(br) 1760(sh),1590(w)	10
$Mo(CO)_3(\eta^6\text{-}C_6H_6)$ (pentane solution)	25°C, 2.5h	$Mo(CO)_3$(ads) PDA powder (Nujol mull)	1981,1928,1861(br) 1738(w),~1580(sh)	This work
	100°C, 2h	"	2020(w),1972,1929 1858(br),1750(sh) ~1570(sh)	"
$Mo(CO)_3(\eta^6\text{-}C_6H_6)$ (benzene solution)	25°C, 2h	"	1983,1925,1851(br) 1738	"
	100°C, 1h	"	1970,1933,1860(br) 1741(w),~1570(sh)	"

[a] (w) = weak, (br) = broad, (sh) = shoulder

[b] Peaks in parentheses are assigned to adsorbed acetone and its reaction products on PDA (Chapter 7).

Table 4

Carbon Monoxide Evolution During Adsorption of $Mo(CO)_3(\eta^6\text{-}C_6H_6)$ on PDA

Activation Temperature	Solvent	CO/Mo(ads)	benzene/Mo(ads)	$Mo(CO)_6$/Mo(ads)[a]	Number of Runs
25°C	pentane	0.21 ± 0.1	0.41 ± 0.1	0.0013 ± 0.001	5
25°C	benzene	0.04 ± 0.03		N.D.[b]	9
100°C, 2h	benzene	0.074 ± 0.08			9
100°C, 7h	benzene	0.56			1
150°C, 1h	benzene	0.45			1

[a] quantified by UV spectroscopy
[b] not detected by UV spectroscopy

The infrared spectra for the supported carbonyls generated from $Mo(CO)_3(\eta^6\text{-}C_6H_6)$ and $Mo(CO)_6$ are remarkably similar. These were obtained from Nujol mulls and are shown in Figure 4. The upper spectrum was obtained by adsorbing $Mo(CO)_3(\eta^6\text{-}C_6H_6)$ onto PDA from pentane solution followed by activation for 2 h at 100°C in flowing helium. This material proved to be active for propylene metathesis. The lower spectrum shows $Mo(CO)_6$ adsorbed on PDA from pentane solution after activation for 3 h at 100°C in flowing helium. This material was also active for propylene metathesis. The peak values are given in Table 3. Two major peaks are observed at 1970 and 1860 cm^{-1} in both spectra. These are similar to those reported by Burwell, et al.[11,14,15] and Howe[4,10] but they are shifted slightly to lower wavenumber. The spectra shown in Figure 4 were obtained from samples in Nujol mulls and not from in situ pressed pellets as Burwell[11] and Howe[10] reported. The bands below 1600 cm^{-1} have been attributed by previous researchers to carbonyl ligands involved in various modes of interaction with neighboring sites on the PDA surface as discussed in Chapter 1. The nature of the species responsible for these bands will not be discussed in this chapter but it should be noted here that the bands at 1655 and 1556 cm^{-1} shown in Figure 4 were present on the PDA itself.

The supported $Mo(CO)_3(\eta^6\text{-}C_6H_6)$ complexes generated either from pentane or benzene solutions show similar activity for the metathesis of propylene at a temperature of about 50°C as observed for supported complexes generated from $Mo(CO)_6$.

3E PROPYLENE METATHESIS ACTIVITY

The activities of the supported molybdenum carbonyls for propylene metathesis are shown in Table 5. The activities are listed as the percent conversion of propylene in the first pulse which represents the activities of the fresh catalysts. Also shown are the turnovers per pulse. For comparision, the data of Brenner is shown which was obtained under similar conditions.[5]

Active catalysts were synthesized from both $Mo(CO)_6$ and $Mo(CO)_3(\eta^6\text{-}C_6H_6)$ and the activities of the catalysts on a per molybdenum basis are very similar. However, catalysts generated from $Mo(CO)_3(CH_3CN)_3$ were inactive for metathesis. Poisoning experiments performed on active

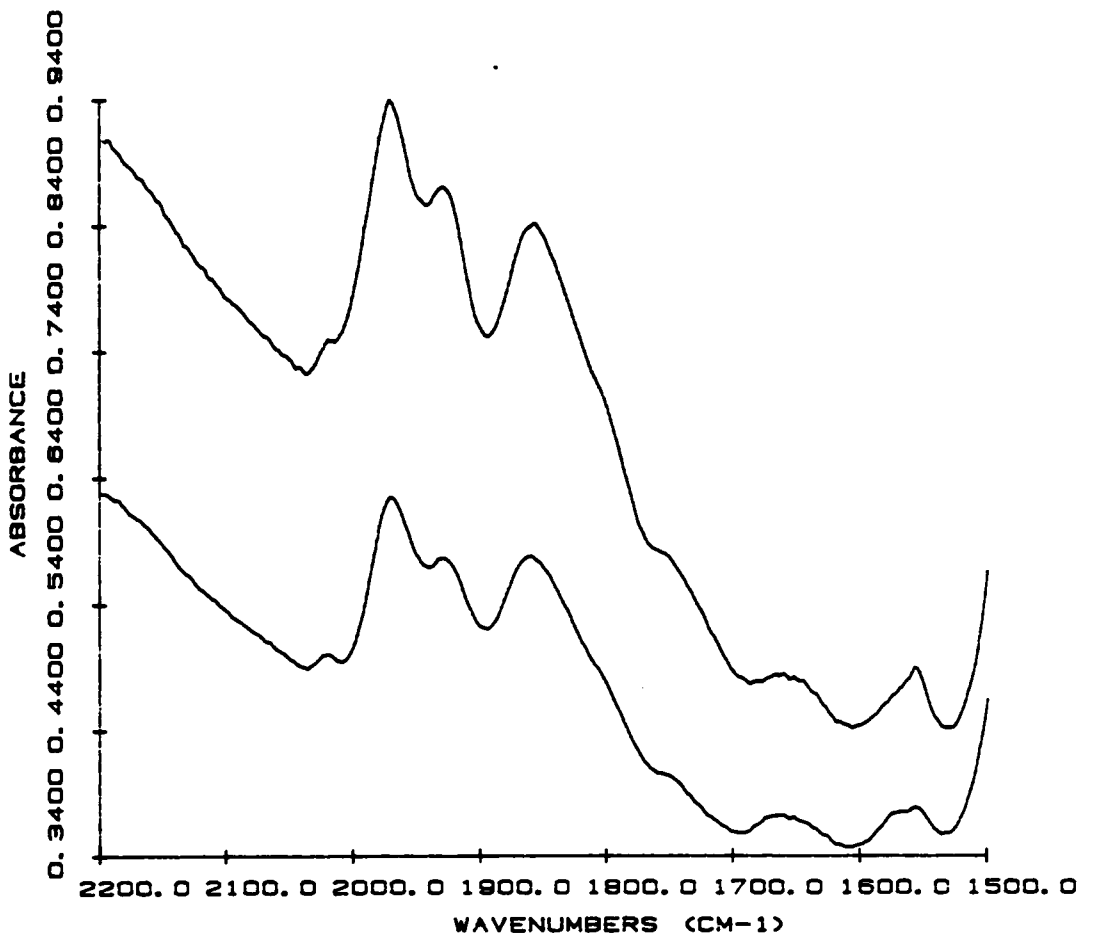

Figure 4. $Mo(CO)_3(\eta^6\text{-}C_6H_6)$ and $Mo(CO)_6$ Adsorbed on PDA

Table 5

Activity for Propylene Metathesis for Various Catalysts

Catalyst Precursor	Activation Temperature	Wt% Mo	Activity[a](%)	Turnover[b](s^{-1})
$Mo(CO)_6$/pentane	100°C	0.92	8.9 @ 54°C	0.0056
above + acetone	100°C	"	not active	
$Mo(CO)_6$/pentane	100°C	1.3	7.6 @ 54°C	0.0033
above + benzene	100°C	"	8.6 @ 53°C	0.0038
$Mo(CO)_6$/acetone	100°C	1.1	not active @ 100°C	
$Mo(CO)_3(CH_3CN)_3$/acetone	100°C	0.54	not active @ 100°C	
$Mo(CO)_3(\eta^6\text{-}C_6H_6)$/pentane	100°C	0.79	10.7 @ 55°C	0.0079
$Mo(CO)_3(\eta^6\text{-}C_6H_6)$/benzene	100°C	0.76	9.7 @ 52°C	0.0074
$Mo(CO)_6$/pentane[c]	100°C	0.56	0.8 @ 53°C	0.013[d]

[a] Activities are reported as percent conversion of propylene for the first pulse.
[b] Turnovers are reported as moles propylene consumed per mole molybdenum per second. The contact time of a propylene pulse in the reactor used in this work was measured to be 5.5 s.
[c] Reference 5
[d] Reported for a contact time of 1.6 s.

metathesis catalysts generated from $Mo(CO)_6$ showed that both acetonitrile and acetone were poisons for the catalysts whereas benzene had no effect on the catalytic activities. Thus, materials synthesized from either acetonitrile or acetone solvents or from carbonyl complexes containing nitrile ligands would be inactive for metathesis.

3F DISCUSSION

The attempted reactions for generating $Mo(CO)_3$(ads) on PDA are shown in equations 3.1 and 3.2. There is a great deal of precedent for these reactions in the organometallic literature but the results presented in this chapter indicate that acetonitrile is not an appropriate leaving group when using PDA surface OH^- and O^{2-} groups as potential ligands.

$$Mo(CO)_3(CH_3CN)_3 + \gamma\text{-}Al_2O_3 \rightarrow Mo(CO)_3(ads) + 3\ CH_3CN \qquad 3.1$$

$$Mo(CO)_3(\eta^6\text{-}C_6H_6) + \gamma\text{-}Al_2O_3 \rightarrow Mo(CO)_3(ads) + C_6H_6 \qquad 3.2$$

When the reaction represented by equation 3.2 was performed in pentane, some decomposition of $Mo(CO)_3(\eta^6\text{-}C_6H_6)$ to yield $Mo(CO)_6$ was observed. Also, 0.25 equivalents of CO per adsorbed Mo were evolved at 25°C. Carbon monoxide evolution is not predicted by equation 3.2 and was most likely due to the direct adsorption of $Mo(CO)_6$ which was generated in situ. A similar quantity of CO was observed during the adsorption of $Mo(CO)_3(CH_3CN)_3$ from acetone (equation 3.1) at 25°C. Although $Mo(CO)_6$ was not observed in this case, a pathway involving the formation of $Mo(CO)_6$ cannot be ruled out. As will be discussed below, IR spectroscopy suggests that only two acetonitrile ligands were lost from each tris-acetonitrile complex after adsorption onto PDA at 25°C. Also, addition of CH_3CN to $Mo(CO)_3$(ads) generated from $Mo(CO)_6$ resulted in a suface species that had an infrared spectrum similar to $Mo(CO)_3(CH_3CN)_3$ adsorbed on PDA.

The reaction stoichiometry predicted by equation 3.2 was most closely approximated when $Mo(CO)_3(\eta^6\text{-}C_6H_6)$ was adsorbed from benzene. Benzene loss could not be easily quantitated in this case but the combination of observations: (i) virtually no CO loss at 25°C, (ii) no $Mo(CO)_6$ formation and (iii) complete extraction of $Mo(CO)_3(\eta^6\text{-}C_6H_6)$ from solution, suggest that equation 3.2 is a reasonable representation of the adsorption process. Furthermore, at 100°C in flowing he-

lium, the adsorbed complex lost CO very slowly. These are the conditions at which $Mo(CO)_3$(ads) would be expected to be stable. Under the same conditions, the adsorbed carbonyl generated from $Mo(CO)_3(CH_3CN)_3$ lost CO much more rapidly. Finally, the IR spectrum of $Mo(CO)_3(\eta^6\text{-}C_6H_6)$ adsorbed on PDA at 25°C is nearly indistinguishable from the spectrum obtained for $Mo(CO)_6$ adsorbed on PDA after activation at 100°C. Therefore, the results suggest that equation 3.2 is a viable pathway to $Mo(CO)_3$(ads) under ambient conditions.

Two principal CO stretches were observed for $Mo(CO)_3$(ads) on PDA by Laniecki and Burwell[11] at 1994 and 1885 cm^{-1}. Also, a band at 1584 cm^{-1} was assigned to the interaction of a terminal carbonyl with a surface OH^- group via the carbonyl carbon. Kazusaka and Howe[10] reported values of 2000 and 1900 cm^{-1} in the terminal carbonyl region and observed that adsorption of ammonia-d_3 caused the peaks to shift to 1900 and 1780 cm^{-1}. They suggested that the shifts were caused by ND_3 coordination to the surface complex to form $Mo(CO)_3(ND_3)$(ads). After partial removal of the adsorbed ND_3, Kazusaka and Howe noted a further 20 cm^{-1} shift which they attributed to a solvent effect. In the case of $Mo(CO)_3(CH_3CN)_3$ adsorbed on PDA, the presence of two carbonyl stretches is consistent with formation of a tricarbonyl complex being formed on the surface. However, the supported complex appears to have retained a coordinated acetonitrile ligand as suggested by the similarity of the IR bands at 1907 and 1770 cm^{-1} with those reported for $Mo(CO)_3(ND_3)$(ads).[10] After heating, excess acetonitrile and acetone solvent were removed from the surface and the bands shifted to 1917 and 1786 cm^{-1} which may have been due to a solvent effect. This assignment is supported by a catalyst poisoning experiment in which $Mo(CO)_3$(ads) generated from $Mo(CO)_6$ was reacted with acetonitrile at 25°C and activated at 100°C. The IR spectrum of the resulting material had two CO stretches at 1908 and 1772 cm^{-1} and a small peak at 2020 cm^{-1} which is in good agreement with the spectrum obtained by the direct adsorption of $Mo(CO)_3(CH_3CN)_3$ onto PDA from acetone solution. Furthermore, reacting the active $Mo(CO)_3$(ads) catalyst (from $Mo(CO)_6$) with acetonitrile poisoned the catalyst for propylene metathesis. When $Mo(CO)_3$(ads) (from $Mo(CO)_6$) was reacted with acetone at 25°C and activated

at 100°C, two major peaks at 1906 and 1768 cm^{-1} and a small peak at 2002 cm^{-1} were observed in the IR spectrum of the material which was also poisoned for metathesis. When $Mo(CO)_6$ was reacted with PDA from an acetone solution and activated at 100°C, two major peaks were present in the IR spectrum of the material at 1905 and 1771 cm^{-1} and a smaller peak at 2036 cm^{-1} and this material was also inactive for metathesis. Thus, acetone not only prevented the formation of the catalytically active $Mo(CO)_3$(ads) but also poisoned the catalyst as acetonitrile did. It appeared that acetone was able to coordinate to molybdenum to cause the large shifts observed in the IR spectra of the materials as was proposed for acetonitrile. This phenomenon was also observed by ^{13}C NMR for the complex, $Mo(CO)_3$(diglyme), dissolved in acetone-d_6 and will be discussed in Chapter 5. Therefore, the species formed in the reaction of $Mo(CO)_3(CH_3CN)_3$ is postulated to be $Mo(CO)_3(CH_3CN)$(ads) which decomposes at elevated temperatures as evidenced by CO evolution.

The γ-alumina supported molybdenum carbonyls generated from $Mo(CO)_3(\eta^6\text{-}C_6H_6)$ and $Mo(CO)_6$ are indistinquishable based on IR spectroscopy and olefin metathesis activity. Thus, the use of an arene ring as a leaving group was demonstrated as a viable low temperature reaction pathway to supported metal complexes.

CHAPTER 4
DETECTION OF MOLYBDENUM SUBCARBONYLS ON γ-ALUMINA BY CROSS POLARIZATION-MAGIC ANGLE SPINNING ^{13}C NMR

4A EXPERIMENTAL

The alumina was heated at 450°C for 1 h in flowing helium to yield partially dehydroxylated γ-alumina (PDA).[9] Hydroxylated γ-alumina (HA) was generated from PDA by passing helium saturated with water vapor through the alumina while the temperature was raised from 23 to 300°C. The temperature was held at 300°C for 0.5 h and then lowered to 100°C and purged with dry helium for 1 h.[9] Dehydroxylated γ-alumina (DA) was formed by heating at 950°C in flowing helium for 2 h.[9]

^{13}CO enriched $Mo(CO)_6$ was prepared by UV irradiating a stirred solution of the hexacarbonyl in THF along with a small amount of a 10% Pd/charcoal catalyst (Englehard Industries) under a ^{13}CO atmosphere. ^{13}CO was obtained from Isotec, Inc. The enriched $Mo(CO)_6$ was purified by sublimation.

The pentane used for impregnating the γ-alumina with the hexacarbonyl was freshly distilled from NaK/benzophenone prior to use.

The impregnating solution was prepared by dissolving a weighed amount of the enriched $Mo(CO)_6$ in pentane which was then degassed by three freeze-pump-thaw cycles. A measured aliquot of the solution was injected into the reactor containing the activated γ-alumina. The solvent volume injected was designed to contain a slight excess amount of $Mo(CO)_6$ than was necessary to achieve the maximum loading of 2.2% Mo reported by Brenner and Burwell[9] which corresponds to a monolayer coverage. Excess $Mo(CO)_6$, which sublimed off the γ-alumina, was trapped at -196°C and quantified by UV spectroscopy.

Samples were packed in Kel-F bullet type sleeve rotors and sealed with Plasticine (a modeling material manufactured by Colorforms, Ramsey NJ 07446) to prevent decomposition of the samples during data aquisition. A small amount of hexamethylbenzene was packed in the rotors to serve as a chemical shift reference. Samples prepared in this manner showed no deterioration by NMR

over a period of several days and the spectrum of an aged sample yielded the same relative intensities for the observed signals. Samples directly exposed to air bleached in a few minutes.

NMR spectra were recorded on a JEOL FX60QS spectrometer equipped with a solids accessory manufactured by Chemagnetics. The observation frequency for carbon was 15.0 MHz.

4B DISCUSSION

As pointed out in Chapter 1, molybdenum subcarbonyls on γ-alumina have been postulated to be in the form of discreet surface complexes having definite stoichiometries which can be selectively formed under appropriate conditions. Also, the surface ligands have been shown to be either OH^- or O^{2-} depending on the degree of surface hydroxylation. These factors suggest that solid state magic angle spinning (MAS) ^{13}C NMR, which has been widely used to study other metal carbonyl complexes, would be a viable method to characterize the molybdenum subcarbonyl species present on the surface.

However, a problem exists with supported molybdenum subcarbonyls since only loadings of up to about 2.2% Mo have been achieved.[9] In effect, this greatly reduces the number of ^{13}C spins achievable in an NMR sample as compared to the number present in a conventional metal carbonyl complex NMR sample. Enriching the $Mo(CO)_6$ used to make the supported subcarbonyls with ^{13}CO helps to overcome this problem and enrichments up to 45% yield no additional line broadening due to homonuclear dipolar interactions (^{13}C-^{13}C) as evidenced by MAS ^{13}C NMR spectra of the hexacarbonyl.

As in other solid Group VI metal carbonyls, T_1's are very long and was measured to be 480 s[70] for solid $Mo(CO)_6$ at 15 MHz by the progressive saturation technique.[71] This problem can be overcome by using the cross polarization (CP) technique.[48] This is possible since, on a hydroxylated γ-alumina (HA) or partially dehydroxylated γ-alumina (PDA) surface, OH^- groups serve as ligands for the molybdenum subcarbonyls which allows for the necessary ^1H-^{13}C dipolar interactions. Physisorbed $Mo(CO)_6$ would not be observable by CP due to the absence of direct bonds to the surface OH^- groups. However, $Mo(CO)_6$(phys) was detectable by MAS ^{13}C NMR

since T_1 for the complex was greatly reduced to 120 ms as measured by the inversion recovery technique.[71]

The CP-MAS ^{13}C NMR spectra for molybdenum hexacarbonyl supported on PDA are shown in Figure 5. The two large peaks appearing in each spectrum are due to hexamethylbenzene which was used as an internal standard for chemical shift calibration. The sample yielding the bottom spectrum in Figure 5 was activated for 1 h at 30°C in flowing helium and was bright yellow. Only one resonance is observable in the carbonyl region at 203 ppm which is close to the values reported for complexes of the type $Mo(CO)_5L$.[32] This peak is assigned to the species $Mo(CO)_5$(ads), which was proposed by Brenner and Burwell[6] as an intermediate in the formation of $Mo(CO)_3$(ads). The $Mo(CO)_5$(ads) species should possess C_{4v} symmetry,[8] with a surface OH^- group occupying the sixth coordination site of the molybdenum atom. This would yield a ratio of 1:4 for the axial and equatorial ligands, respectively. However, the signal for the axial ligand was not detected and may be obscured due to either an accidental degeneracy of the signals or a dynamic process in which the axial and equatorial CO ligands are rapidly exchanging. Initial low-temperature NMR results showed a slight broadening of the 203 ppm resonance at -40°C, which may be indicative of a dynamic process. The dynamics of the molybdenum subcarbonyls were further investigated in later work and these results will be presented in Chapter 6.

The middle and top spectra in Figure 5 show the CP-MAS ^{13}C NMR spectra obtained from samples activated at 100°C in flowing helium for 1 and 3 h, respectively. These samples were both yellow-brown. In these spectra, a broad peak at 223 ppm appeared and its intensity became greater with respect to the peak at 203 ppm as the activation time was increased. This peak is assigned to $Mo(CO)_3$(ads) as it was proposed by Brenner and Burwell[6] to be the stable molybdenum subcarbonyl species formed at 100°C in flowing helium. Also, the chemical shift of this species is in close agreement with the values reported for (arene)$Mo(CO)_3$ complexes.[32] A single resonance would be expected for a species of C_{3v} symmetry, two for mirror-plane symmetry and three for a tricarbonyl group possessing no symmetry. Due to the nature of the PDA surface,[23] it would be

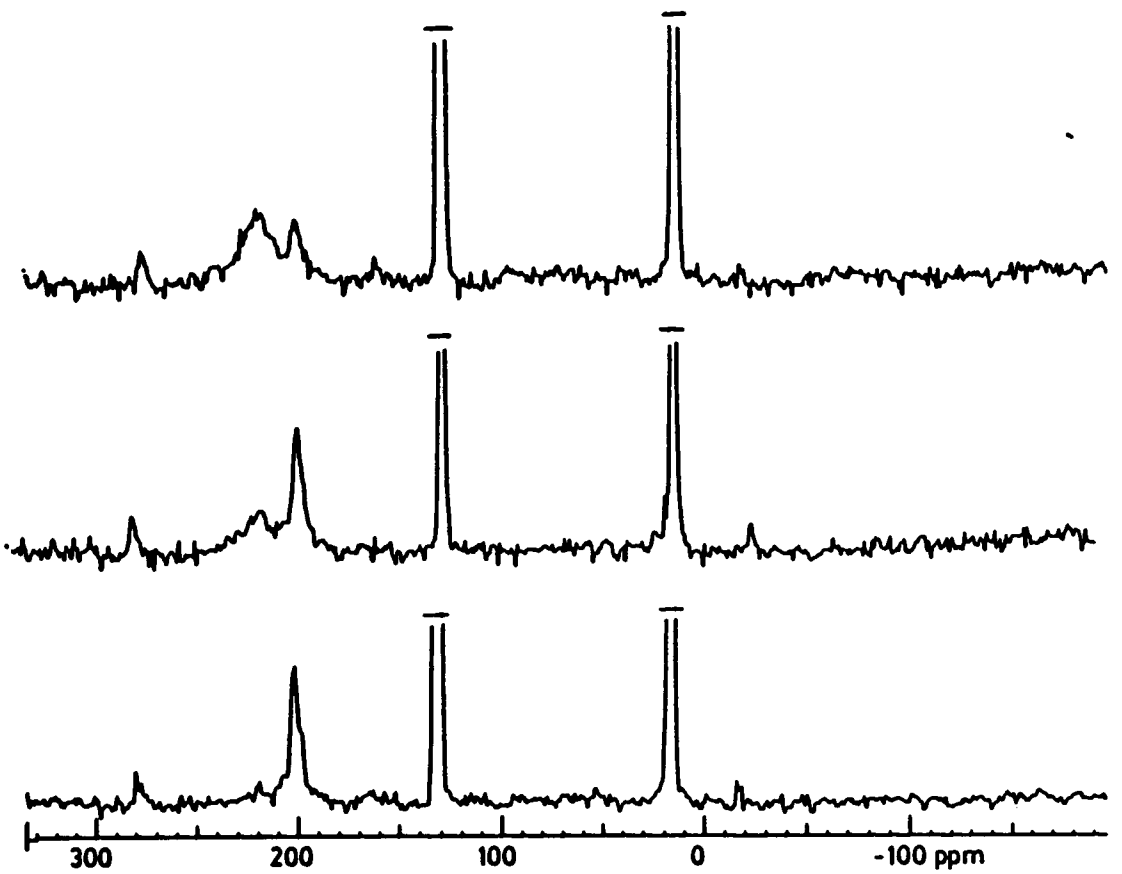

Figure 5. CP-MAS ^{13}C NMR Spectra of $Mo(CO)_6$ on PDA

nearly impossible for the $Mo(CO)_3$(ads) species to be adsorbed at sites having three-fold rotational symmetry and, therefore, more than one resonance would be expected. The fact that a single broad peak is observed for $Mo(CO)_3$(ads) suggests that a fluxional tricarbonyl group is adsorbed on the surface as is observed in many complexes containing metal carbonyl groups.[34,44,47]

The surface species, $Mo(CO)_3$(ads), has been suggested to be bimolecular, $Mo_2(CO)_6$(ads).[10] The analogous model compounds, $(\eta^5\text{-}C_5H_5)_2Mo_2(CO)_6$[32] and (arene)$Mo(CO)_3$,[32] have chemical shifts at 228.6 ppm and about 222 ppm, respectively. Both of these values are within the range of chemical shift values observed for zerovalent molybdenum tricarbonyl complexes (see Chapter 5) and this fact alone cannot differentiate between a mononuclear and bimolecular species. However, the latter complex shows coalescence of the carbonyl resonances at temperatures below 0°C, whereas the bimolecular complex shows coalescence close to 100°C. Therefore, the results for $Mo(CO)_3$(ads) are more consistent with a mononuclear complex.

Recording the NMR spectra of the previous samples using a single carbon 90° pulse with or without proton decoupling (i.e. no cross polarization) yields a single resonance at 201 ppm which is assigned to residual physisorbed $Mo(CO)_6$. This species was not observable using cross polarization due to the absence of any appropriate bonds to surface OH^- groups. The presence of the unreacted $Mo(CO)_6$ in the sample activated at 30°C was probably due to the incomplete removal of the excess complex (via sublimation in flowing helium) which was used to insure a monolayer coverage. In the samples activated at 100°C, the unreacted $Mo(CO)_6$ could be a result of the relatively low helium flow rates (30 mL/min) and activation times which were not sufficient to completely convert the hexacarbonyl to the tricarbonyl. This observation is in agreement with the equilibrium postulated by Brenner and Burwell:

$$Mo(CO)_6(phys) \underset{+CO}{\overset{-CO}{\rightleftharpoons}} Mo(CO)_5(ads) \underset{+CO}{\overset{-CO}{\rightleftharpoons}} Mo(CO)_3(ads)$$

Thus, if the reaction is stopped prematurely, then $Mo(CO)_6$(phys) could be generated in the sealed rotors. The results of Brenner and Burwell[6] were confirmed on small samples (250 mg alumina)

at low weight percent loadings (0.3 to 0.7% Mo); where after activation for 2 h at 100°C, 2.95 ± 0.06 equivalents of CO per equivalent of Mo were evolved (average value of five runs).

On hydroxylated γ-alumina, the results are essentially the same as reported for partially dehydroxylated γ-alumina. On dehydroxylated γ-alumina, $Mo(CO)_3$(ads) and $Mo(CO)_5$(ads) could not be detected by MAS ^{13}C NMR but a signal could be seen for $Mo(CO)_6$(phys) as was the case in the other samples. This was due to an increased T_1 caused by anchoring the chemisorbed subcarbonyl species to the surface. The chemical shift for $Mo(CO)_6$(phys) on dehydroylated γ-alumina is 201 ppm; the same value observed for the physisorbed hexacarbonyl on partially dehydroxylated γ-alumina.

CHAPTER 5
DYNAMICS OF METAL TRICARBONYL MODEL COMPOUNDS

5A GENERAL

Intramolecular motions in metal carbonyl complexes are well documented and have been detected and characterized by solution and solid state NMR spectroscopy.[42,44,72-74] Rearrangements in mononuclear and polynuclear metal carbonyls have been described in terms of polytopal rearrangements of their ligand polyhedra.[75-77] For example, the axial-equatorial exchange observed in iron pentacarbonyl was explained by the Berry pseudorotation mechanism.[75] Also, rearrangements in the tetranuclear clusters, $M_4(CO)_{12}$, were postulated as being an expansion of the icosahedron of carbonyl ligands into an intermediate cubooctahedron structure.[76,77] On the basis of MAS ^{13}C NMR results, it has been suggested that metal clusters may reorient independently from the polyhedron expansion of the clusters, $Fe_3(CO)_{12}$[78] and $Co_4(CO)_{12}$.[79] This possibility of metal cluster reorientation has also been supported by molecular mechanics simulations of $Co_4(CO)_{12}$.[80,81]

Although there are many examples of direct intramolecular carbonyl exchange for complexes in solution which do not involve either polytopal reorganization of the ligands or metal cluster reorientations, there are no well-documented cases for carbonyl motion in complexes in the solid state. In fact, many complexes which are fluxional in solution are static in the solid state. One example of this is given by $(\eta^5\text{-}C_5H_5)_2Fe_2(CO)_4$ which undergoes bridge-terminal exchange in solution,[82] but is static in the solid state.[43]

Perhaps the simplest example of intramolecular carbonyl exchange in solution is represented by the rotation of a metal carbonyl group which is bonded to a larger molecule.[44] This involves a minimum of motion and may be expected to occur in the solid state also. Many precedents exist for three-fold rotations in the solid for pendant methyl groups[53] as well as somewhat larger trifluoromethyl groups[83] in organic molecules. However, both CH_3 and CF_3 are smaller than metal tricarbonyl groups and would be expected to rotate much more readily.

A solution ^{13}C NMR study[36] of monosubstituted (η^6-arene)$Cr(CO)_3$ complexes indicates that an equilibrium exists between two conformations via a rotation about the chromium-arene bond. In one conformation, the three carbonyl ligands are eclipsed with ring carbons 2, 4 and 6 and in the other with carbons 1, 3 and 5. These conformations are shown in Figure 6. Evidence for these two conformations, which are in rapid equilibrium, is given by changes in the chemical shifts of the appropriate ring carbon atoms with temperature. For (η^6-$C_6H_5CH_3$)$Cr(CO)_3$, the conformation in which the carbonyl groups are eclipsed with ring carbons 1, 3 and 5 is the preferred structure at 25°C and becomes increasingly predominant at lower temperatures. Interestingly, this conformation is also adopted by the complex in the solid state.[84] Exchange between these conformations remains rapid at low temperatures. Another study dealing with substituted (η^6-arene)$Cr(CO)_3$ complexes[35] supports these findings and further shows that in the sterically hindered complex, (1,3-di-t-butylbenzene)$Cr(CO)_3$, rotation about the chromium-arene bond is rapid even at a temperature of -60°C as evidenced by the lack of broadening of the carbonyl resonances in the ^{13}C NMR spectra. For the related cycloheptatriene molecules, (η^6-C_7H_8)$Cr(CO)_3$ and (η^6-C_7H_8)$Mo(CO)_3$, solution ^{13}C NMR spectroscopy indicates a broadening of the carbonyl signals at -28°C and -13°C, respectively.[34] At lower temperatures, these split into two peaks with relative areas 1:2. The peaks were assigned to the two different carbonyl ligand types present in the crystal structures of the complexes. The estimated activation energies for the motions of the cycloheptatriene rings relative to the carbonyl ligands are 11 and 12 kcal/mol for the chromium and molybdenum compounds, respectively.

A study of crystalline (η^6-C_6H_6)$Cr(CO)_3$ by broadline ^1H NMR investigated the rotation of the coordinated benzene ring in the solid state.[45] By measuring the linewidth of the proton signal at various temperatures, two line narrowing regions were observed and occur at about -165°C and -45°C. The activation energy of the motion at -165°C is 3.4 ± 0.4 kcal/mol and was attributed to a hindered ring rotation which compares favorably with the value of 4.4 kcal/mol measured for solid benzene.[53] The activation energy of the motion causing the line narrowing at -45°C was estimated

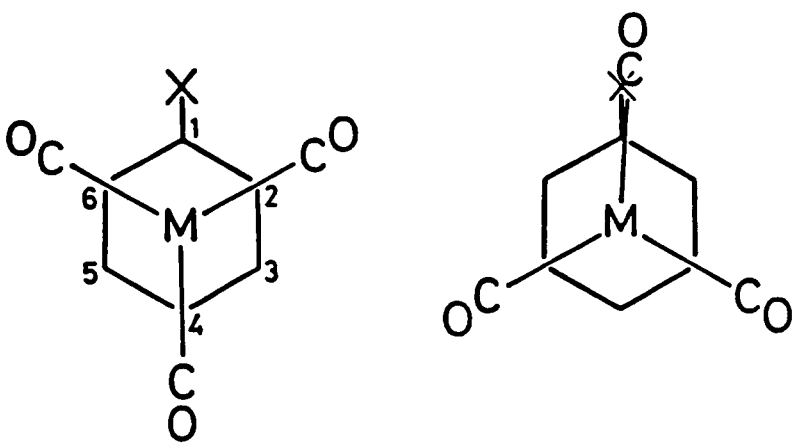

Figure 6. Conformations of Monosubstituted (arene)$M(CO)_3$ Complexes in Solution

to be 7.2 ± 0.6 kcal/mol. However, the type of motion responsible for this proton line narrowing was not deduced. It was noted, though, that solid benzene is characterized by the onset of a molecular motion at a relatively high temperature (greated than -40°C) with an activation energy of approximately 16 kcal/mol and that the two motions may be related. In solid benzene, this high activation barrier process is thought to be due to rotation of the benzene molecule about axes in the plane of the ring.[53] Ring rotations in the solid state have also been detected for coordinated cyclooctatetraene ligands in the complexes, $(\eta^4\text{-}C_8H_8)Fe(CO)_3$, $(\mu\text{-}\eta^8\text{-}C_8H_8)Fe_2(CO)_5$ and $(\mu\text{-}\eta^8\text{-}C_8H_8)_2Ru_3(CO)_4$, using broadline ^1H NMR[37-39] and MAS ^{13}C NMR.[40] The corresponding activation energies are 9.1, 2.6 and 5.2 kcal/mol, respectively.[41] Rotation of coordinated rings is also well documented for these molecules, and others, in solution.[85] NMR spectroscopy is a powerful tool to detect motions in solids and is complementary to x-ray diffraction techniques which may detect disorders but not dynamic processes.

The temperature dependence of CP-MAS NMR linewidths has been previously discussed by Rothwell and Waugh.[86] The relationship they derived is applicable to a system where ^{13}C spins are coupled to ^1H spins through dipole-dipole interactions where the protons are subjected to an rf decoupling of intensity ω_1. The spins are assumed to possess a rotational motion with a correlation time τ_c. The relevant equations are presented below. For this type of system, two ^{13}C line narrowing regions are predicted: one at $\omega_1\tau_c << 1$ (short correlation limit, equation 5.2) and the other at $\omega_1\tau_c >> 1$ (long correlation limit, equation 5.3). The point of maximum broadening occurs at $\omega_1\tau_c = 1$. Arrhenius type activation energies for motional processes can be calculated by measuring the NMR linewidths as a function of temperature. Then since T_2^{-1} is proportional to the linewidth, the slope of the line of a plot of ln (τ) (where τ = linewidth) vs. T^{-1} (in Kelvin degrees) is simply E_a/R (equation 5.4). The intercept yields the inverse frequency factor, τ_0, given by equation 5.5 where T′ is the temperature where maximum broadening occurs. Using CP-MAS ^{13}C NMR, Rothwell and Waugh have illustrated this behavior for a number of hydrocarbon compounds which possess rotational motions in the solid state.[86] These compounds, e.g.

adamantane and hexamethylbenzene, undergo solid state rotations but do not exchange carbons with different environments. Therefore, these are not fluxional molecules.

$$\frac{1}{T_2} = \frac{[4\gamma_I^2\gamma_S^2h^2]I(I+1)}{15r^6}\frac{\tau_c}{(1+\omega_1^2\tau_c^2)} \qquad 5.1$$

$$\frac{1}{T_2} = \frac{[4\gamma_I^2\gamma_S^2h^2]I(I+1)}{15r^6}\tau_c,\ \omega_1\tau_c << 1 \qquad 5.2$$

$$\frac{1}{T_2} = \frac{[4\gamma_I^2\gamma_S^2h^2]I(I+1)}{15r^6}\frac{1}{(\omega_1^2\tau_c)},\ \omega_1\tau_c >> 1 \qquad 5.3$$

$$\tau = \tau_0\exp[E_a/(RT)] \qquad 5.4$$

$$\tau_0 = \omega_1^{-1}\exp[-E_a/(RT)] \qquad 5.5$$

In this chapter, the results of variable temperature solution ^{13}C NMR and CP-MAS ^{13}C NMR studies of metal tricarbonyl complexes will be presented with emphasis on metal tricarbonyl group rotations in the solid state. These complexes will serve as model compounds for γ-alumina supported $Mo(CO)_3$(ads). The results for $Cr(CO)_3(\eta^6\text{-}C_6H_5CH_3)$ and $Mo(CO)_3(\eta^6\text{-}C_6H_5CH_3)$, which demonstrate novel tricarbonyl group rotations in the solid state, have been previously published.[87]

5B EXPERIMENTAL

The ^{13}CO enriched $Mo(CO)_3(CH_3CN)_3$ complex was prepared by stirring the reaction mixture from the synthesis of $Mo(CO)_3(CH_3CN)_3$ (see Chapter 3) under a ^{13}CO atmosphere for 3 days. Some $Mo(CO)_6$ formed and was converted back to $Mo(CO)_3(CH_3CN)_3$ by additional refluxing. An enrichment of about 30% ^{13}CO was estimated by IR spectroscopy.

The $Mo(CO)_3$(diglyme) (diglyme = $CH_3OCH_2CH_2OCH_2CH_2OCH_3$) complex was prepared by refluxing $Mo(CO)_3(\eta^6\text{-}C_6H_5CH_3)$ (see below) in a 30% v/v diglyme/pentane solution. This resulted in a light yellow precipitate which was filtered and washed with pentane. This compound was characterized by satisfactory elemental analysis and two infrared carbonyl stretching frequencies at 1915 and 1752 cm^{-1} (KBr) which were distinctly different from those reported for the toluene complex at 1983 and 1913 cm^{-1} (hexane).[68] These bands are different than those reported by

Werner and Coffield at 1905 and 1835 cm^{-1} (KBr)[22] and the reason for this discrepancy is not clear. The complex was soluble in water, acetone, THF, methanol and ethanol but insoluble in pentane and diethylether. The ^{13}CO enriched diglyme complex was prepared similarly from ^{13}CO enriched $Mo(CO)_3(\eta^6\text{-}C_6H_5CH_3)$ (see below). An enrichment of about 30% ^{13}CO was estimated by IR spectrocopy.

The $Mo(CO)_3(\eta^6\text{-}C_6H_6)$ complex was prepared as described in Chapter 3.

The ^{13}CO enriched $Cr(CO)_3(\eta^6\text{-}C_6H_5CH_3)$ complex was synthesized from $Cr(CO)_3(CH_3CN)_3$ by refluxing the latter compound in toluene. The ^{13}CO enriched $Cr(CO)_3(CH_3CN)_3$ complex was prepared in a manner analogous to ^{13}CO enriched $Mo(CO)_3(CH_3CN)_3$ (see above). The isotopically normal toluene complex prepared in this manner yielded two carbonyl IR stretches at 1977 and 1908 cm^{-1} (Nujol) which corresponded well with the literature values of 1980 and 1912 cm^{-1} (hexane).[68] An enrichment of 10% ^{13}CO was estimated by IR spectroscopy.

The ^{13}CO enriched $Mo(CO)_3(\eta^6\text{-}C_6H_5CH_3)$ complex was synthesized by refluxing $Mo(CO)_6$ in toluene. The reaction mixture was then stirred under an atmosphere of ^{13}CO for 2 days. Some $Mo(CO)_6$ formed during this process and the solution was additionally refluxed to convert the hexacarbonyl back to the toluene complex. The isotopically normal complex prepared in this manner yielded two carbonyl IR stretching frequencies at 1985 and 1914 cm^{-1} in agreement with the literature values of 1983 and 1913 cm^{-1}.[68] An enrichment of 15% ^{13}CO was estimated by IR spectroscopy.

Acetone-d_6 (99.8% D) was obtained from Cambridge Isotopes. Ethanol-d (99.5% D) and methanol-d (99.5% D) were obtained from Aldrich Chemical Company.

Solution NMR samples of $Mo(CO)_3$(diglyme) were prepared under an inert atmosphere using degassed deuterated NMR solvents. The solutions were filtered through a glass frit and then syringed into a degassed 10 mm o.d. NMR tube through a septum. This procedure avoided exposure of the samples to air.

Solution 20.12 MHz ^{13}C NMR spectra were obtained using a Bruker NR-80 NMR spectrometer.

Variable temperature solution 50.3 MHz ^{13}C NMR spectra were obtained on a Bruker WP-200 NMR spectrometer equipped with a Bruker variable temperature controller. A pulse delay time of 10 sec was used and was adequate to observe the carbonyl signals in the diglyme complex. Samples were allowed to equilibrate for at least 5 min before scanning. Temperatures were maintained by the controller to ± 1°C. Dry nitrogen gas, from liquid nitrogen boil off, was used for sample spinning at subambient temperatures.

All solid state NMR samples were prepared under nitrogen.

Variable temperature 22.6 MHz CP-MAS ^{13}C NMR spectra were obtained using a Chemagnetics 2 T superconducting magnet, a Chemagnetics probe and variable temperature controller which was interfaced to a JEOL FX60QS NMR console. Using this instrument, NMR samples were packed in bullet type sleeve rotors machined from either Kel-F or delrin which were employed for above-ambient and subambient temperature work, respectively. The rotors were sealed with plasticine to prevent decomposition of the samples during data acquisition. The delrin rotor material yields a signal at 89.3 ppm (TMS) which was used as the chemical shift reference. Dry nitrogen gas, from liquid nitrogen boil off, was used as the spinner and bearing gas at subambient temperatures. House air was used at room temperature and above for the spinning and bearing. Temperatures were measured by a thermocouple placed in the spinner air stream immediately before the sample. The sample was allowed to equilibrate for at least 10 min before acquiring data. Temperatures varied no more than ± 3°C during data acquisition.

Variable temperature 75.5 MHz CP-MAS ^{13}C NMR spectra were obtained using a Bruker MSL-300 NMR spectrometer equipped with a Bruker variable temperature controller. Samples were packed in standard Bruker aluminum oxide rotors utilizing boron nitride endcaps. The hole in the endcap was sealed with either rubber cement or plasticine to prevent sample decomposition. Dry nitrogen gas, from liquid nitrogen boil off, was used as the drive and bearing gas for all work.

This aided in preserving the samples during data aquisition. Samples were allowed to equilibrate at a given temperature for at least 10 min before scanning. Temperatures were maintained to ± 1°C by the temperature controller. A separate spectrum of admantane was obtained for chemical shift calibration.

5C RESULTS FOR SOLID $Mo(CO)_3(CH_3CN)_3$

The 22.63 MHz CP-MAS ^{13}C NMR spectrum of ^{13}CO enriched $Mo(CO)_3(CH_3CN)_3$ shown in Figure 7, yields a single sharp resonance in the carbonyl region at 227 ppm (TMS) along with an array of spinning sidebands at 25°C. This would be expected as a result of the C_{3v} symmetry of the complex in the absence of any slow CO exchange process. As the temperature of the sample was lowered to -64°C the linewidth of the carbonyl resonance broadened only slightly. Also, warming the sample to 55°C merely caused the linewidth to narrow to a very slight extent. From this data, it would not be possible to speculate about the fluxionality of the carbonyl ligands due to the very slight broadening and narrowing of the carbonyl resonance upon cooling and heating the sample. However, the very intense array of spinning sidebands associated with the carbonyl peak indicates a very large chemical shift anisotropy. By inspection of the sideband intensities,[89,90] the chemical shift anisotropy ($\sigma_{\parallel}$-$\sigma_{\perp}$) is estimated to be ca. 400 ± 50 ppm, which is near the value expected for a static carbonyl of axial symmetry.[91] Therefore, $Mo(CO)_3(CH_3CN)_3$ appears to be static in the solid state.

5D RESULTS FOR $Mo(CO)_3$(diglyme) IN SOLUTION

Of all the model compounds studied, $Mo(CO)_3$(diglyme) has a structure most similar to γ-alumina supported $Mo(CO)_3$(ads) in that the metal tricarbonyl group is coordinated to oxygen electron lone pairs. This compound was studied by both variable temperature solution and solid state NMR since no previous NMR studies have been reported for this complex.

The 20.12 MHz and 50.323 MHz ^{13}C NMR spectra of $Mo(CO)_3$(diglyme) in acetone-d_6 at 25°C are shown in Figure 8. The singlet at 206 ppm and multiplet at 29.8 ppm are due to the solvent. The signal at 29.8 ppm was used as the chemical shift reference. There is only one

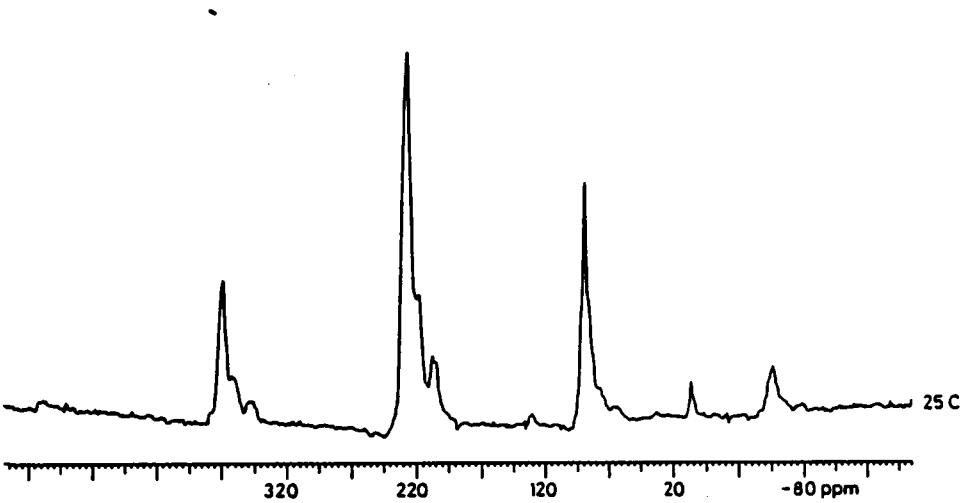

Figure 7. 22.63 MHz CP-MAS ^{13}C NMR Spectrum of ^{13}CO Enriched $Mo(CO)_3(CH_3CN)_3$ at 25°C

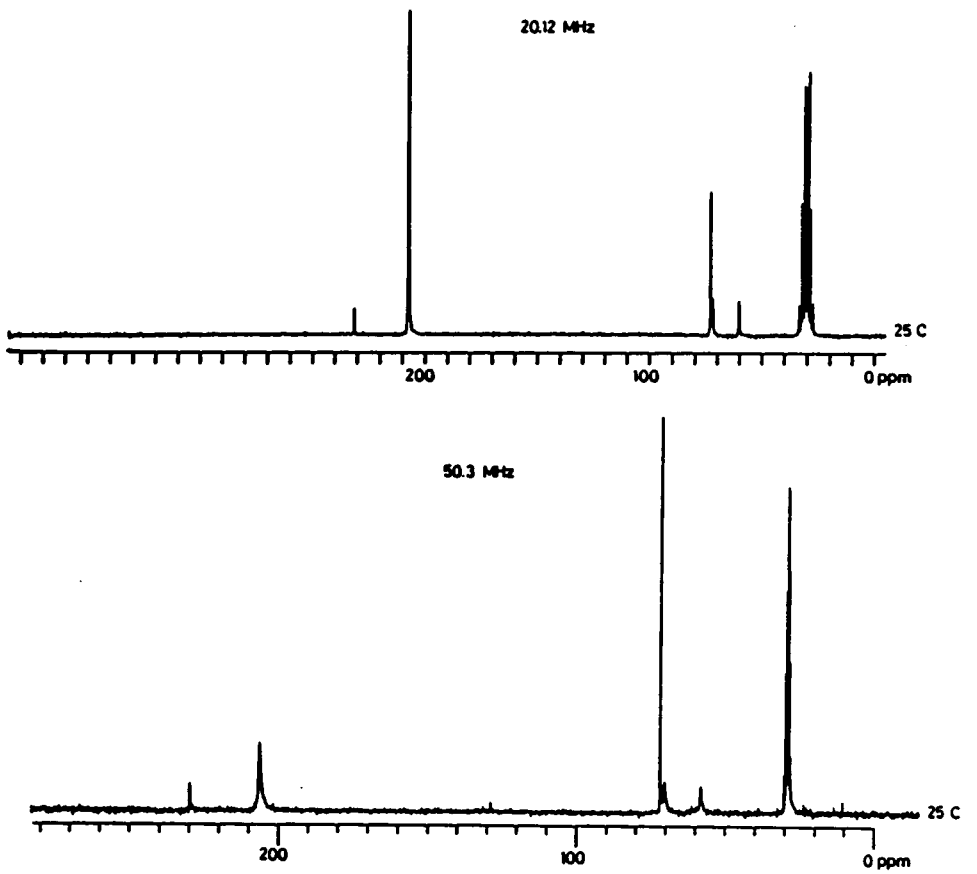

Figure 8. Solution ^{13}C NMR Spectra of $Mo(CO)_3$(diglyme) in Acetone-d_6 at 25°C

resonance in the carbonyl region at 230.7 ppm (TMS). Signals can also be observed for the diglyme ligand at 72.6, 71.5 and 59.2 ppm, which are barely shifted from the uncomplexed ligand (72.7, 71.3 and 58.8 ppm measured in acetone-d_6 at 20.12 MHz). The broadness of the diglyme ligand peaks at 71.5 and 59.2 ppm seems to be due to a concentration effect since very dilute solutions of the complex yield sharp resonances for the various carbons in the ligand as is observed in solution ^{13}C NMR spectra for the uncomplexed ligand. The assignments for the signals in the diglyme molecule are not clear. However, it is reasonable to assume that the peak at 59.2 ppm is due to the pair of methyl carbons and the peaks at 72.7 and 71.3 ppm are due to the two pairs of methylene carbons.

The structure of the complex presented by Werner and Collfield[22] implies that the methyl groups of the diglyme ligand are directed toward each other as the ligand is wrapped around the molybdenum atom in order for the oxygens to occupy three coordination sites in a facial manner, as shown in Figure 9 (a). As a result of steric repulsions, the methyl groups are forced to bend in opposite directions, thereby introducing an asymmetry into the complex. In this case, three resonances would be expected for the three carbonyl ligands and a separate signal would be observed for each carbon in the complexed diglyme ligand. However, these features are not observable in the 25°C spectra in Figure 8.

An alternative structure for the complex is one in which the methyl groups are directed away from each other as shown in Figure 9 (b). A simple "ball and stick" model of the $Mo(CO)_3$(diglyme) complex, using an octahedral molybdenum center and tetrahedral configurations for all of the carbon and oxygen atoms in the diglyme ligand, indicates that this structure is less sterically hindered than the structure depicted in Figure 9 (a). Furthermore, the non-interacting methyl groups do not require the complexed ligand to twist to relieve the steric repulsions of the methyl groups. Thus, this structure would possess mirror plane symmetry if a C_{3v} arrangement of the carbonyl ligands is assumed. This symmetry would account for the single resonance observed for each pair of carbons present in the complexed diglyme ligand. However, if the methyl groups of the structure shown in Figure 9 (a) are involved in a rapid motion so that they both aquire the

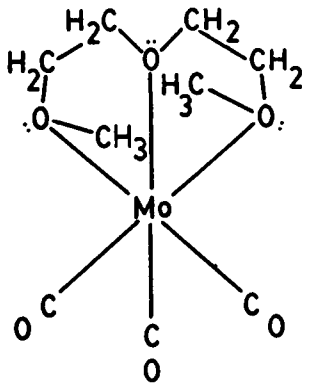

(a)

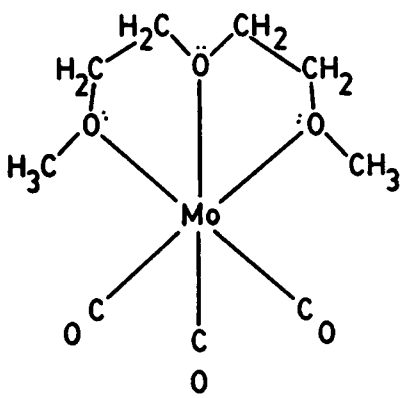

(b)

Figure 9. Proposed Structures for $Mo(CO)_3$(diglyme)

same averaged environments, then this structure would possess pseudo-mirror plane symmetry and would also fit the observable ^{13}C NMR spectrum at 25°C. In the case of either structure, the presence of a single carbonyl resonance is not predicted. This may be due to either an accidental degeneracy of the chemical shifts or a motional process in which the carbonyls are rapidly exchanging positions. Many precedents exist for tricarbonyl group rotation in (arene)$M(CO)_3$ complexes in solution.[34-36,44] However, the bonds between the metal atom and the arene ring are not directional (which may account for the low rotational barriers observed in these complexes) whereas in the diglyme complex, the directional nature of the molybdenum-oxygen bonds may present a very high barrier for rotation of the tricarbonyl group. The carbonyl groups have a longer T_1 than the diglyme ligand carbons as evidenced by the relative enhancement of the carbonyl resonance by either increasing the delay time between pulses or by the addition of the relaxation agent, $Cr(acac)_3$. These treatments have little effect on the diglyme ligand signals.

At the higher field strength of 50.323 MHz, the ^{13}C NMR spectrum of $Mo(CO)_3$(diglyme) in acetone-d_6 at 25°C (Figure 8) shows essentially the same features as the corresponding lower field spectrum (Figure 8) except that the signals for the diglyme ligands at 71.5 and 59.2 ppm are broadened to a greater extent due to the greater concentration of this sample.

A series of spectra of $Mo(CO)_3$(diglyme) in acetone-d_6 recorded at subambient temperatures is shown in Figure 10. Where indicated, the acetone-d_6 solvent peaks have been truncated to allow amplification of the weaker signals of the complex. At 284 K (top spectrum), the peaks due to the methyl group pair and one pair of methylene groups have sharpened considerably and by 264 K they have attained approximately the same intensity and linewidth of the signal due to the other pair of methylene groups. This again suggests that the methyl groups adopt positions which allow mirror plane symmetry for the diglyme ligand.

At about 244 K, a new signal appears in the carbonyl region at 220.0 ppm and increases in intensity relative to the carbonyl resonance as the temperature is lowered. However, in the low temperature spectra of ^{13}CO enriched $Mo(CO)_3$(diglyme) in acetone-d_6 solution shown in Figure

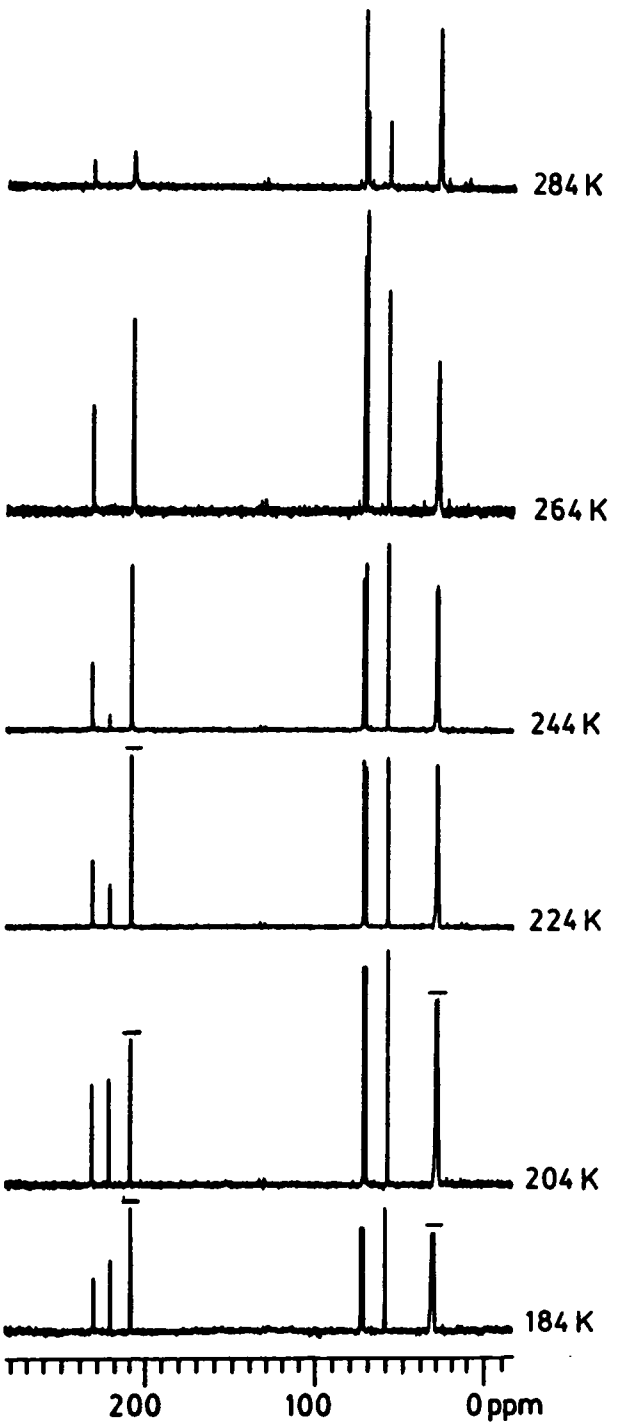

Figure 10. Variable Temperature 50.3 MHz ^{13}C NMR Spectra of $Mo(CO)_3$(diglyme) in Acetone-d_6

11, the new peak is very weak compared to the carbonyl signal; suggesting that the peak orignates from the acetone-d_6 solvent molecules rather than the carbonyl ligands. Thermodynamic data[62] for ligand displacement reactions indicate that the diglyme ligand should be stable towards displacement by acetone at subambient temperatures. Thus, it appears that acetone molecules are able to interact with the diglyme complex, thereby causing a dramatic change in the chemical shift of the acetone carbonyl resonance, although the nature of this interaction is unclear. The chemical shift of the acetone methyl groups appears not to be greatly affected by this interaction since their resonance could not be resolved from the solvent peak. In the lower temperature spectra, the area of the interacting acetone-d_6 solvent molecules is approximately equal to the area of the three carbonyl ligands, which indicates that three acetone molecules are interacting with the diglyme complex at the lower temperatures. However, peaks due to diglyme ligand in interacting and non-interacting complexes are not resolved in the spectra, which is not unexpected since the chemical shifts of complexed and non-complexed diglyme ligand differ by less than 0.4 ppm. At 184 K, all the linewidths of the signals begin to broaden slightly which may be indicative of a motional process in which the tricarbonyl group is undergoing a three-fold rotation with respect to the diglyme ligand. An alternative explanation is that the complex is crystallizing out of solution at this low temperature. Also, this temperature is near the freezing point of acetone and, therefore, a solvent with a lower freezing point would be necessary in order to determine if a fluxional process is present.

The subambient temperature 50.323 MHz ^{13}C NMR spectra of $Mo(CO)_3$(diglyme) in ethanol-d are shown in Figure 12. The peaks at 56.8 and 17.2 ppm are due to the ethanol-d solvent. The 56.8 ppm signal was used as the chemical shift reference. The ambient temperature spectrum (top spectrum) is virtually identical to the corresponding spectrum obtained in acetone-d_6. The carbonyl resonance is at 228.8 ppm and the signals for the diglyme ligand are at 71.4, 69.8 and 52.7 ppm. Lowering the temperature of the sample again causes the signals at 69.8 and 52.7 ppm to sharpen in the lower temperature spectra. However, at 254 K a new peak at 62.0 ppm begins to grow in and attains the same relative intensity of the signals due to the methyl and methylene

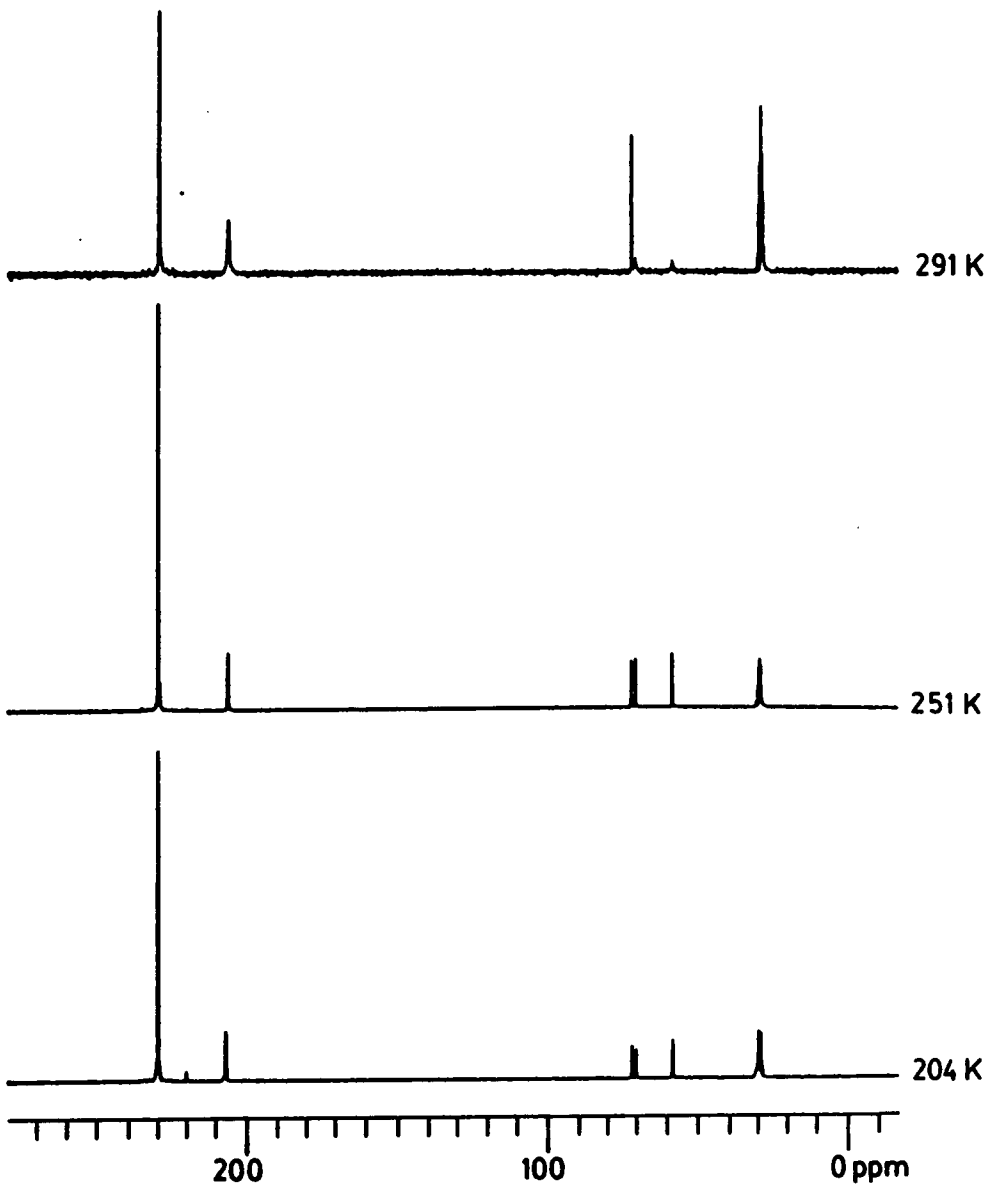

Figure 11. Variable Temperature 50.3 MHz ^{13}C NMR Spectra of ^{13}CO Enriched $Mo(CO)_3$(diglyme) in Acetone-d_6

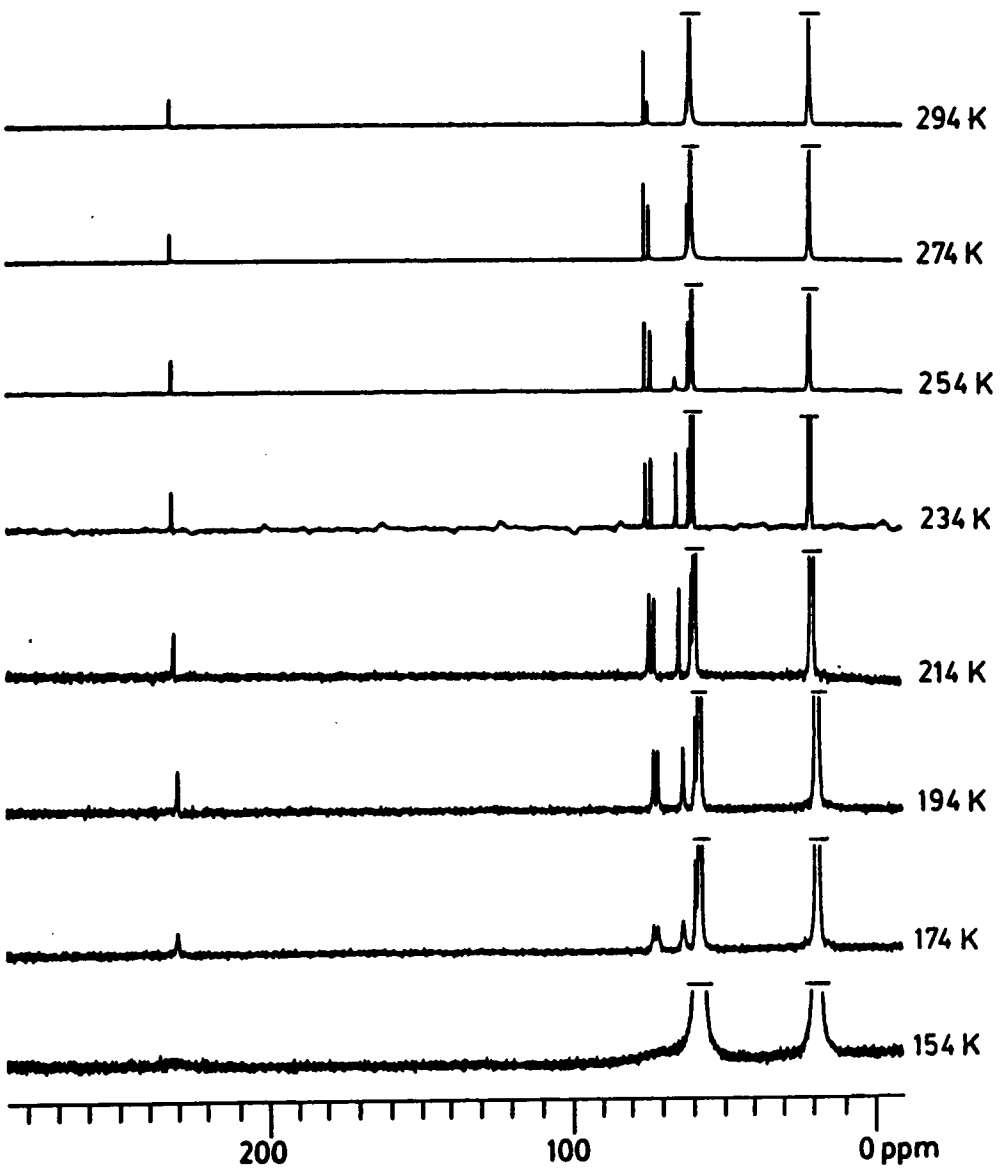

Figure 12. Variable Temperature 50.3 MHz ^{13}C NMR Spectra of $Mo(CO)_3$(diglyme) in Ethanol-d

carbons in the diglyme ligand at 234 K. At the lower temperatures, the area of this new peak approaches a value which is 1.5 times the areas of the individual diglyme ligand signals which suggests that the peak represents three molecules. Again, thermodynamic data[62] suggests that diglyme should not be displaced by monodentate oxygen donating ligands at subambient temperatures. Therefore, this new peak is assigned to the methylene groups of ethanol-d molecules interacting with the diglyme complex at the lower temperatures in a manner analogous to acetone-d_6. However, the corresponding signal for the interacting ethanol-d methyl groups is not resolved from the solvent peak. Again, the peaks due to diglyme ligand in interacting and non-interacting complexes are not resolved. As the temperature is lowered further, the resonances due to the carbonyl ligands and methyl and methylene groups of the diglyme ligand as well as the methylene signal of the interacting ethanol-d molecules begin to broaden considerably. It should be noted that the peak due to the methyl groups in the diglyme ligand at 58.2 ppm broadens at a slower rate than the other signals. At 154 K, the peaks are so severely broadened that they are barely discernible in the spectrum. However, this temperature is very near the freezing point of ethanol which may account for the broadened lines. The signal due to the methyl groups of the diglyme ligand would broaden at a slower rate since they would have greater mobility than the other carbons in the sample. Therefore, lower temperatures would have to be achieved in order to determine the dymanics of the carbonyl ligands in the diglyme complex. In order to further substantiate the assignment of the peak at 62.0 ppm to interacting ethanol-d molecules, it was decided use methanol-d as the solvent to determine if a similar interaction process would occur at low temperatures.

A series of variable temperature solution 50.3 MHz ^{13}C NMR spectra of $Mo(CO)_3$(diglyme) in methanol-d is shown in Figure 13. In the 293 K spectrum, the peaks are at 229.6 ppm (carbonyl ligands), 72.0 and 70.4 ppm (methylene groups of the diglyme ligand) and 58.2 ppm (methyl groups of the diglyme ligand). The methanol-d solvent peak is at 49.0 ppm and was used as the chemical shift reference. At 293 K, the peaks at 70.4 and 58.2 ppm are not as severely broadened as in the corresponding spectra in the other solvents since this sample was very dilute. Again, lowering the

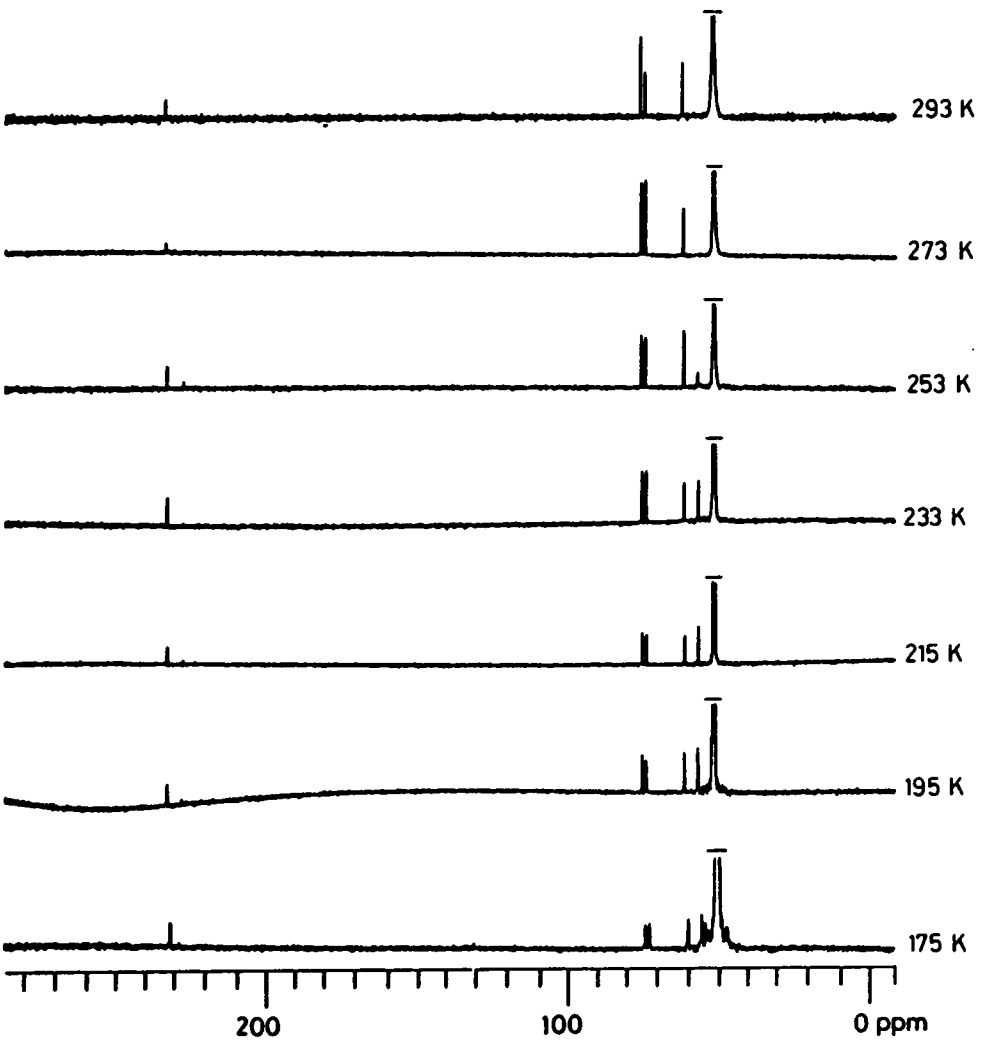

Figure 13. Variable Temperature 50.3 MHz ^{13}C NMR Spectra of $Mo(CO)_3$(diglyme) in Methanol-d

temperature of the sample causes the signals of all three pairs of carbon atoms in the diglyme ligand to attain nearly equal intensities. In the 253 K spectrum, a new peak begins to appear at 53.7 ppm. In the lower temperature spectra, the ratio of the area of the new peak to the area of the diglyme methyl peak approaches a value of 1.5. Thermodynamic data[62] again suggests that monodentate oxygen donating ligands should not displace diglyme at subambient temperatures. Therefore, this indicates that three methanol-d molecules are interacting per molybdenum complex which causes the observed shift of the interacting methanol-d methyl groups from 49.0 to 53.8 ppm. Thus, as in the previous solvents, methanol-d is interacting with the diglyme complex at the lower temperatures. Again, the signals for diglyme ligand in interacting and non-interacting complexes are not resolvable.

In the solution ^{13}C NMR spectra of this dilute sample of $Mo(CO)_3$(diglyme) in methanol-d, no significant broadening of the signals was observed at the lower temperatures. Thus, it appears that the broadening observed in the lower temperature spectra of the previous solvents was due to either the complex crystallizing out of solution or merely an increase of the sample viscosity since the spectra were obtained near the freezing points of the acetone-d_6 and ethanol-d solvents. Therefore, the temperature range accessible using these solvents did not allow for the direct observation of any motional process involving the tricarbonyl group of the diglyme complex in solution. Only a single signal was observed for the diglyme methyl groups in the low temperature spectra which is consistent with the structure in Figure 9 (b), although a motional process exchanging the positions of the methyl groups in the structure shown in Figure 9 (a) can not be ruled out. The use of variable temperature CP-MAS ^{13}C NMR would yield information on both the dynamics of the complex in the solid state and the orientation of the diglyme ligand methyl groups. This would also avoid solvent effects.

5E RESULTS FOR SOLID $Mo(CO)_3$(diglyme)

The variable temperature 75.5 MHz CP-MAS ^{13}C NMR spectra of ^{13}CO enriched $Mo(CO)_3$(diglyme) are shown in Figure 14. In the 299 K spectrum, a single sharp carbonyl peak

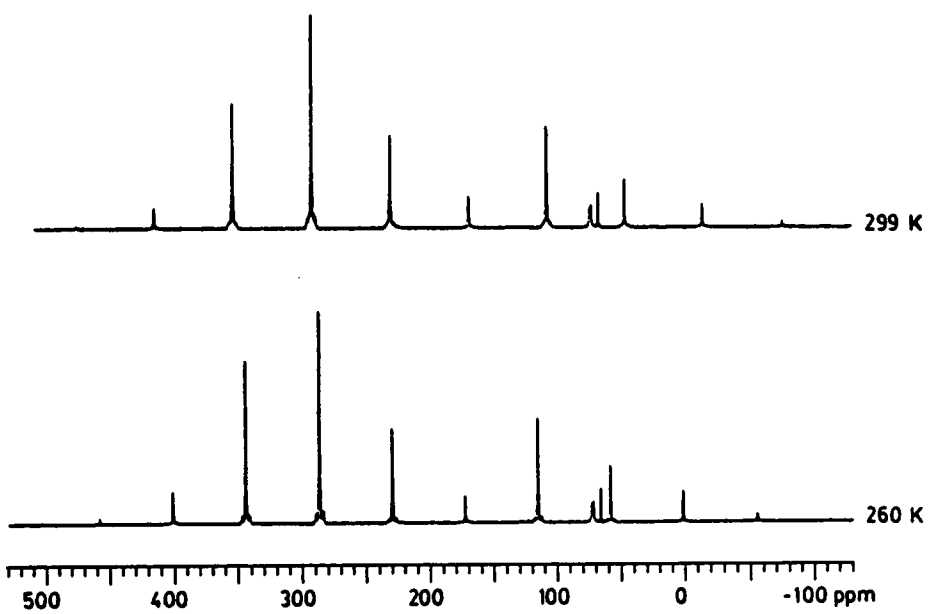

Figure 14. Variable Temperature 75.5 MHz CP-MAS ^{13}C NMR Spectra of ^{13}CO Enriched $Mo(CO)_3$(diglyme)

is present at 230.7 ppm and is very close to the solution value. The diglyme ligand resonances are at 74.1, 72.8 and 67.3 ppm. The peak due to the diglyme methyl groups at 67.3 ppm is slightly enhanced relative to the methylene groups. The other peaks present in the spectrum are due to spinning sidebands of the carbonyl peak. The spectrum obtained at 260 K is virtually unchanged except that the sidebands have moved towards the carbonyl peak at 230.5 ppm as a result of the slower spin rate. The spinning rates were at about 4600 Hz and 4300 Hz in the 299 K and 260 K spectra, respectively. The presence of only a single sharp resonance for each pair of methyl and methylene groups indicates that the ligand probably has mirror plane symmetry in the solid state as previously suggested by the model shown in Figure 9 (b). The presence of a single sharp resonance for the carbonyl ligands at both temperatures with nearly identical linewidths suggests that the complex is static in the solid state and that the chemical shifts for the carbonyl ligands are degenerate. Furthermore, an inspection[89,90] of the intense array of spinning sidebands indicates a very large chemical shift anisotropy of ca. 400 ± 50 ppm for the carbonyl ligands which is close to the value of about 400 ppm expected for a static metal carbonyl.[91] Therefore, the $Mo(CO)_3$(diglyme) complex appears to be static in the solid state.

5F RESULTS FOR SOLID $Mo(CO)_3(\eta^6\text{-}C_6H_6)$

A series of variable temperature 75.5 MHz CP-MAS ^{13}C NMR spectra obtained from $Mo(CO)_3(\eta^6\text{-}C_6H_6)$ at various temperatures is shown in Figure 15. The 300 K spectrum yields two resonances at 99 ppm and 223 ppm. The other peaks in the spectrum are due to spinning sidebands from these two peaks. The sidebands can be observed to move inward in the lower temperature spectra as a result of the slower spin rates which varied between about 4600 Hz at 328 K to 3800 Hz at 230 K. The peak at 99 ppm indicates that all the ring carbons are equivalent as expected since the complex probably has a structure analogous to $Cr(CO)_3(\eta^6\text{-}C_6H_6)$ in which the carbonyl groups are in a C_{3v} arrangement and staggered with respect to the benzene ring.[88] Also, it has been previously shown that rotation of the benzene ring in crystalline $Cr(CO)_3(\eta^6\text{-}C_6H_6)$ is very rapid at ambient temperatures with an activation energy of 3.4 kcal/mol and that line

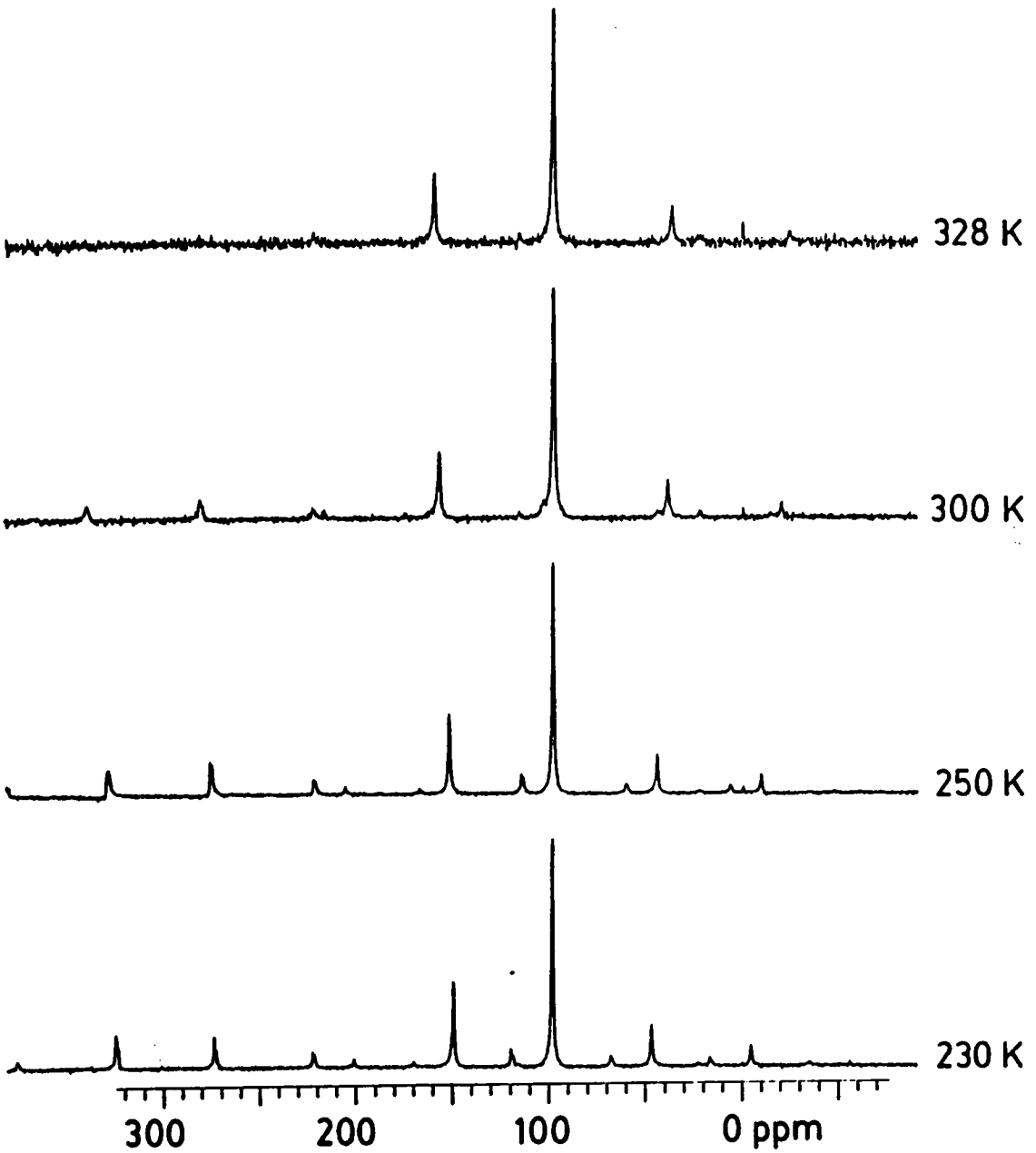

Figure 15. Variable Temperature 75.5 MHz CP-MAS ^{13}C NMR Spectra of $Mo(CO)_3(\eta^6\text{-}C_6H_6)$

broadening is not observed in broadline 16 MHz ^{1}H NMR spectra until about 133 K.[45] Thus, even if the complex did not possess three-fold symmetry, all of the ring carbons would be averaged to a single resonance by rapid rotation of the benzene ring. However, the temperature range of the spectra (> 230 K) did not allow for the direct observation of this motional process as the linewidth of the ring carbon signal did not vary significantly at the different temperatures.

In Figure 16, the carbonyl regions of the spectra shown in Figure 15 are amplified in order to allow the signals for the carbonyl ligands to be more clearly observed. A single broad resonance at 223 ppm is present for the carbonyl ligands at 300 K. At 328 K, the signal is severely broadened and is not discernible in this spectrum and is further obscured by a spinning sideband from the ring carbon signal which is coincidentally in the vicinity of 223 ppm. In the subambient spectra, the carbonyl resonance sharpens and two overlapping peaks are present which are separated by about 1 ppm. The ratio of the peak areas is approximately 1:2 and is more clearly demonstrated by the left spinning sideband in the 230 K spectrum.

The crystal structure of $Cr(CO)_3(\eta^6\text{-}C_6H_6)$ shows that this complex possesses a plane of mirror symmetry in the crystal lattice.[88] Thus, one carbonyl ligand is in the mirror plane while the other two carbonyl ligands are bisected by the plane. Therefore, there are two types of carbonyl ligands present in the crystal lattice. If the molybdenum complex adopts an analogous structure, then the presence of two types of carbonyl ligands in a ratio of 1:2 would explain the two signals observed in the low temperature NMR spectra. The chemical environments are very similar, however, since their chemical shift difference is only about 1 ppm. The carbonyl ligands appear to be involved in a motional process which averages and broadens their signals at the higher temperatures of 300 and 328 K. The low signal to noise ratio of these spectra would not allow for an accurate calculation[86] of the activation energy for this process. However, a very rough estimate of about 4 kcal/mol can be obtained by using the linewidths of the spinning sidebands in the 300 and 250 K spectra which indicates a low rotational barrier for the carbonyl ligands in the solid state. This barrier is higher than that for the hindered rotation of the benzene ring in the molybdenum complex since the

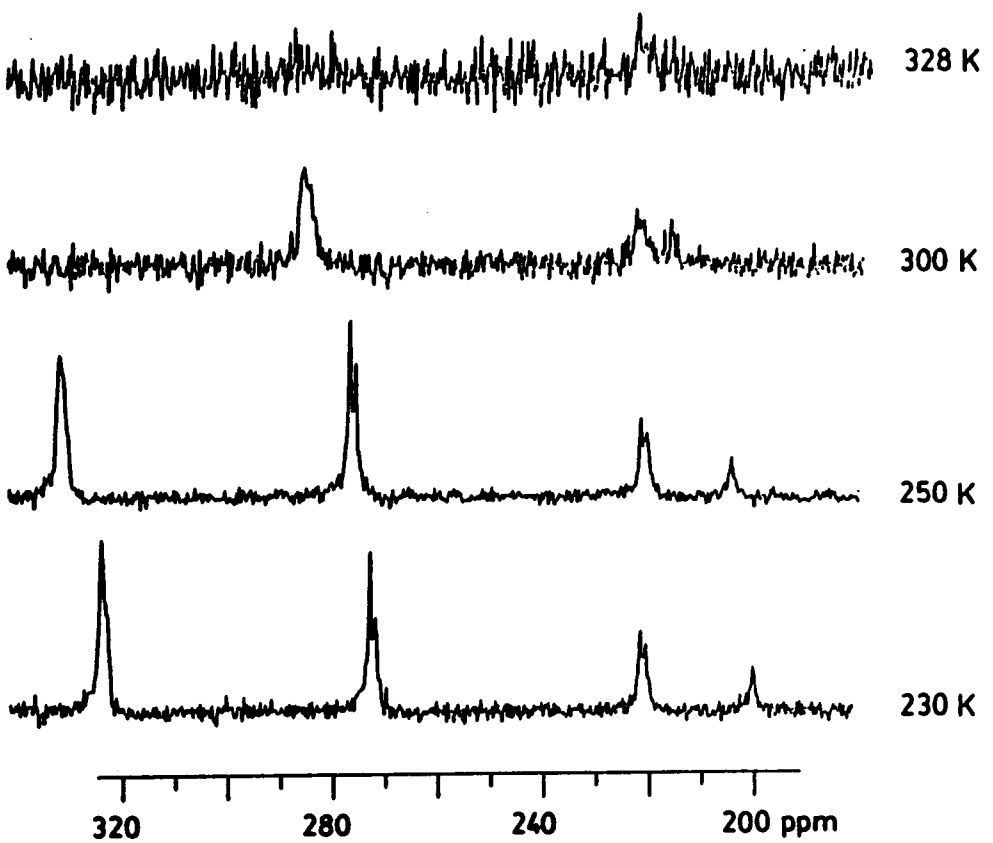

Figure 16. Enhanced Carbonyl Regions of the Variable Temperature 75.5 MHz CP-MAS ^{13}C NMR Spectra of $Mo(CO)_3(\eta^6\text{-}C_6H_6)$

motion of the ring was rapid even at 230 K as evidenced by the narrow linewidth of the ring carbon signal at this temperature. Thus, the complex $Mo(CO)_3(\eta^6\text{-}C_6H_6)$ exhibits two different motional processes in the solid state; one involving rotation of the benzene ring and the other involving rotation of the tricarbonyl ligands.

5G RESULTS FOR SOLID $Cr(CO)_3(\eta^6\text{-}C_6H_5CH_3)$ AND $Mo(CO)_3(\eta^6\text{-}C_6H_5CH_3)$

As shown in Figure 17, a single broad resonance is observed at 25°C in the carbonyl region of the 22.63 MHz CP-MAS ^{13}C NMR spectrum of ^{13}CO enriched $Cr(CO)_3(\eta^6\text{-}C_6H_5CH_3)$. The peak is centered at about 236 ppm (TMS) and has a linewidth of 2140 Hz. Heating the sample to 60°C causes the carbonyl signal to narrow to a single peak at 236 ppm with a linewidth of 164 Hz. Cooling the sample below 25°C again causes a narrowing of the carbonyl signal to a single peak at 236 ppm which continues to narrow as the temperature is lowered. The chemical shift remains constant. The peak widths and corresponding temperatures are as follows: 539 Hz at 13°C, 195 Hz at 0°C, 117 Hz at -10°C and 117 Hz at -36°C. However, at -77°C the linewidth increases to 180 Hz and a shoulder is present at 233 ppm. This is probably due to two different carbonyl environments within the complex and will be discussed later. The individual carbonyl signals are not resolvable due to their linewidths and close proximity. Other features in the spectra include signals due to the ring carbons (which are most prominent at 25°C due to the large number of scans), the signal at 89.3 ppm due to the delrin rotor used in obtaining the lower temperature spectra, and spinning sidebands which begin to appear in the -10, -36 and -77°C spectra due to the slower spin rates at these temperatures. The spinning rate varied from 2000 to 4000 Hz from -77 to 60°C. No significant changes in the chemical shifts and linewidths of the ring carbon signals were observed as a function of temperature.

The 22.63 MHz CP-MAS ^{13}C NMR spectra of ^{13}CO enriched $Mo(CO)_3(\eta^6\text{-}C_6H_5CH_3)$ are shown in Figure 18. At 25°C, a single broad carbonyl resonance is observed at 224 ppm with a linewidth of 684 Hz. When the spectrum is recorded at 40°C, the carbonyl peak narrows to 200 Hz and at 60°C it narrows further to 31 Hz. Also, as the sample is cooled to 10°C, the peak

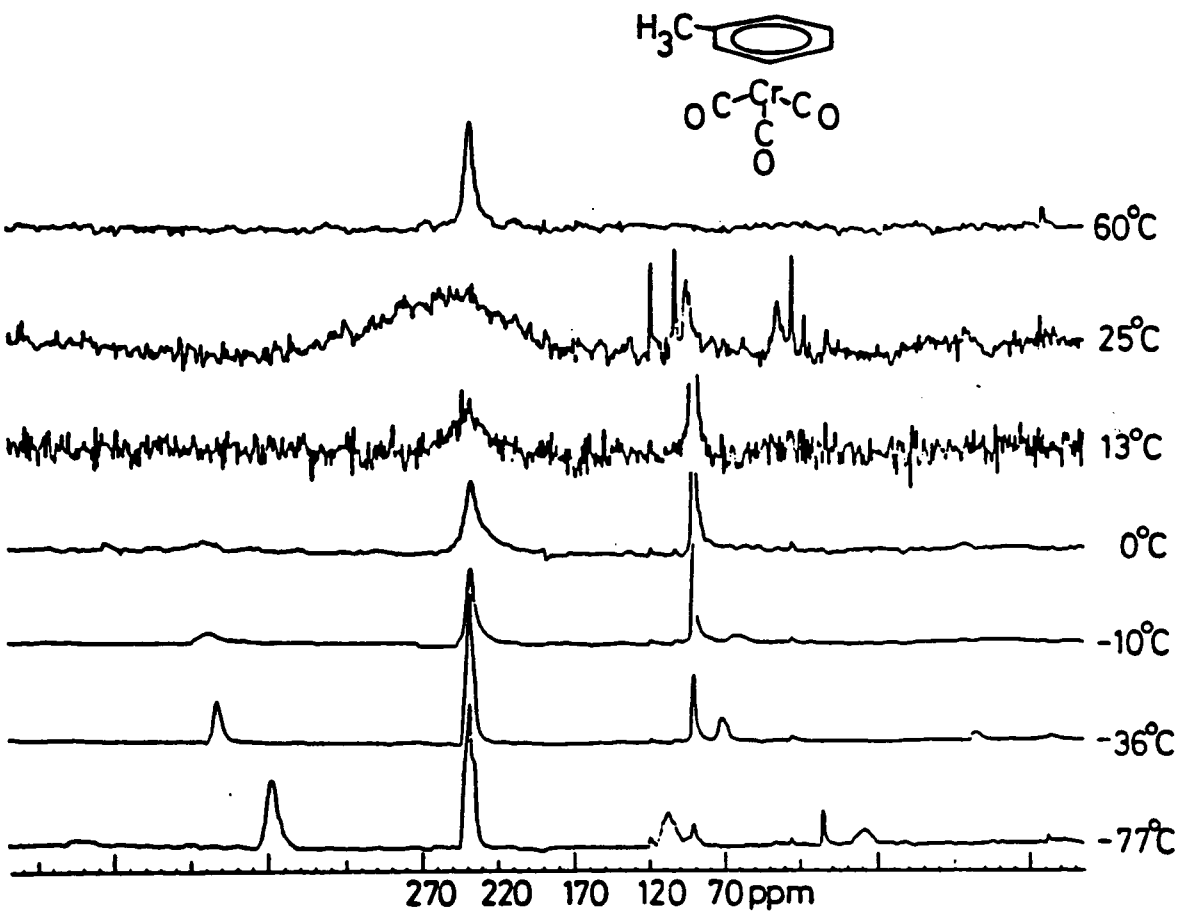

Figure 17. Variable Temperature 22.63 MHz CP-MAS ^{13}C NMR Spectra of ^{13}CO Enriched $Cr(CO)_3(\eta^6\text{-}C_6H_5CH_3)$

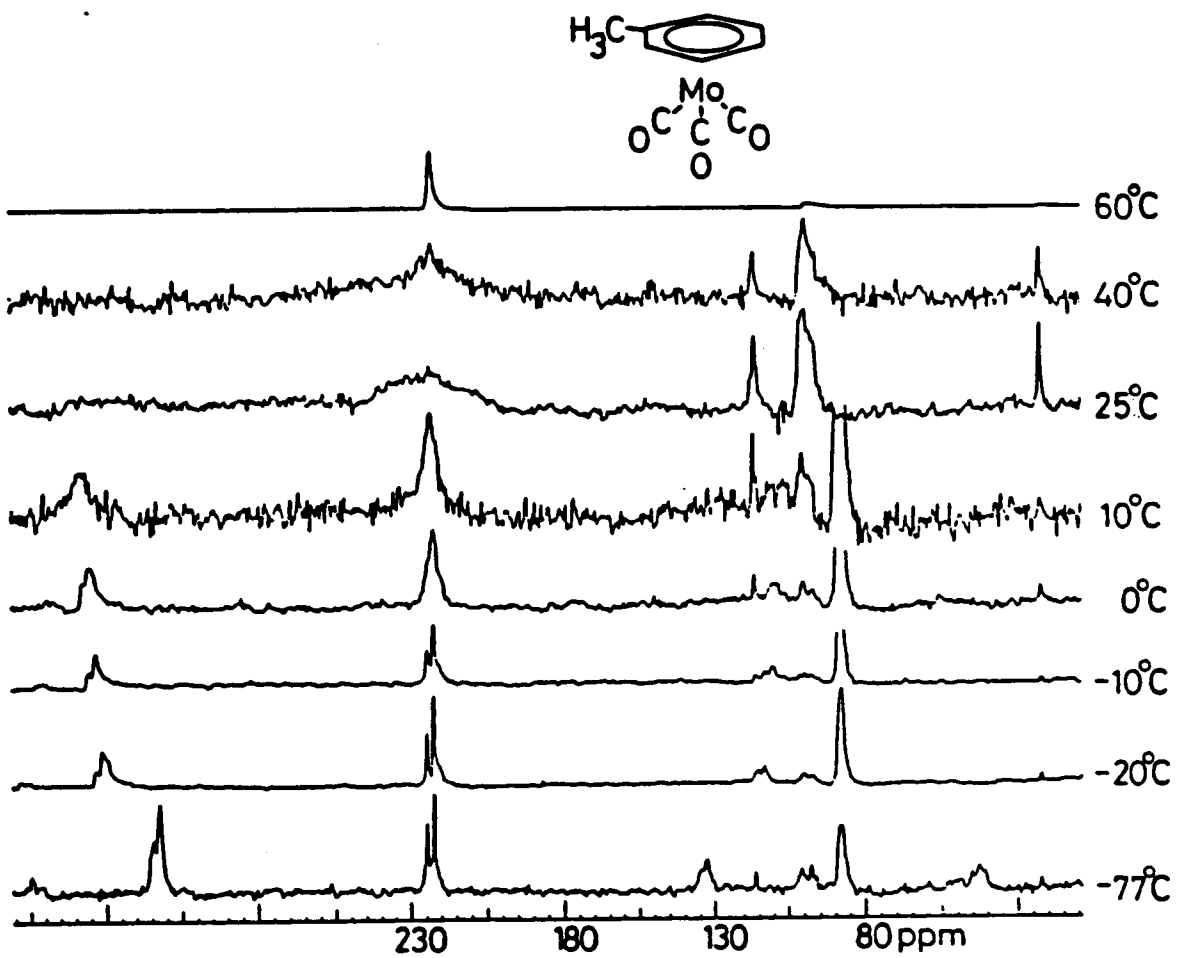

Figure 18. Variable Temperature 22.63 MHz CP-MAS ^{13}C NMR Spectra of ^{13}CO Enriched $Mo(CO)_3(\eta^6\text{-}C_6H_5CH_3)$

sharpens to a single resonance at 224 ppm with a linewidth of 94 Hz. However, at -10°C, two overlapping signals are present at 226 and 223 ppm, both having a linewidth of 21.5 Hz. At -20°C, the resonances sharpen to 15.6 Hz and are well resolved. The relative intensities of the peaks at 226 and 223 ppm are approximately 1:2. This is attributable to two different types of carbon monoxide ligands present in different chemical environments within the molecule. Spinning sidebands are evident in the lower temperature spectra as is the delrin signal at 89.3 ppm. The signals due to the ring carbons are also observed but do not demonstrate any chemical shift or linewidth changes at different temperatures.

The NMR data for $M(CO)_3(\eta^6\text{-}C_6H_5CH_3)$ (M = Cr, Mo), shown in Figures 17 and 18, show two distinct linebroadening regions. This is most easily seen in the data for the molybdenum compound in Figure 18. From -77 to 0°C, the signals due to two different carbonyl environments collapse into a single broad line. These sharpen from 0°C to 10°C and then broaden extensively at room temperature. The low temperature linebroadening region is easily explained by exchange of carbonyl ligands between the two different environments present in the molecule. This represents typical solution-like behavior for a fluxional process. The high temperature linebroadening is more complicated but is probably due to the same motional process responsible for carbonyl exchange. Analyses of the linewidths at various temperatures[86] for both complexes yield activation energies for rotation of the tricarbonyl groups in $Cr(CO)_3(\eta^6\text{-}C_6H_5CH_3)$ and $Mo(CO)_3(\eta^6\text{-}C_6H_5CH_3)$ of 15.5 and 17 kcal/mol, respectively. These values are presented in Table 6 along with the value calculated for $Mo(CO)_3(\eta^6\text{-}C_6H_6)$.

The results indicate that the aromatic rings in both the chromium and molybdenum compounds are static in the solid state since the linewidths due to the ring carbons do not vary as the temperature (and, hence, the correlation times for any rotational motions) is changed. Furthermore, the chemical shifts remain unchanged which indicates that only one rotational conformation is present in the solid state. Thus, the methyl group on the ring effectively prevents rotation of the aromatic ligand in contrast to the rapid rotation observed for the benzene rings in solid

Table 6

Activation Energies for Tricarbonyl Group Rotations in Crystalline $M(CO)_3$(arene) Complexes

Compound	E_a (kcal/mol)
$Cr(CO)_3(\eta^6\text{-}C_6H_5CH_3)$	15.5
$Mo(CO)_3(\eta^6\text{-}C_6H_5CH_3)$	17
$Mo(CO)_3(\eta^6\text{-}C_6H_6)$	~4

$Cr(CO)_3(\eta^6\text{-}C_6H_6)$[45] and $Mo(CO)_3(\eta^6\text{-}C_6H_6)$ (Section 5F). This is consistent with the x-ray structure determined for $Cr(CO)_3(\eta^6\text{-}C_6H_5CH_3)$.[84] However, at 25°C, the broadness of the carbonyl signals for both complexes is consistent with a rotational motion of the tricarbonyl group. The rate is near the point of maximum line broadening, i.e. $\omega_1\tau_c \cong 1$, in a manner analogous to $Mo(CO)_3(\eta^6\text{-}C_6H_6)$. As the samples are heated to 60°C, the linewidths narrow as the correlation times decrease so that the rates of the rotational motions for the two complexes approach the short correlation limit where $\omega_1\tau_c < 1$. The long correlation limit for the rotational motions of the tricarbonyl groups is neared as the samples are cooled and the correlation times increase so that $\omega_1\tau_c > 1$ as evidenced by a narrow line for the carbonyls at 10°C for $Mo(CO)_3(\eta^6\text{-}C_6H_5CH_3)$. At even lower temperatures, the rotational motion is sufficiently slow so that the distinct carbonyl ligands present in different chemical environments within the complexes are distinguishable by NMR. This is particularly evident for the molybdenum compound (Figure 18) and accounts for the shoulder in the -77°C spectrum of $Cr(CO)_3(\eta^6\text{-}C_6H_5CH_3)$. In these cases, the distinct carbonyl ligands are separated by about 3 ppm whereas in the case of $Mo(CO)_3(\eta^6\text{-}C_6H_6)$, the observed separation was only 1 ppm. This suggests that the symmetry of a ligand within a complex affects the chemical environments of the carbonyl ligands to a greater extent than the symmetry imposed by neighboring molecules in the crystal lattice.

5H DISCUSSION

The chemical shifts of the molybdenum tricarbonyl model compounds discussed in this chapter lie in a rather narrow range between 230 and 223 ppm. Chemical shifts reported for other zerovalent molybdenum tricarbonyl complexes in solution also fall within this range.[32] In view of the wide variety of ligands present in these zerovalent molybdenum tricarbonyl compounds, this narrow chemical shift range of 7 ppm appears to be very descriptive for this particular metal tricarbonyl fragment. Therefore, one would expect the chemical shifts of other types of molybdenum tricarbonyl complexes to lie near this range. This was observed for the chemical shift of alumina supported $Mo(CO)_3$(ads) which had a value of 223 ppm as noted in Chapter 4.

Of all the model compounds studied, only the arene-metal tricarbonyl complexes demonstrated tricarbonyl group rotation in the solid state. The complexes $Mo(CO)_3(CH_3CN)_3$ and $Mo(CO)_3$(diglyme) were assessed to be static in the solid state for two reasons. The first reason is that the linewidths of the carbonyl signals were sharp at ambient temperatures and did not broaden in lower temperature spectra. Secondly, the very intense sideband patterns indicated a large chemical shift anisotropy for the carbonyl ligands. These values were estimated by inspection[89,90] to be about 400 ± 50 ppm for both $Mo(CO)_3(CH_3CN)_3$ and $Mo(CO)_3$(diglyme) and is close to the value of 400 ppm expected for a static metal carbonyl.[91] The chemical shift anisotropies of the carbonyl ligands in the arene-metal tricarbonyl complexes are less than about 300 ppm (estimated for $Mo(CO)_3(\eta^6\text{-}C_6H_5CH_3)$) at ambient temperatures and decrease dramatically at elevated temperatures due to accelerated motional averaging. However, the chemical shift anisotropies were seen to increase at subambient temperatures as the motional averaging was decreased and approached the value expected for a static metal carbonyl.[91]

Therefore, fluxional molybdenum tricarbonyl groups are characterized by both a definite chemical shift range, 230 - 223 ppm, and a reduced chemical shift anisotropy at higher temperatures. Furthermore, a broadened signal is observed at ambient temperatures only for those complexes in which the carbonyl ligands are involved in a motional process where the rate of the tricarbonyl group rotation is near the point of maximum broadening, i.e. $\omega_1\tau_c \cong 1$.[86]

CHAPTER 6
DYNAMICS OF γ-ALUMINA SUPPORTED $Mo(CO)_3$(ads) AND $Mo(CO)_5$(ads)

6A GENERAL

As demonstrated in Chapter 5, the ^{13}C NMR signals of static zerovalent molybdenum tricarbonyl groups are characterized by a narrow linewidth (< 6 ppm at 22.6 MHz for $Mo(CO)_3(CH_3CN)_3$ at 25°C) and their chemical shift values lie within a range of 7 ppm. Also, the presence of very intense sidebands indicates a large chemical shift anistropy which is not reduced by a motional process. However, in the case of fluxional molybdenum tricarbonyl groups, the carbonyl ^{13}C NMR signals have a broad linewidth at ambient temperatures (> 30 ppm for $Mo(CO)_3(\eta^6\text{-}C_6H_6)$ at 22.6 MHz at 25°C) which is much greater than the 7 ppm range of chemical shift values observed in the compounds studied. These broad carbonyl signals were then observed to narrow at high and low temperatures which clearly demonstrated the presence of fluxional processes in the (arene)$M(CO)_3$ compounds. Furthermore, as indicated by the lack of spinning sidebands, the chemical shift anistropy was reduced for these complexes as a result of the motional averaging. The results of Shirley[92] indicated reduced chemical shift anisotropies for $Mo(CO)_3$(ads) and $Mo(CO)_5$(ads) which were explained by motional processes involving the carbonyl ligands. This chapter discusses experimental results which further demonstrate the dynamic behavior of these γ-alumina supported molybdenum subcarbonyls.

6B RESULTS FOR $Mo(CO)_3$(ads)

The linewidth of the 15.0 MHz CP-MAS ^{13}C NMR spectrum of $Mo(CO)_3$(ads) shown in Figure 5 (Chapter 4) is broad at 25°C and has a linewidth of about 16.4 ppm. It was mentioned in Chapter 4 that a motional process involving the tricarbonyl group may be responsible for the broad linewidth. An alternative explanation is that the heterogeneity of the γ-alumina surface would cause the molybdenum tricarbonyl groups to reside in sites possessing different chemical environments which would result in a different chemical shift for a tricarbonyl group adsorbed to each different site. However, in view of the narrow range of chemical shifts (< 7 ppm) observed

for the carbonyl signals in the molybdenum tricarbonyl model compounds, which possess a wide variety of coordinated ligands, it would be difficult to suppose that the various surface sites on the γ-alumina surface could cause the large distribution of chemical shifts (> 16 ppm) observed in the 15.0 MHz spectrum of $Mo(CO)_3$(ads) at 25°C. Furthermore, there is an absence of spinning sidebands for the carbonyl ligands in $Mo(CO)_3$(ads) which indicates a chemical shift anistropy that is lower than the value of about 400 ppm expected for a static metal carbonyl.[91] Shirley[92] estimated a value of 390 ± 50 ppm for the chemical shift anistropy of $Mo(CO)_3$(ads) and indicated that any motional process present must be occuring at a frequency of less than 15 kHz. Therefore, the nature of the 15.0 MHz CP-MAS ^{13}C NMR spectrum of $Mo(CO)_3$(ads) at 25°C is consistent with a fluxional molybdenum tricarbonyl group on the γ-alumina surface.

It was decided to obtain variable temperature CP-MAS ^{13}C NMR spectra of $Mo(CO)_3$(ads) in order to clearly demonstrate the presence of a motional process involving the molybdenum tricarbonyl group. However, attempts at achieving these spectra were plagued by a significant reduction in signal-to-noise at higher and lower temperatures as demonstrated in Figure 19 by a pair of 75.5 MHz CP-MAS ^{13}C NMR spectra obtained for $Mo(CO)_3$(ads) at 302 K and 325 K. The 302 K spectrum consisted of 2706 scans and the 325 K spectrum was the result of 2792 scans. Attempts at recording subambient temperature spectra were also subject to similar difficulties. This reduced signal-to-noise may be due to either an alteration of the spinning angle at higher and lower temperatures or a change in the Hartmann-Hahn matching condition for cross polarization. The dilute nature of the ^{13}C spins in a sample of $Mo(CO)_3$(ads) did not allow for recalibration of the magic angle or retuning at a sustained non-ambient temperature (magic angle calibration and tuning were performed at ambient temperatures using samples of hexamethylbenzene and admantane). However, the cause of the reduction in signal-to-noise at non-ambient temperatures was not determined and adequate variable temperature spectra were not obtained for $Mo(CO)_3$(ads).

In the course of this work, different spectrometers were used to obtain ambient temperature CP-MAS ^{13}C NMR spectra for $Mo(CO)_3$(ads) at three different field strengths. These spectra,

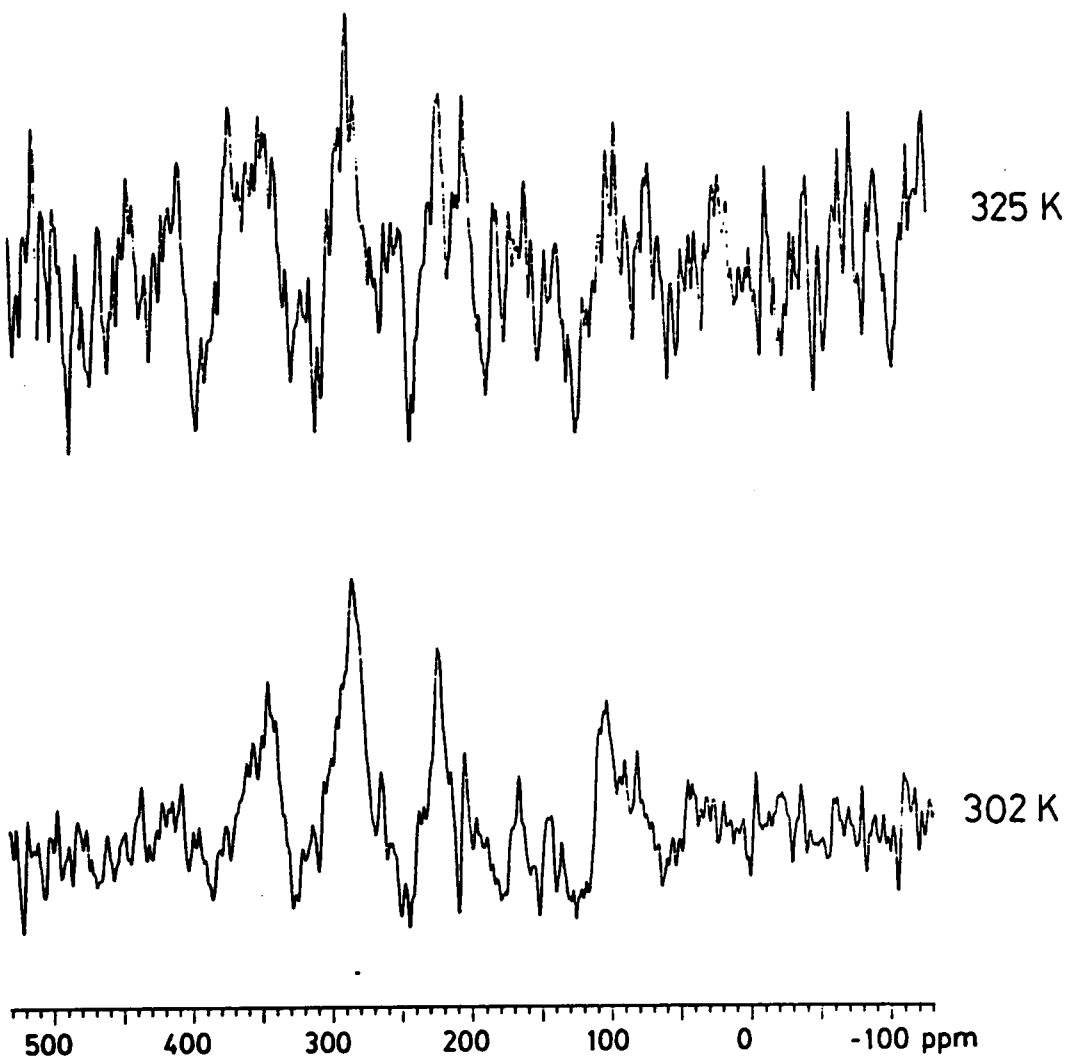

Figure 19. Variable Temperature 75.5 MHz CP-MAS ^{13}C NMR Spectra of $Mo(CO)_3$(ads)

which are shown together in Figure 20, show that the linewidth of the tricarbonyl signal (expressed in ppm) decreases in the higher field spectra. The linewidths of the spectra are as follows: 16.4 ppm at 15.0 MHz, 13.0 ppm at 22.6 MHz and 7.4 ppm at 75.5 MHz. If the natural logarithm (ln) of the linewidths (in ppm) is plotted against the natural logarithm of the field strengths (in MHz), a straight line results having a slope of -0.5. This demonstrates a linewidth dependence on the field strength which varies approximately as the inverse of the square root of the magnetic field. The dependence of ^{13}C NMR linebroadenings have been investigated for various organic solids,[93] but none of the linebroadening mechanisms reported fit the observed inverse square root dependence on the field strength.

One possible explanation for the linenarrowing at the higher fields is that a faster sample spinning rate was used. The spin rates were about 2200 Hz in the 15.0 MHz spectrum and about 4600 Hz in the 75.5 MHz spectrum. Comparing these values gives a power dependence of the linewidth (in ppm) on the spinning rate of -1.1. However, a similar analysis of the linewidths obtained for $Mo(CO)_3(\eta^6\text{-}C_6H_6)$ at 25°C with spinning rates of 2350 Hz at 22.6 MHz and 4400 Hz at 75.5 MHz yields a power dependence of -0.75 for the linewidth (in ppm). The disagreement of these dependences suggests that a different mechanism is responsible for the linenarrowing at higher fields. It is noteworthy that the dependence of the carbonyl linewidth of the fluxional $Mo(CO)_3(\eta^6\text{-}C_6H_6)$ complex on the field strength is -0.4 which is close to the value of -0.5 observed for $Mo(CO)_3$(ads). The dependences of the linewidths of the carbonyl signals on both field strength and spinning rate are summarized in Table 7 for $Mo(CO)_3$(ads) and $Mo(CO)_3(\eta^6\text{-}C_6H_6)$.

Another possible explanation is that a quadrupolar coupling between molybdenum and carbon is causing the line-narrowings at the higher fields. However, a very narrow linewidth of about 0.7 ppm was obtained for the static $Mo(CO)_3$(diglyme) complex at 25°C at 75.5 MHz. Furthermore, the linewidths of the complexes $Mo(CO)_3(\eta^6\text{-}C_6H_6)$ and $Mo(CO)_3(\eta^6\text{-}C_6H_5CH_3)$ obtained at very low temperatures at 75.5 MHz and 22.6 MHz, respectively, were also about 0.7 ppm indicating that

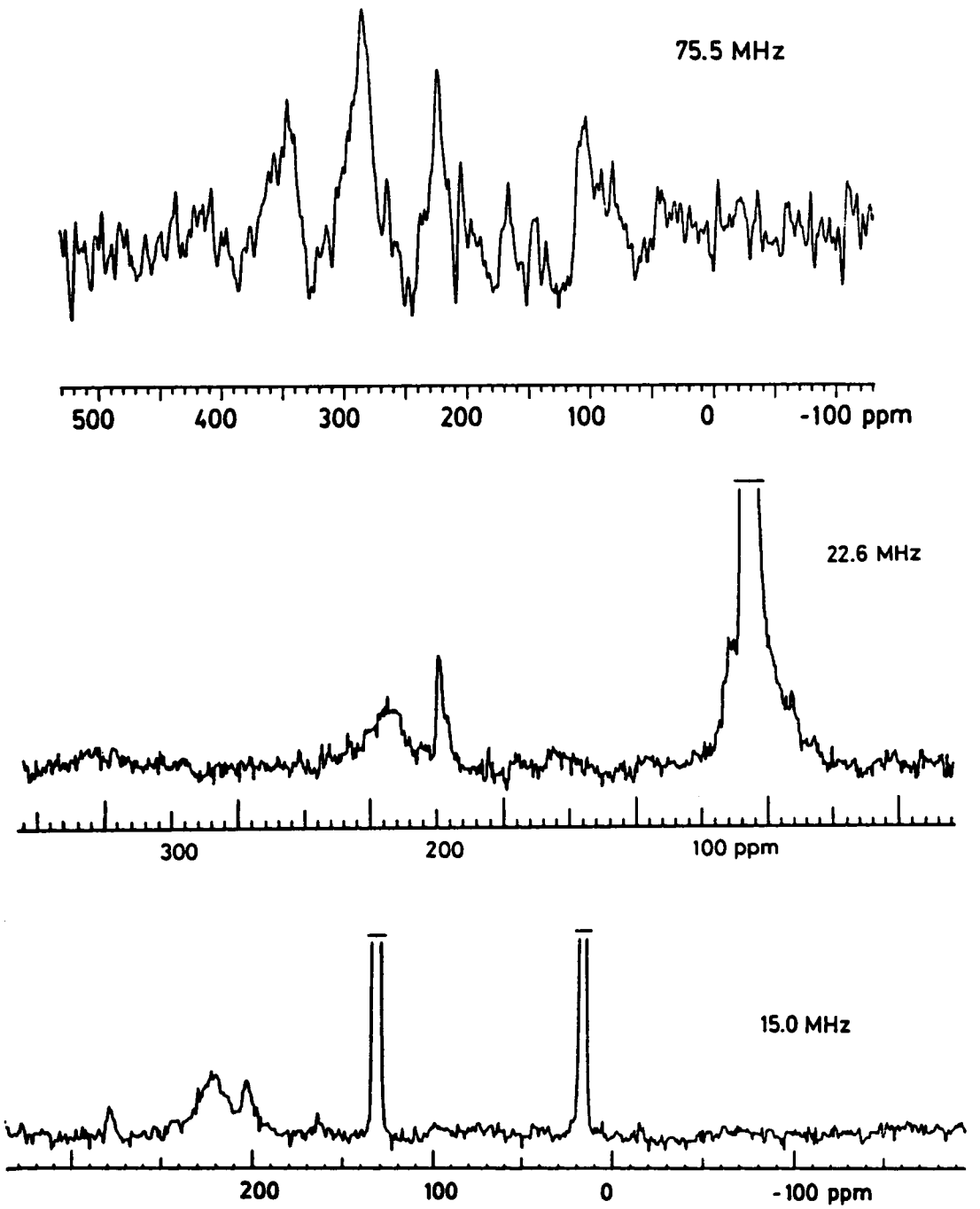

Figure 20. CP-MAS ^{13}C NMR Spectra of $Mo(CO)_3$(ads) at Various Field Strengths

Table 7

CP-MAS ^{13}C NMR Linewidth Dependences for Carbonyl Resonances in Molybdenum Tricarbonyl Complexes

Complex	T_K	Field Strength (B_0)	Spin Rate (ν_{rot})	Linewidth	Dependence[a] B_0	ν_{rot}
$Mo(CO)_3(\eta^6\text{-}C_6H_6)$	298 K	22.6 MHz	2350 Hz	3.2 ppm	-0.4	-0.75
	298 K	75.5 MHz	4400 Hz	2.0 ppm		
	230 K	75.5 MHz	3900 Hz	0.7 ppm		
$Mo(CO)_3$(ads)	298 K	15.0 MHz	2200 Hz	16.4 ppm	-0.5	-1.1
	298 K	22.6 MHz	----	13.0 ppm		
	298 K	75.5 MHz	4600 Hz	7.4 ppm		

[a] Values are exponents for a power law dependence on the given variable.

the motions of the carbonyl ligands were in the slow exchange regime, i.e. $\omega_1\tau_c > 1$, which narrowed the linewidths. These very narrow linewidths, obtained in the absence of motional averaging, demonstrate that there is very little quadrupolar coupling between molybdenum and carbon and, furthermore, that there is no dependence of the static linewidths (in ppm) of the carbonyl signals on the field strength or spinning rate.

The most likely explanation is that a motional process is responsible for the line-narrowings observed in the higher field spectra of $Mo(CO)_3$(ads). Thus, at the higher fields, the difference between the frequency of the motional process (which remains constant at ambient temperature) and the observation frequency is increasing. This causes a narrowing of the linewidths since the product of the correlation time and the decoupling field strength approaches the slow exchange regime, i.e. $\omega_1\tau_c > 1$.[86]

The power dependence of the linewidth on the field strength does not fit the theoretical value[93] since the rate of the motional process is not in the slow exchange regime, i.e. $\omega_1\tau_c >> 1$.[86]

Therefore, there is good evidence for a motional process involving the carbonyl ligands in $Mo(CO)_3$(ads). This process is perhaps best visualized as a rotation of the molybdenum tricarbonyl group in a manner analogous to the (arene)$M(CO)_3$ complexes discussed in Chapter 5; although a pairwise exchange of the carbonyl ligands cannot be ruled out. The detection of this motional process relies on the observation that the linewidth of the carbonyl signal (in ppm) in $Mo(CO)_3$(ads) narrows at higher fields with a power dependence of -0.5 which is close to the value of -0.4 obtained for the fluxional complex, $Mo(CO)_3(\eta^6\text{-}C_6H_6)$. Also, the broadness of the 15.0 MHz spectrum at 25°C and the reduced chemical shift anisotropy support the presence of a fluxional process. The chemical shift anisotropy of the carbonyl signal in the 75.5 MHz spectrum was estimated to be about 300 ± 50 ppm, which is less than the value expected for a static carbonyl,[91] and is in agreement with Shirley's result of 390 ± 50 ppm at 37.7 MHz[92] (although slightly reduced at the higher field). Alternative line-broadening mechanisms such as quadrupolar coupling and sample spinning rates were rejected as these factors did not influence the carbonyl

linewidths of the molybdenum tricarbonyl model complexes in spectra obtained at higher fields and faster spinning rates (in the absence of motional processes). However, variable temperature CP-MAS ^{13}C NMR spectra were not obtained for $Mo(CO)_3$(ads) and, therefore, an activation energy was not calculated for the motional process involving the carbonyl ligands. This calculation was not possible since the dependence of the NMR linewidths vs. field strength at constant temperature is not as straightforward as the dependence of NMR linewidths vs. temperature at constant field.[86] Nevertheless, the CP-MAS ^{13}C NMR results for $Mo(CO)_3$(ads) are best explained by a motional process involving the carbonyl ligands.

6C RESULTS FOR $Mo(CO)_5$(ads)

The 15.0 MHz CP-MAS ^{13}C NMR spectrum of $Mo(CO)_5$(ads) at 25°C has a linewidth of 3.37 ppm which is much narrower than the linewidth of $Mo(CO)_3$(ads). However, the linewidth is much broader than those observed in the model molybdenum tricarbonyl complexes in the absence of any motional processes (about 0.7 ppm). Also, the absence of any spinning sidebands indicates a chemical shift anisotropy which is less than about 300 ppm, which is much less than the chemical shift anistropy expected for a static metal carbonyl.[91] Shirley[92] estimates a chemical shift anistropy of 203 ± 40 ppm for $Mo(CO)_5$(ads) at 37.7 MHz and proposed that the reduced chemical shift anistropy was due to anisotropic motions of the carbonyl ligands. Furthermore, one would expect the presence of both axial and equatorial carbonyl ligands in the $Mo(CO)_5$(ads) structure, but only a single signal is observed. It was mentioned in Chapter 4 that this factor suggested that a motional process may be present in $Mo(CO)_5$(ads) and may also be responsible for the observed reduction in chemical shift anistropy of the carbonyl ligands.

Attempts at obtaining variable temperature CP-MAS ^{13}C NMR spectra for $Mo(CO)_5$(ads) were unsuccessful; probably for the same reasons discussed in the preceding section (6B). However, spectra were obtained at two different field strengths which indicated a narrowing of the linewidth (in ppm) at the higher field. These spectra are shown in Figure 21. The linewidths were 3.37 ppm and 2.9 ppm at the field strengths of 15.0 and 22.6 MHz, respectively. These values yield a power

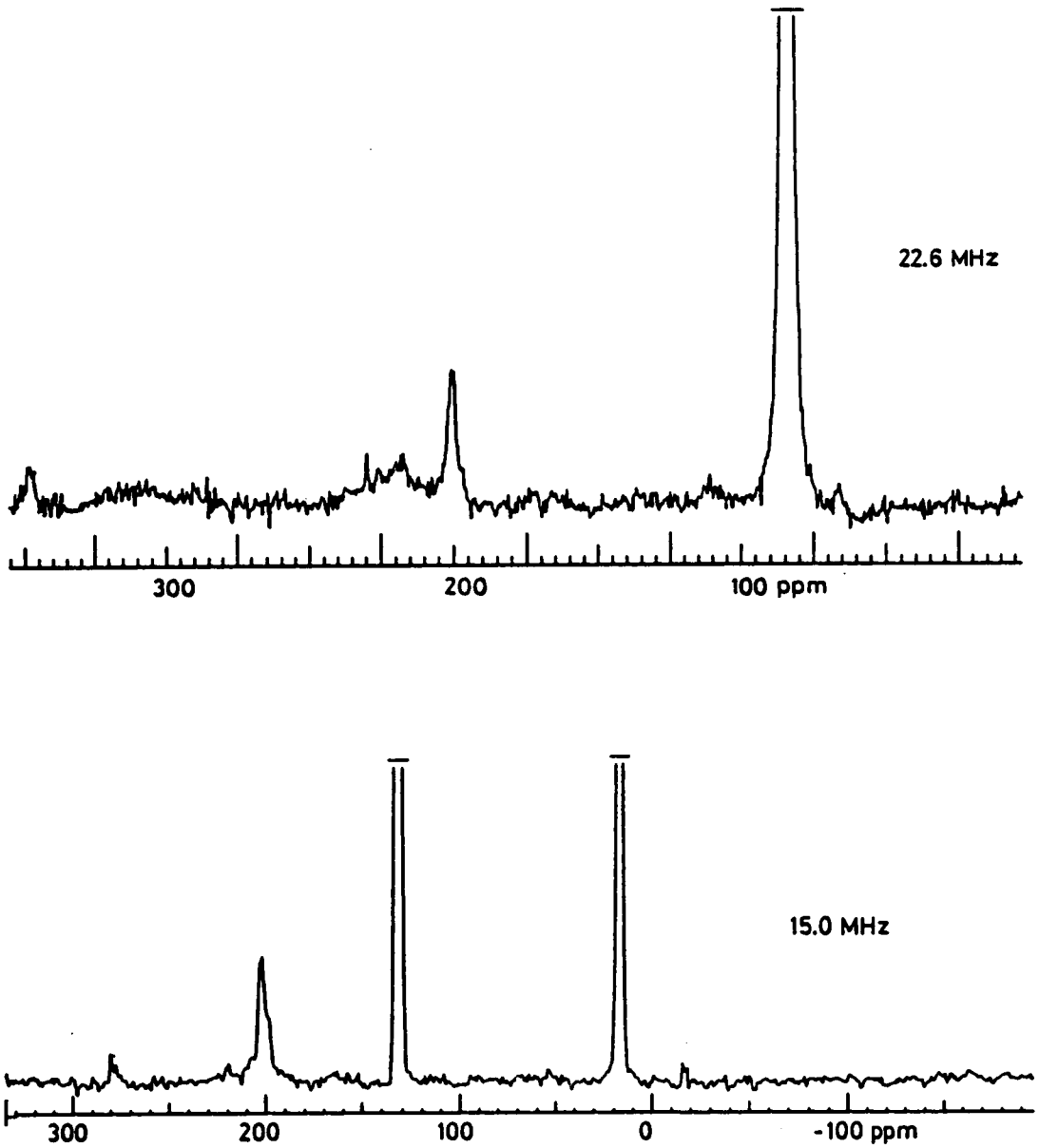

Figure 21. CP-MAS ^{13}C NMR Spectra of $Mo(CO)_5$(ads) at Two Different Field Strengths

dependence of the linewidth on the field strength of -0.4 which is near the values observed for the linewidth dependence of the signals for $Mo(CO)_3$(ads) and $Mo(CO)_3(\eta^6\text{-}C_6H_6)$ vs. field strength (Table 7). The spinning rates at the two fields were 2200 Hz at 15.0 MHz and about 3300 Hz at 22.6 MHz. These values yield a linewidth dependence on the spinning rate of -0.4 which does not correlate with the spinning rate dependences observed in the tricarbonyl complexes (Table 7). This fact also suggests that variation in spinning rate is not responsible for the observed line narrowings at higher fields.

If it is assumed that there is an absence of significant quadrupolar coupling in $Mo(CO)_5$(ads), as was demonstrated for the molybdenum tricarbonyl model compounds (Section 6B), then the only reasonable mechanism which could account for the observed line narrowings at higher field strengths is a motional process in agreement with Shirley's results.[92] This motional process may involve a pairwise exchange between axial and equatorial ligands, in a manner similar to the Berry pseudorotation mechanism.[75] A process such as this would explain the observation of only a single resonance for the carbonyl ligands in $Mo(CO)_5$(ads). An alternative mechanism would be a C_4 rotation of the equatorial ligands causing the observed broadening of their single carbonyl signal which may then be occluding the resonance of the unique axial carbonyl ligand signal in $Mo(CO)_5$(ads). However, molybdenum pentacarbonyl model compounds were not studied in this dissertation and, therefore, no analogies can be drawn to suggest one mechanism over the other as was possible for $Mo(CO)_3$(ads). Nevertheless, the CP-MAS results for $Mo(CO)_5$(ads) suggest that the carbonyl ligands are involved in a motional process which causes a narrowing of the carbonyl signal in higher field spectra and a reduced chemical shift anisotropy.

CHAPTER 7
INTERACTION OF ACETONE WITH PARTIALLY DEHYDROXYLATED γ-ALUMINA

7A GENERAL

As mentioned in Chapter 1, acetone is highly reactive with the alumina surface and has been the subject of many previous studies.[56-59] This study was undertaken in order to identify the various adsorbed acetone species as well as the reaction intermediates. This knowledge was critical in interpreting the results for the adsorption of $Mo(CO)_3(CH_3CN)_3$ onto alumina from acetone solution given in Chapter 3.

Although isotopically substituted acetones (acetone-d_6 and acetone-2-^{13}C) were also studied, only the results for isotopically normal acetone will be presented here. The isotopically substituted molecules aided in the assignment of IR adsorption bands and these results as well as those for isotopically normal acetone have been published elsewhere.[65]

7B EXPERIMENTAL

The γ-alumina studied was produced by the hydrothermal conversion of high purity bayerite to boehmite in a Parr bomb. In a typical preparation, the Parr bomb was charged with 100 g of bayerite, 10 g of water and heated to 510 K for 2 h. Boehmite was converted to γ-alumina by heating to 820 K for 2 h in flowing air in 100 g lots. Gamma-alumina was confirmed by the x-ray diffraction pattern of the material. The alumina was sieved through 100 mesh; the surface area was determined to be 67 m^2g^{-1}. Iron content of the material was determined to be 0.001% by elemental analysis.

Acetone, HPLC grade; acetone-d_6, 100.0 mole %; and iodomethane, 99%, were obtained from Aldrich Chemical Company. Acetone labeled with ^{13}C at the carbonyl carbon (99 mole %) was obtained from Cambridge Isotopes. The solvents were stored over molecular sieves after opening. The liquids were outgassed prior to introducing their vapor to the IR cell by three freeze-pump-thaw cycles.

All in situ infrared spectra were recorded on an IBM-98 FTIR spectrometer equipped with a liquid nitrogen cooled narrow band MCT detector. The resolution was 4 cm^{-1}; 128 scans were collected for each spectrum. A schematic representation of the high vacuum cell used in this work is shown in Figure 22. The window materials consist of KRS-5 which were held in place with 2 1/8 inch diameter conflat flanges and sealed with viton-A O-rings. The vacuum cell is connected to an Inficon Quadrex 200 quadrupole mass spectrometer. Data aquisition, temperature and pressure programming are controlled by a Bruker Aspect 2000 computer.

In a typical experiment, 15 to 25 mg of alumina powder was pressed at 33.5 MPa into a pellet 13 mm in diameter. The pellet was then mounted in the infrared cell where it was preated at 700 K for 1 h at 10^{-6} torr. This treatment yields a γ-alumina with a partially dehydroxylated surface. The pellet was then cooled in vacuo to the desired temperature and the appropriate liquid vapor was allowed to contact the wafer. In repeat experiments, absorbance values vary no more than 10% when corrected for the weight of the pellet.

7C RESULTS

Infrared spectra of acetone adsorbed on γ-Al_2O_3 at 300 K are shown in Figure 23 as a function of acetone pressure. The pellet for this sample was preheated to 700 K under vacuum to yield a partially dehydroxylated surface. All spectra in the series are referenced to the pellet before exposure to acetone. Thus, as acetone is introduced, the negative peaks centered at 3750 cm^{-1} are due to loss of isolated surface hydroxyl groups. With increasing acetone pressure, a broad band at 3500 cm^{-1} grows in intensity. This indicates the concurrent formation of hydrogen bonded surface hydroxyl groups with loss of isolated hydroxyl groups.

The C-H stretching region is dominated by aliphatic C-H stretches; however, a small but significant band occurs above 3000 cm^{-1}. This is consistent with a small amount of unsaturated hydrocarbon on the surface. After evacuation, most of the intensity above 3000 cm^{-1} disappears.

At pressures of 1 torr and higher, gas phase acetone is observed in the infrared spectra. The carbonyl stretch at 1738 cm^{-1} is due to acetone in the gas phase. Comparision with the spectrum

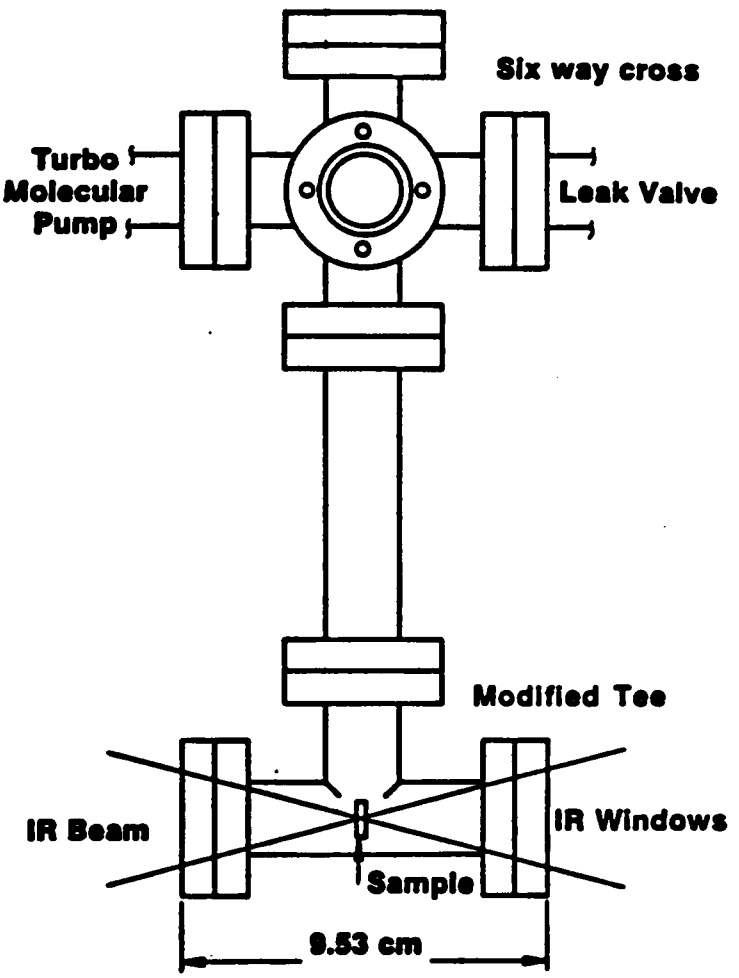

Figure 22. Diagram of In Situ UHV Infrared Cell

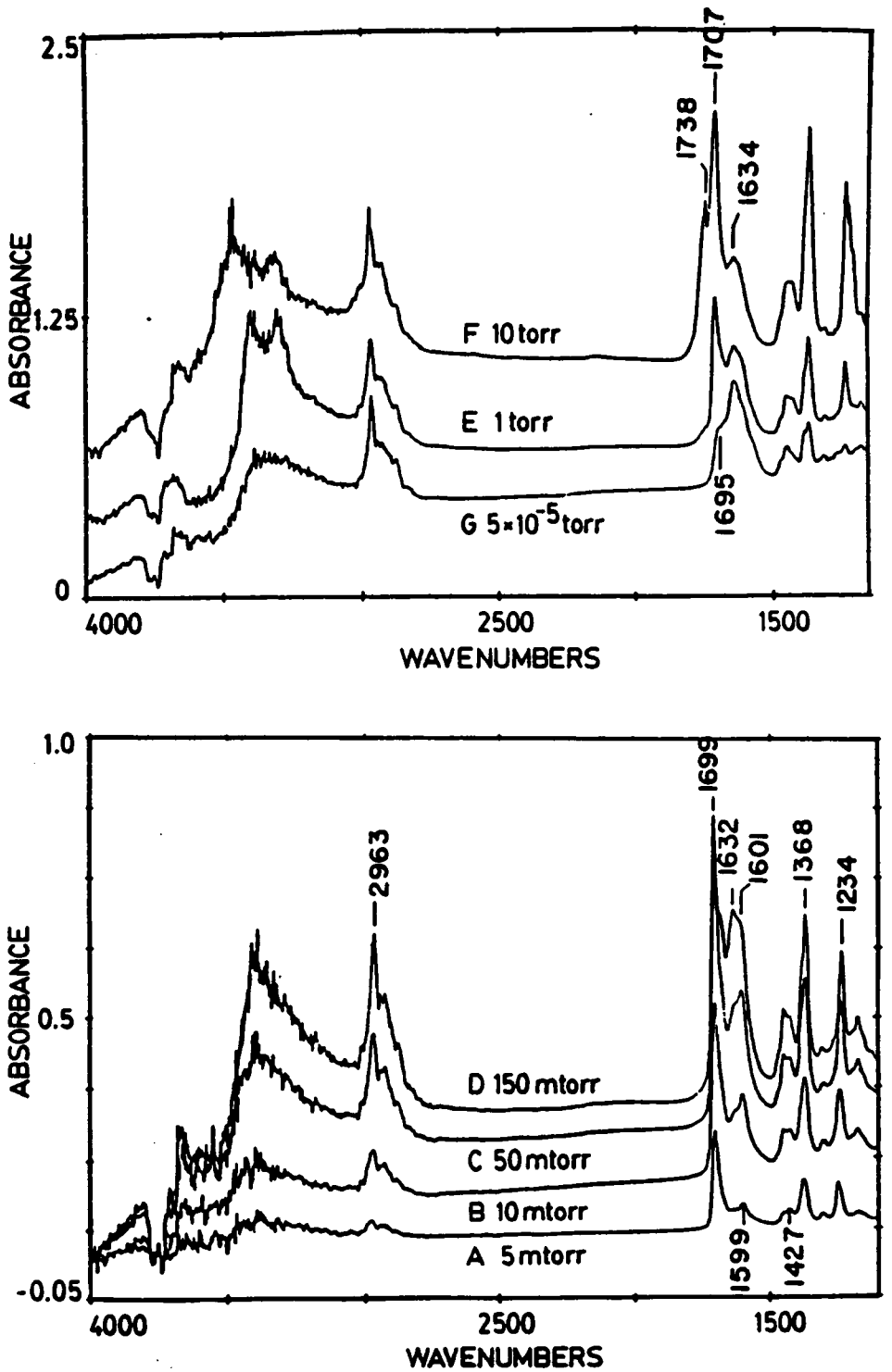

Figure 23. Infrared Spectra for the Adsorption of Acetone on γ-Alumina at 300 K

of gas phase acetone allows the assignment of peaks at 1427 and 1368 cm^{-1} to CH_3 bending modes and the 1234 cm^{-1} peak to the C-C stretch of acetone. These are not perturbed upon adsorption.

In the carbonyl region, the most prominent band occurs at 1697 cm^{-1} at a low pressure of acetone. The position of this band moves to higher wavenumbers with an increasing pressure of acetone until it appears at 1707 cm^{-1} at 10 torr. A band assigned to liquid acetone is observed at 1711 cm^{-1}. Additional bands are observed at 1632 cm^{-1} and 1599 cm^{-1} at low pressure (Figure 23 (a)). As the pressure of acetone increases, the 1632 cm^{-1} band increases in relative intensity with respect to the 1599 cm^{-1} band (Figures 23 (b), (c)). The 1599 cm^{-1} band shifts sightly to higher wavenumber with increasing pressure.

Upon evacuation, the major band in the carbonyl region occurs at 1634 cm^{-1} with a shoulder at ca. 1695 cm^{-1} (Figure 23 (g)). The total intensity of the C-H region compared to the carbonyl region is greater in the evacuated spectrum than observed at lower pressures (compare the 150 millitorr spectrum with the 5×10^{-5} torr spectrum, Figures 23 (d) and (g)).

7D DISCUSSION

Adsorption of acetone on γ-alumina at 300 K (Figure 23) results in the appearance of two peaks at 1696 and 1596 cm^{-1}. The high frequency band is assigned to acetone adsorbed at a Lewis acid site consistent with the literature[94-97] and is represented in Figure 23 (a). Miyata, et al.[95,96] assigned a low frequency band at 1580 cm^{-1} for acetone on NiO to a different Lewis acid site for acetone adsorption. This is a very large shift in frequency (more than 130 cm^{-1} compared to gas phase acetone) for acetone to have retained its structure; i.e., a discrete carbonyl group. A more plausible explanation is the formation of an acetone enolate on the surface. Miyata, et al.[95,96] and Griffiths and Rochester[97] assign the enolate structure to the more slowly developing bands at $\sim$1545 cm^{-1} and 1430 cm^{-1}. It is proposed that these bands are more appropriately assigned to surface carboxylate structures (vide infra).

Structural and infrared data for some isolated alkali metal enolates are compiled in Table 8.[98,99] For pinacolone, the C-O bond length in the enolate is significantly longer than that for

Table 8

Data for Enolates

Molecule	Infrared Stretching Frequencies (C-H (cm^{-1}))(C=O,C_2L(cm^{-1}))	Bond Lengths (Å) d C-O[b]	d C-C[b]
Li-pinacolone enolate	3118w 1615s 1586m 1540m[a]	1.342(6)	1.330(6)
Na-pinacolone enolate	3112vw 3081w 1598s 1555sh[a]	1.308(4)	1.350(6)
K-pinacolone enolate	3090w 1560s 1526w[a]	1.306(4)	1.350(4)
Li-acetone enolate	3086w 1610s 1572m 1542sh[a]		
Li-di-n-propyl enolate	1634s[a]		
Li-di-isopropyl enolate	1638s[a]		
alumina acetone (100 mtorr)	1596		
alumina acetone-d_6 (100 mtorr)	1585		
alumina acetone-2-^{13}C (100 mtorr)	1570		

[a] Reference 98
[b] Reference 99

pinacolone.[98] Moreover, the C-C bond length is in the region for a normal double bond. The frequency of the C=C stretching mode varies from 1560 cm^{-1} to 1638 cm^{-1} and is a function of the alkali metal and the ketone. For Li-acetone enolate, the C=C stretch is observed at 1610 cm^{-1}.[99] From the pinacolone data, the frequency shifts to a lower wavenumber for Li, Na and K enolates. For acetone at 300 K (Figure 23), the corresponding band is observed at 1599 cm^{-1} at 5 mtorr pressure. At 1599 cm^{-1}, the frequency is within the region of values for either a carbonyl or an olefin functional group. In the experiment at 300 K, this band shifts to higher wavenumber with increasing coverage. This suggests either that the structure of the surface enolate is strongly dependent on local surface environment or that the band postion is shifted by the growth of a more intense peak at higher wavenumber.

In Figure 23, for acetone adsorbed at 300 K, a frequency shift is observed from 1595 cm^{-1} to 1605 cm^{-1}. Adsorption of mesityl oxide on γ-alumina leads to bands at 1688 and 1613 cm^{-1} (Figure 24). The shift is consistent with mesityl oxide formation on the surface. Mesityl oxide is a dimer of acetone and is generated via acetone enolate. The shift from 1595 cm^{-1} to 1605 cm^{-1} is consistent with formation of acetone enolate followed by production of mesityl oxide (Figure 23 (a)).

The band assigned to acetone at a Lewis acid site (1697 cm^{-1}) also shifts to higher wavenumber with increasing pressure. This phenomenon has been observed by others.[94] At 1 torr, the position of the band (1707 cm^{-1}) corresponds closely to liquid acetone. It is suggested that physisorbed acetone obscures the band due to acetone at Lewis acid sites. Evacuation removes the liquid-like acetone and a band remains as a shoulder at 1690 cm^{-1} (Figure 23). This may be due to either strongly adsorbed acetone or mesityl oxide which gives a similar band (vide supra).

With time and/or increasing pressure (Figure 23), a new band grows in the region 1632 - 1638 cm^{-1} until it becomes the most dominant peak in this region of the spectrum. Additionally, upon evacuation to 10^{-5} torr, this peak is the most intense peak in the C=C, C=O region of the spectrum.

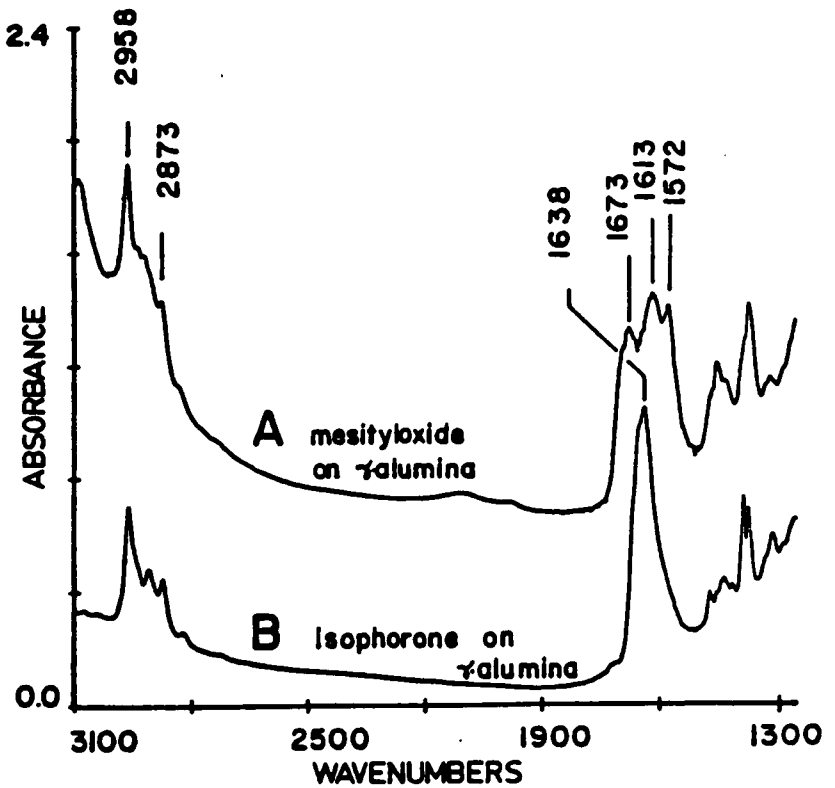

Figure 24. Mesityl Oxide and Isophorone Adsorbed on γ-Alumina at 300 K

The reaction sequence: acetone→acetone enolate→mesityl oxide→isophorone can account for all of the spectral changes observed in the first several hours at 300 K and 400 K. For acetone-2-^{13}C adsorbed on γ-alumina at 400 K (not shown), the growth of the 1630 - 1640 cm^{-1} band occurs concurrently with the increase in C-H intensity relative to the C-O stretching region (Figure 25). It is concluded that a surface species develops which has lost a significant amount of unsaturation. The formation of mesityl oxide and phorone (a dimer and trimer of acetone, respectively) are not good candidates since both contain C=C double bonds in place of carbonyl groups. Significantly, mesityl oxide adsorption alone does not give a band at 1640 cm^{-1}; therefore oligomerization or polymerization of surface mesityl oxide cannot be responsible for growth of the bands at 1630 - 1640 cm^{-1}. Isophorone is a good candidate in that it loses a C=C bond upon cyclization. Furthermore, isophorone on γ-alumina gives an intense band at 1638 cm^{-1} (Figure 24). Production of isophorone accounts for the more rapid growth in the C-H region vs. the C=O, C=C region in the first hour at 400 K (Figure 25).

After long exposures at 300 K, a pair of bands are observed to grow at 1564 and 1443 cm^{-1} for acetone-d_6 (not shown). These are assigned to the asymmetric and symmetric stretches of adsorbed carboxylate and would be near the values for isotopically normal acetone adsorption. Oxidation of adsorbed acetone is much slower than dimerization or trimerization at 300 and 400 K. In experiments at higher temperatures (500 to 700 K), the 1564 and 1443 cm^{-1} bands are the only ones observed in the spectrum of adsorbed acetone-d_6. Oxidation to surface carboxylate is accelerated at elevated temperatures.

To confirm the 1585 cm^{-1} band assignment to adsorbed acetone enolate, an experiment with CH_3I was performed on a sample in which this band was clearly evident. Thus, at 300 K and 100 mtorr of acetone-d_6, a spectrum analogous to Figure 23 (b) was obtained for a fresh pellet of γ-alumina. Treatment with CH_3I caused the 1585 cm^{-1} band to decrease in intensity relative to the 1690 cm^{-1} band. However, the expected desorption product ($CD_3C(O)CD_2CH_3$; 2-butanone) of the reaction between CH_3I and acetone enolate was not observed in the mass spectrum upon

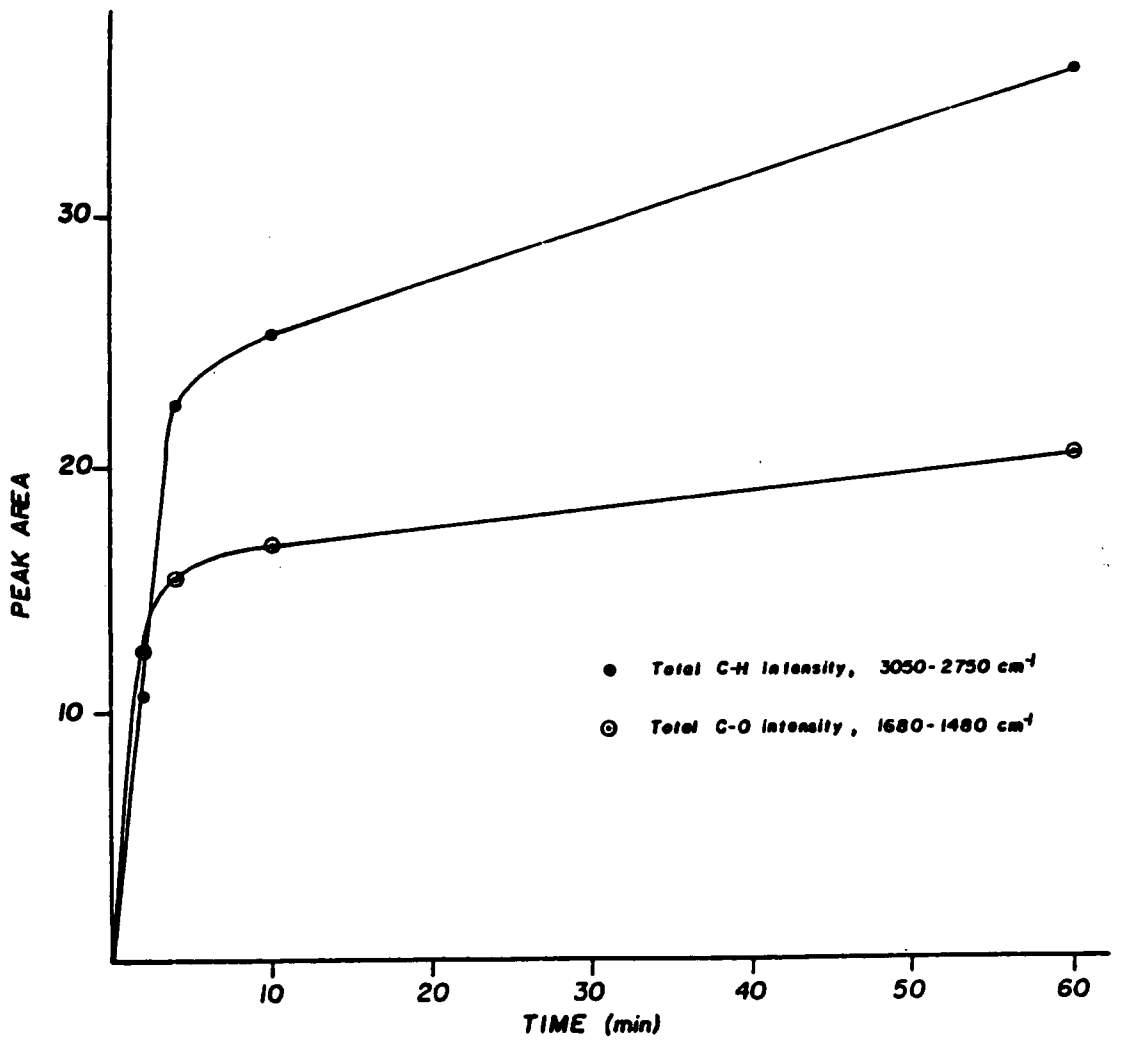

Figure 25. Plot of the Relative Intensities of Integrated Peak Areas of the C-H vs. C-O Regions for Acetone-2-^{13}C Adsorbed on γ-Alumina at 400 K (3050 to 2750 cm^{-1} and 1680 to 1480 cm^{-1}, Respectively)

thermal desorption (TPD). As indicated by IR spectra, most of the adsorbed carbonyl containing species were lost from the surface after evacuation of the IR cell just prior to the TPD experiments. In the absence of mass spectroscopic evidence, the presence of enolate on the surface and the assignment of the 1585 cm^{-1} band to this species relies on spectroscopic evidence. Methyl and methylene groups are present on the surface even after thermal desorption as evidenced by the presence of C-H stretches in the 2750 - 2950 cm^{-1} region.

In summary, the reaction sequence may be outlined in the following way. Acetone interacts with γ-alumina to initially adsorb at Lewis acid sites both through the carbonyl oxygen and as acetone enolate. For clarity these structures are shown in Figure 26. Interconversion of structures I and II in Figure 26 leads to the observed deuterium exchange with surface OH^- by acetone-d_6. For acetone, the appropriate infrared bands are observed at about 1697 cm^{-1} and 1599 cm^{-1} for adsorbed acetone and acetone enolate, respectively. The first of these assignments is in accord with the literature for a number of metal oxides including γ-alumina.[94] The assigment of the 1599 cm^{-1} band to acetone enolate differs from the literature on two counts. In one case, this band is assigned to acetone bonded through the carbonyl oxygen on MgO[95,96] and, in another, acetone enolate is assigned to the more slowly developing bands at 1545 and 1430 cm^{-1} on TiO^2.[97] Three lines of evidence implicate the 1599 cm^{-1} band as acetone enolate: (i) comparison with model compounds (Table 8) which places the C=C stretch in the 1560 to 1630 cm^{-1} region, (ii) the concurrent exchange of surface OH^- with the development of a band at 1585 cm^{-1}, and (iii) the fact that acetone enolate is a rational precursor to mesityl oxide and isophorone which appear more slowly in the infrared spectra as illustrated in Figure 26. The presence of mesityl oxide and isophorone is identified by independent adsorption of these molecules and it is suggested that formation of isophorone is responsible for the more rapid growth of the intensity in the C-H vs. C=O, C=C region of the infrared spectra.

The enolization of acetone on γ-alumina as represented in Figure 26 requires the close proximity of both Lewis acid and Lewis base sites on the surface. A model for the surface of partially

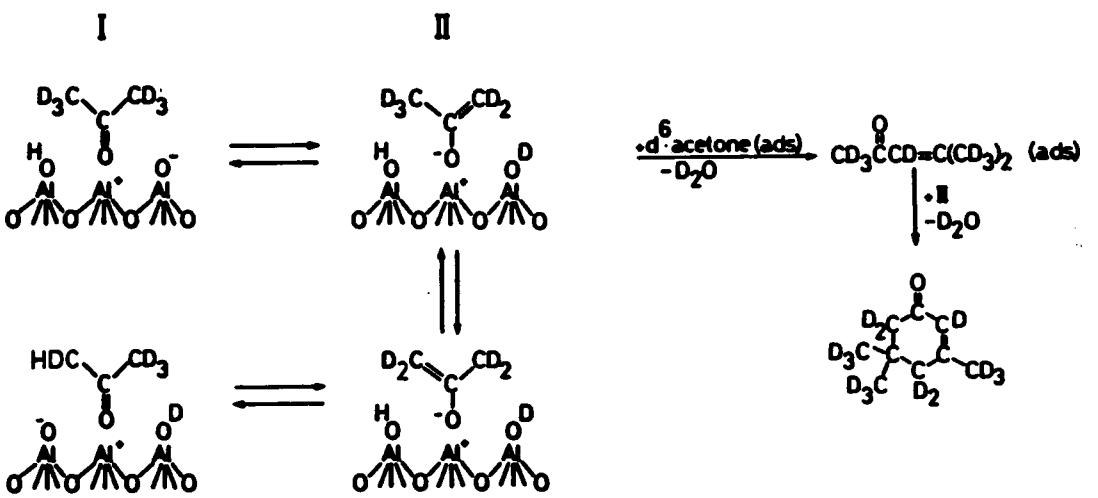

Figure 26. Mechanism of Acetone-d_6 Adsorption at Lewis Acid Sites Indicating Pathways for Surface H-D Exchange and Production of Mesityl Oxide and Isophorone

dehydroxylated γ-alumina indicates that this requirement is satisfied.[23]

Mesityl oxide is formed via nucleophilic attack of the enolate on an adjacent adsorbed acetone molecule followed by dehydration. Attack of acetone enolate or adsorbed mesityl oxide gives a linear trimer of acetone which may then cyclize to give isophorone. Addition without cyclization will yield oligomers of acetone which may not be thermally desorbed during TPD (vide supra). All of the surface species shown in Figure 26 are capable of polymerization under a variety of conditions. This is particularly true for mesityl oxide.

Methyl iodide is observed to displace many of the above species as previously discussed. This may be explained by formation of Al-O-CH_3 and Al-I bonds on the surface. Figure 27 represents this reaction for the displacement of acetone but may be generalized for the displacement of other adsorbed ketones.

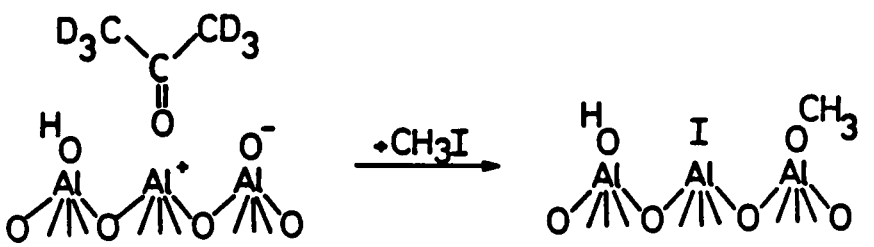

Figure 27. Mechanism for Methyl Iodide Displacement of Adsorbed Ketones

CHAPTER 8
CONCLUSIONS

The main conclusions of this dissertation fall under two categories: a) new synthetic routes to $Mo(CO)_3$(ads) and b) characterization of γ-alumina supported molybdenum subcarbonyls and model compounds by CP-MAS ^{13}C NMR.

The first major conclusion is that $Mo(CO)_3$(ads) can be synthesized using a molybdenum tricarbonyl complex via a ligand displacement reaction with the γ-alumina surface as demonstrated in Chapter 3. This synthesis was designed by analogy with known solution chemistry methods. It is shown that benzene is easily displaced by the γ-alumina surface at 25°C whereas acetonitrile remains coordinated to the surface complex. It is also demonstrated that the solvent used in the displacement reaction is an important consideration since both acetonitrile and acetone were found to poison active $Mo(CO)_3$(ads) olefin metathesis catalysts, presumably by coordinating to the surface complexes. Benzene did not alter metathesis activities. The success of this synthetic approach gives additional confirmation for the formation of mononuclear $Mo(CO)_3$(ads) from $Mo(CO)_6$.

Another facet of this research, namely the interaction of acetone with γ-alumina (Chapter 7), led to the spectroscopic identification of acetone enolate on the γ-alumina surface as well as associated polymerization products.

The second major conclusion of this dissertation is the detection of γ-alumina supported molybdenum subcarbonyls by CP-MAS ^{13}C NMR discussed in Chapter 4. These results indicate the possibility that the $Mo(CO)_3$(ads) species is involved in a motional process. This led to the variable temperature CP-MAS ^{13}C NMR studies of molybdenum tricarbonyl model complexes in Chapter 5. The $Mo(CO)_3$(arene) complexes demonstrate unprecedented tricarbonyl group rotation in the solid state which suggests that this type of motion may be present in $Mo(CO)_3$(ads). Although adequate variable temperature CP-MAS ^{13}C NMR spectra were not obtained for $Mo(CO)_3$(ads) and $Mo(CO)_5$(ads), it is shown that the NMR linewidths of the two species narrow at higher field strengths. This indicates the last major conclusion that the carbonyl ligands of the

γ-alumina supported molybdenum subcarbonyls are dynamic in nature, but the exact identity of these motional processes can not be determined by this data.

REFERENCES

1. Banks, R. L.; Bailey, G. C. I. & E. C. Prod. Res. Dev., 3 (1964) 170.
2. Mol, J. C.; Moulijn, J. A. Advan. Catal., 24 (1975) 131.
3. Davie, E. S.; Whan, D. A.; Kemball, C. J. Chem. Soc., Chem. Comm., (1969) 1430.
4. Howe, R. F.; Davidson, D. E.; Whan, D. A. J. Chem. Soc., Faraday Trans. I, 68 (1972) 2266.
5. Brenner, A.; Ph.D. Dissertation, Northwestern University, 1975.
6. Brenner, A.; Burwell, R. L., Jr. J. Am. Chem. Soc., 97 (1975) 2565.
7. Burwell, R. L., Jr.; Brenner, A. J. Mol. Catal., 1 (1975/76) 77.
8. Howe, R. F. Inorg. Chem., 15 (1976) 486.
9. Brenner, A.; Burwell, R. L., Jr. J. Catal., 52 (1978) 353.
10. Kazusaka, A.; Howe, R. F. J. Mol. Catal., 9 (1980) 183.
11. Laniecki, M.; Burwell, R. L., Jr. J. Coll. Inter. Sci., 75 (1980) 95.
12. Davie, E. S.; Whan, D. A.; Kemball, C. J. Catal., 24 (1972) 272.
13. Brenner, A.; Burwell, R. L., Jr. J. Catal., 52 (1978) 364.
14. Bowman, R. G.; Burwell, R. L., Jr. J. Catal., 88 (1984) 388.
15. Bowman, R. G.; Burwell, R. L., Jr. J. Catal., 63 (1980) 463.
16. Brenner, A.; Hucul, D. A. J. Am. Chem. Soc., 102 (1980) 2484.
17. Herisson, J. L.; Chauvin, Y. Makromol. Chem., 141 (1970) 161.
18. Calderon, N.; Ofstead, E. A.; Judy, W. A. Angew. Chem. Int. Ed. Engl., 15 (1976) 401.
19. Mango, F. D. J. Am. Chem. Soc., 99 (1977) 6117.
20. Calderon, N.; Chen, H. Y.; Scott, K. W. Tetrahedron Lett., (1967) 3327.
21. Bailey, G. C. Catal. Rev., 3 (1969) 37.
22. Werner, R. P. M.; Collfield, T. H. Chem. Ind., (1960) 936.
23. Peri, J. B. J. Phys. Chem., 69 (1965) 220.
24. "Tables of Interatomic Distances and Configuration in Molecules and Ions," Special Publication No. 11. Chemical Society London 1958.

25. Casey, C. P.; Burkhardt, T. J. J. Am. Chem. Soc., 96 (1974) 7808.

26. Chatt, J.; Haines, R. J.; Leigh, G. J. J. Chem. Soc., Chem. Comm., (1972) 1202.

27. Yoshida, T.; Ueda, Y.; Otsuka, S. J. Am. Chem. Soc., 100 (1978) 3941.

28. Casey, C. P.; Andrews, M. A.; Rinz. J. E. J. Am. Chem. Soc., 101 (1979) 741.

29. Brown, T. L. J. Mol. Catal., 12 (1981) 41.

30. Herrmann, W. A.; Ziegler, M. L.; Wienhammer, K.; Biersack, H. Angew. Chem. Int. Ed. Engl., 18 (1979) 960.

31. Herrmann, W. A.; Biersack, H.; Ziegler, M. L.; Weinhammer, K.; Siegal, R.; Rehder, D. J. Am. Chem. Soc., 103 (1981) 1692.

32. Todd, L. J.; Wilkinson, J. R. J. Organometal. Chem., 77 (1974) 1.

33. Cozak, D.; Butler, I. S.; Hickey, J. P.; Todd, L. J. J. Magn. Res., 33 (1979) 149.

34. Kreiter, C. G.; Lang, M. J. Organometal. Chem., 55 (1973) C27.

35. Jackson, W. R.; Pincombe, C. F.; Rae, I. D.; Thapebinkarn, S. Aust. J. Chem., 28 (1975) 1535.

36. Roques, B. P.; Segard, C. J. Organometal. Chem., 73 (1974) 327.

37. Campbell, A. J.; Fyfe, C. A.; Maslowsky, E., Jr. J. Am. Chem. Soc., 94 (1972) 2690.

38. Cottrell, C. E.; Fyfe, C. A.; Senoff, C. V. J. Organometal. Chem., 43 (1972) 203.

39. Campbell, A. J.; Cottrell, C. E.; Fyfe, C. A.; Jeffrey, K. R. Inorg. Chem., 15 (1976) 1321.

40. Lyerla, J. R.; Fyfe, C. A.; Yannoni, C. S. J. Am. Chem. Soc., 101 (1979) 1351.

41. Fyfe, C. A. Mol. Cryst. Liq. Cryst., 52 (1979) 1.

42. Lyerla, J. R.; Yannoni, C. S.; Fyfe, C. A. Acc. Chem. Res., 15 (1982) 208.

43. Dorn, H. C.; Hanson, B. E.; Motell, E. J. Organometal. Chem., 224 (1982) 181.

44. Cotton, F. A.; Hanson, B. E. Israel J. Chem., 15 (1976/77) 165.

45. Delise, P.; Allegra, G.; Magnaschi, E. R.; Chierico, A. J. Chem. Soc., Faraday Trans. II, 71 (1975) 207.

46. Cotton. F. A.; Hanson, B. E. Inorg. Chem., 15 (1976) 2806.

47. Cotton, F. A.; Lahuerta, P.; Stults, B. R. Inorg. Chem., 15 (1976) 1866.

48. Yannoni, C. S. Acc. Chem. Res., 15 (1982) 201.

49. Rothwell, W. P.; Waugh, J. S. J. Chem. Phys., 74 (1981) 2721.

50. Yannoni, C. S.; Clarke, T. C.; Kendrick, R. D.; Macho, V.; Miller, R. D.; Myhre. P. C. Mol. Cryst. Liq. Cryst., 96 (1983) 305.

51. Eades, R. G.; Jones, G. P.; Llewellyn, J. P.; Terry, K. W. Proc. Phys. Soc., 91 (1967) 124.

52. Albert, S.; Gutowsky, H. S.; Ripmeester, J. A. J. Chem. Phys., 56 (1972) 2844.

53. Van Steenwinkel, R. Z. Naturforsch., 24a (1969) 1526.

54. Fyfe, C. A.; Lyerla, J. R.; Yannoni, C. S. J. Magn. Res., 31 (1978) 315.

55. Haupt, J.; Muller-Warmuth, W.; Schulz, G. Z. Angew. Phys., 18 (1964) 132.

56. Bell, V. A.; Gold, H. S. J. Catal., 79 (1983) 286.

57. Schulz, W.; Knozinger, H. J. Phys. Chem., 80 (1976) 1502.

58. Reichle, W. T. J. Catal., 63 (1980) 295.

59. Fink, P. Rev. Roum. Chim., 14 (1969) 811.

60. Papee, D.; Tertian, R.; Biais, R. Bull. Soc. Chim. Fr., (1958) 1301.

61. Lippens, B. C.; De Boer, J. H. Acta Cryst., 17 (1964) 1312.

62. Nolan, S. P.; de la Vega, R. L.; Hoff, C. D. Organometallics, 5 (1986) 2529.

63. Wagner, G. W.; Hanson, B. E. Organometallics, in press.

64. Brenner, A.; Hucul, D. A. Inorg. Chem., 18 (1979) 2836.

65. Hanson, B. E.; Weiserman, L.; Wagner, G. W.; Kaufman, R. Langmiur, in press.

66. Hanson, B. E.; Wagner, G. W.; Davis, R. J.; Motell, E. Inorg. Chem., 23 (1984) 1635.

67. Ross, B. L.; Grasselli, J. G.; Ritchey, W. M.; Kaesz, H. D. Inorg. Chem., 2 (1963) 1023.

68. Brown, D. A.; Hughes, F. J. J. Chem. Soc. (A), (1968) 1519.

69. Evdokimova, M. G.; Yavorskii, B. M.; Trembovler, V. N.; Baranetskaya, N. K.; Krivykh, V. V.; Zaslavskaya, G. B. Dol. Akad. Nauk SSSR, 239 (1978) 1393.

70. Hanson, B. E., unpublished results.

71. Farrar, T. C.; Becker, E. D. "Pulse and Fourier Transform NMR"; Academic Press, New York (1971).

72. Adams, R. A.; Cotton, F. A. Chapter 9 in "Dynamic Nuclear Magnetic Resonance Spectroscopy," L. M. Jackman and F. A. Cotton, eds., Academic Press, New York (1975).

73. Rosenberg, E.; Thorsen, C. B.; Milone, L.; Aime, S. Inorg. Chem., 24 (1985) 231.

74. Hanson, B. E. p. 89 in "Advances in Dynamic Stereochemistry," M. Gielen, ed., Freund, London (1985).

75. Berry, R. S. J. Chem. Phys., 32 (1960) 933.

76. Johnson, B. F. G.; Benfield, R. E. J. Chem. Soc., Dalton Trans., (1978) 1554.

77. Benfield, R. E.; Johnson, B. F. G. in "Transition Metal Clusters," B. F. G. Johnson, ed., J. Wiley, New York (1980).

78. (a) Dorn, H. C.; Hanson, B. E.; Motell, E. Inorg. Chim. Acta, 54 (1981) L71.

(b) Hanson, B. E.; Lisic, E. C.; Petty, J.; Iannaccone, G. Inorg. Chem., 25 (1986) 4062.

79. Hanson, B. E.; Lisic, E. C. Inorg. Chem., 25 (1986) 715.

80. Lauher, J. L. J. Am. Chem. Soc., 108 (1986) 1521.

81. Clare, B. W.; Faras, M. C.; Kepert, D. L.; May, A. S. p. 1 in "Advances in Dynamic Stereochemistry," M. Gielen, ed., Freund, London (1985).

82. Gansow, O. A.; Burke, A. R.; Vernon, W. D. J. Am. Chem. Soc., 98 (1976) 5817.

83. Anderson, J. E.; Slichter, W. P. J. Chem. Phys., 43 (1965) 433.

84. Van Meurs, F.; Van Koningsveld, H. J. Organometallic Chem., 131 (1977) 423.

85. Cotton, F. A. Chapter 10 in "Dynamic Nuclear Magnetic Resonance Spectroscopy," L. M. Jackman and F. A. Cotton, eds., Academic Press, New York (1975).

86. Rothwell, W. P.; Waugh, J. S. J. Chem. Phys., 74 (1981) 2721.

87. Wagner, G. W.; Hanson, B. E. Inorg. Chem., in press.

88. Bailey, M. F.; Dahl, L. F. Inorg. Chem., 4 (1965) 1314.

89. Mariq, M.; Waugh, J. S. Chem. Phys. Lett., 47 (1977) 327.

90. Herzfeld, J.; Berger, A. E. J. Chem. Phys., 73 (1980) 6021.

91. Spiess. H. W.; Grosescu, R.; Haeberlen, U. Chem. Phys., 6 (1974) 226.

92. Shirley, W. M. Z. Phys. Chem., in press.

93. VanderHart, D. L.; Earl, W. L.; Garroway, A. N. J. Magn. Reson., 44 (1981) 361.

94. Hair, M. L.; Chapman, I. D. J. Phys. Chem., 69 (1965) 3949.

95. Miyata, H.; Toda, Y.; Kabokawa, Y. J. Catal., 32 (1974) 155.

96. Miyata, H.; Wakamiya, M.; Kabokawa, Y. J. Catal., 34 (1974) 117.

97. Griffiths, D. M.; Rochester, C. H. J. Chem. Soc., Faraday Trans. I, 74 (1978) 403.

98. Ueda, W.; Yokoyama, T.; Moro-Oka, Y.; Ikawa, T. J. Chem. Soc., Chem. Comm., (1984) 39.

99. Willard, P. G.; Carpenter, G. B. J. Am. Chem. Soc., 108 (1986) 462.

The two page vita has been removed from the scanned document. Page 1 of 2

The two page vita has been removed from the scanned document. Page 2 of 2